

ACTA PHARMACEUTICA SCIENCIA

International Journal in Pharmaceutical Sciences, Published Quarterly

ISSN: 1307-2080,
Volume: 56, No: 2, 2018
Formerly: Eczacılık Bülteni
Acta Pharmaceutica Turcica

ACTA PHARMACEUTICA SCIENCIA

International Journal in Pharmaceutical Sciences

Published Quarterly

ISSN: 1307-2080,

Volume: 56, No: 2, 2018

Formerly: Eczacılık Bülteni/Acta Pharmaceutica Turcica

Founded in 1953 by Kasım Cemal Güven

Editor

Şeref Demirayak

Associate Editors

Gülden Zehra Omurtag

Barkın Berk

Coordinators

M. Eşref Tatlıpınar

Metin Uyar

Language Editors

Recep Murat Nurlu

Mohamed Khalil

Biostatistics Editor

Pakize Yiğit

Address

İstanbul Medipol Üniversitesi

Kavacık Güney Kampüsü

Göztepe Mah. Atatürk Cad.

No: 40 34810 Beykoz/İSTANBUL

Tel: 0216 681 51 00

E-mail

editor@actapharmsci.com

secretary@actapharmsci.com

Web site

<http://www.actapharmsci.com>

Graphic Design

Mesut İlhan

Levent Karabağlı

Editorial Board

Sabahattin Aydın

Ahmet Aydın

Aristidis Tsatsakis

Ayfer Beceren

Dilek Ak

Ebrahim Razzazi-Fazeli

Erçin Erciyas

Erem Memişoğlu Bilensoy

Göknur Aktay

Gülçin Saltan İşcan

Hakan Göker

Hanefi Özbek

Hayati Çelik

İhsan Çalıř

Julide Akbuğa

Kenneth A. Jacobson

Leyla Yurttaş

Mesut Sancar

Nesrin Emekli

Nurşen Başaran

Özgen Özer

Roberta Ciccocioppo

Stefano Constanzi

Tuncer Değim

Yıldız Özsoy

Yusuf Öztürk

Printing Office

Karakış Basım Matbaacılık

Maltepe Mah.

Litros Yolu Sk.

2. Matbaacılar Sitesi 1BF1

Zeytinburnu - İstanbul

Tel: (0212) 544 5820

Contents

Aims and Scope of Acta Pharmaceutica Scientia

Şeref Demirayak

Synthesis of Radioiodinated Thymoquinone Glucuronide Conjugated Magnetic Nanoparticle (^{125}I -TQG- Fe_3O_4) and its Cytotoxicity and In Vitro Affinity

İskender İnce, Zümrüt Biber Müftüler, E. İlker Medine, Özge Kozguş Güldü, Volkan Tekin, Selin Aktar, Erdem Göker, Perihan Ünak

The Effects of Maternal Omega-3 Fatty Acid Supplementation on Breast Milk Fatty Acid Composition

Ezgi Ay, Nihal Büyükuslu, Saime Batirel, Havvanur Yoldaş İlktaş, Muazzez Garipağaoğlu

Synthesis, Characterization and Evaluation of Antifungal Activity of Novel Seven-membered Heterocycles

Rasim Farraj Muslim, Hiba Mahir Tawfeeq, Mustafa Nadhim Owaid, Obaid Hasan Abid

The Essential Oils of Two Achillea L. Species from Turkey

Fatma Tosun, Mine Kürçüoğlu

Renoprotective and Anti-Oxidant Effects of Coleus Forskohlii against Gentamicin Induced Nephrotoxicity in Albino Wistar Rats

Nishat Fatima, Ather Sultana

Polyamine Metabolism and Obesity: Polyamine Metabolic Enzymes Involved in Obesity

Nihal Büyükuslu, Rabia İclal Öztürk

Comparison of 3 Doses of Aloe Vera and Burn Drugs in Market on Burnt Rat Models

Çağlar Macit, M. Eşref Tatlıpınar, Emre Şefik Çağlar, Neda Taner, Senanur Turgut, Elif Görkem Sarıkaya

Aims and Scope of Acta Pharmaceutica Scientia

Acta Pharmaceutica Scientia is a continuation of the former “Eczacılık Bülteni” which was first published in 1953 by Prof. Dr. Kasım Cemal GÜVEN’s editorship. At that time, “Eczacılık Bülteni” hosted scientific papers from the School of Medicine-Pharmacy at Istanbul University, Turkey.

In 1984, the name of the journal was changed to “Acta Pharmaceutica Turcica” and it became a journal for national and international manuscripts, in all fields of pharmaceutical sciences in both English and Turkish. (1984-1995, edited by Prof. Dr. Kasım Cemal GÜVEN, 1995-2001, edited by Prof. Dr. Erden GÜLER, 2002-2011, edited by Prof. Dr. Kasım Cemal GÜVEN)

Since 2006, the journal has been published only in English with the name, “Acta Pharmaceutica Scientia” which represents internationally accepted high-level scientific standards. The journal has been published quarterly except for an interval from 2002 to 2009 in which its issues were released at intervals of four months. The publication was also temporarily discontinued at the end of 2011 but since 2016, Acta Pharmaceutica Scientia has continued publication with the reestablished Editorial Board and also with the support of you as precious scientists.

Yours Faithfully

Prof. Dr. Şeref DEMİRAYAK

Editor



You have only one heart Take care of it

The experienced and specialist academic staff of Medipol University Hospital Cardiology and Cardiovascular Surgery Center, strive for the well being of your heart with the new generation smart technologies which are the "third eye" of the physicians.

Keep in mind,
Cardiovascular Diseases,
Coronary Artery Diseases,
Carotid Artery and Peripheral Artery Diseases,
Arrhythmia,
Cardiac Valve Diseases,
Congenital Heart Valve Diseases
are not irremediable.



MEDIPOL
CALL
CENTER
+90 444 70 44
International WhatsApp Line:
+90 549 794 13 45
www.internationalmedipol.com

**MEDIPOL**
MEGA
MEDIPO
MEGA
HOSPITAL
COMPLEX

UNIVERSITY
HOSPITAL

Synthesis of Radioiodinated Thymoquinone Glucuronide Conjugated Magnetic Nanoparticle ($^{125}\text{I-TQG-Fe}_3\text{O}_4$) and its Cytotoxicity and In Vitro Affinity

İskender İnce^{1,2*}, Zümrüt Biber Müftüler², E. İlker Medine², Özge Kozguş Güldü², Volkan Tekin², Selin Aktar³, Erdem Göker⁴, Perihan Ünak²

¹Ege University, Center for Drug R&D and Pharmacokinetic Applications (ARGEFAR), 35100

²Ege University, Department of Nuclear Application, Institute of Nuclear Sciences, 35100

³Ege University Faculty of Pharmacy, Department of Pharmaceutical Botany, Izmir 35100

⁴Ege University School of Medicine, Division of Medical Oncology, Tulay Aktas Oncology Hospital, 35100

ABSTRACT

The aim of the current study is to develop solid, semisolid or liquid form of radio-nuclide labeled thymoquinone glucuronide conjugated magnetite nanoparticles those targets to the tumor for diagnosis and therapy of cancer.

For this purpose, thymoquinone (TQ), a molecule present in the seeds of *Nigella (Nigella sativa)* used to enhance the affinity of the drug to the tumor cells. TQ was isolated from its microsomes and an enzymatic method applied to synthesize beta glucuronic acid derivatized thymoquinone glucuronide (TQG). TQG attached magnetic nanoparticles (TQG- Fe_3O_4). TQG- Fe_3O_4 were radiolabeled with ^{125}I and ($^{125}\text{I-TQG-Fe}_3\text{O}_4$) its cytotoxic effect and in vitro affinity was investigated.

The IC₅₀ values of TQG- Fe_3O_4 were found 27.31, 18.68, 11.88 ($\mu\text{g/mL}$) respectively 24, 48 and 72 hours against A549 cell line by WST-8 test as a colorimetric way. Incorporation ratios of TQG- Fe_3O_4 with A549 cells is the highest levels. It is seen that TQG- Fe_3O_4 could inhibit the apoptosis on A549 cells but, there is no apoptotic effect of the samples on BEAS-2B cells. Size distribution, cellular uptake and toxicity characteristics of TQG- Fe_3O_4 in this study maintains a useful targeted delivery system in lung cancer diagnosis and therapy.

Keywords: *Nigella* thymoquinone (TQ), glucuronide derivative, beta glucuronidase, radiolabeling with ^{125}I , magnetic nanoparticles, Fe_3O_4 .

INTRODUCTION

Nigella sativa is an annual flowering plant, which is native to India and Pakistan and commonly used as a spice. The oil obtained from the seeds of this plant has traditionally used for the treatment of arthritis, pulmonary disease and hy-

*Corresponding Author: İskender İnce, e-mail: iskender.ince@ege.edu.tr
(Received 23 October 2017, accepted 05 December 2017)

percholesterolemia, especially in Arabian culture. Biological activity of *Nigella* seeds originates from thymoquinone derivatives, which is dominant (30-48%) compound of volatile oil content²⁹. A limited number of clinical trials show that, there is no side effects of thymoquinone on human, even at high dosages of this compound. Therefore, it is highly desirable to form a novel compound, which is hydrolyzed in tumor by beta-glucuronidase with glucuronic acid conjugation of thymoquinone.

It is well-known that, some cancer cells are very rich for beta glucuronidase. Information is available about lung cancer cells have high beta glucuronidase activity²⁰.

Labeling glucuronide derivatives with technetium-99m (^{99m}Tc) or radioiodine with the advantage of higher expression of beta glucuronidase enzymes in tumor tissues rather than normal tissues, have been studied by our group for more than a decade^{1,2,4,5,8-11,13,15,16,21,23-27,29,30}.

Stachulski and Meng reported that glucuronide derivatives of the cytotoxic molecules used in the cancer therapy are significantly reducing the use of glucuronide derivative molecule increased day by day²². Different studies uracil-O-glucuronide are showing that affinity of this molecule in cancer cells is significantly higher than normal cells. For example, production of uracil-O-glucuronide (UOG) significantly increased in HuTu 80 small bowel cancer cells in comparison with normal human intestinal epithelial cells⁶.

Beta-glucuronidase is present in higher levels than in normal tissue, also led this enzyme in tumor tissue to be more active in more acidic environments such as the and relatively easy to measure to some cytotoxic molecules glucuronide derivative of the birth of the idea that can be a good anticancer agents³. Nanoparticles with magnetic properties can be used in imaging, diagnosis and treatment of various diseases and to separate of biological materials. Patient-related, magnetic controlled drug targeting system is reported by Lubbe et al. for the first time. Lubbe and colleagues also states that, directing iron nanoparticles to tumor cells is feasible under 0.5-0.8 Tesla magnetic field strength¹⁴. Mohapatra et al. reported that folic acid-conjugated magnetic nanoparticles retained specifically by folate receptor containing cancer cells. Magnetic nanoparticles were synthesized by precipitation reaction of Fe²⁺/Fe³⁺ and following surface modification with 2-carboxyethyl phosphonic acid. Resulting nanoparticles with a free carboxyl group attached to the folic acid and fluorescein isothiocyanate (FITC) using 2,2- (ethylenedioxy) - bisethylamine¹⁸.

Moritake et al. silanized 3nm sized magnetite nanoparticles with (3-aminopropyl) triethoxysilane and reported that it may also be suitable to attach pharma-

ceuticals and biomolecules after functionalization of surface with amino groups. It is reported that extreme small particles without any other modification may penetrate to inside of cells due to increasing endocytic binding, because of their cationic structures. The cells that bind nanoparticles have continued to proliferate and have not shown any extinguisher effect on mitosis. In addition, when the particles injected under ear skin, they magnetized under outer magnetic field¹⁹.

Thymoquinone compound radiolabeled with ^{99m}Tc is the only thymoquinone derivative that be usable over gamma scintigraphy¹⁷.

The aim of current study is as follows:

- Synthesis of a thymoquinone glucuronide derivative,
- Conjugation with magnetic nanoparticles (Fe₃O₄, nm size),
- Radiolabeling with ¹²⁵I and also other iodine radioisotopes,
- Development of formulations of generated solid radiolabeled nanoparticles showing the magnetic properties in solid, semi-solid and liquid forms.
- Determination of *in vitro* affinity by using Human lung adenocarcinoma cells (A549) and normal human lung epithelial cells (BEAS-2B).

MATERIAL METHOD

Materials

Na¹²⁵I is obtained from the Institute of Isotopes Co. Ltd., Budapest. BEAS-2B and A549 cell lines were obtained from American Type Culture Collection, Rockville, MD, USA and Bio-engineering Department of Ege University, Izmir, Turkey, respectively. WST-8 assay, iodogen (1,3,4,6-tetrachloro-3 α ,6 α -diphenylglycouril), ferrous chloride (FeCl₃) and ferric chloride tetrahydrate (FeCl₂.4H₂O) were purchased from Sigma-Aldrich. All other chemicals purchased from Merck and Lonza. All solvents were reagent grade and, are used without further purification.

Equipment

Transmission electron microscopy (TEM, JEOM JEM 2100F HRTEM), X-ray diffraction (XRD, Philips X'Pert Pro), dynamic light scattering (DLS) (Malvern Nano-ZS) were used for characterization of synthesized Fe₃O₄ nanoparticles. Bi-oscan AR-2000 Imaging Scanner and Packard Tri-Carb-1200 Liquid Scintillation Spectrometer used for Thin Layer Radio Chromatography (TLRC) method and incorporation studies, respectively.

Glucuronidation of Thymoquinone (TQ)

Obtaining of UDP-glucuronyl transferases enzyme (UDPGT) from A549 Cells

Microsome preparates separated from human lung carcinoma cells (A549) used as a UDP-glucuronyl transferase (UDPGT) source, which is required for glucuronidation of thymoquinone. A549 cells were grown in MEM supplemented with 10 % FBS, 2.0 mM glutamine, 0.1 mM nonessential amino acid, 1,5 g/L sodium bicarbonate and 1 mM sodium pyruvate. Mediums removed and cells washed 3 times with PBS. Cells were detached from the surface and cell pellets washed with sucrose/hepes 3 times with centrifugation (4 °C, 1000 rpm and 10 min) in every step. Then cells ruptured with homogenizator for 4 minutes at ice bath. Homogenate was centrifuged at 4 °C, 10500 rpm for 10 minutes and supernatant was centrifuged at 4 °C, 28000 rpm for 10 minutes by ultracentrifuge. After centrifugation supernatant was removed and enzymes were solubilized with pH 7 buffer (0.2 M potassium phosphate, 2 mM mercaptoethanol and 0.4% Triton X100) and stirred for 30 min. at 4 °C. Solubilized enzymes were centrifuged at 4 °C, 28000 rpm for 10 minutes. Protein concentration of the supernatant, which contains microsomal samples determined with bicinchoninic acid method using Thermo Varioskan Flash multimode microplate reader. Absorbance reading was performed at 260 nm and protein concentration was obtained as 3.44 mg/mL.

Enzymatic Synthesis of Thymoquinone Glucuronide (TQG)

34.4 mg microsomal enzyme in 5 mL of 50 mM Tris Buffer (pH = 8) which contains 6 mM CaCl₂, 10 mM UDPGA and 1 mM DTT were stirred at 37 °C for 10 min in a water bath. Then thymoquinone in 10 mg/mL of DMSO was added and incubated at the same temperature for 18 hours. After incubation acetonitrile (300 µL) was added to the solution and centrifuged at 2000 rpm for 20 min. Purity analysis of product was conducted by HPLC (Schimadzu LC10 ATVP).

Preparation of Magnetic Nanoparticle Conjugated TQ and TQG

Synthesis of Magnetic (Fe₃O₄) Nanoparticles

One hundred mL of ferrous salt solution in acidic environment was prepared using 2 M FeCl₃ (12 mL) and 2 M HCl, Then, 0.08 M Na₂SO₃ (50 mL) was added slowly under nitrogen gas. Ammonia (NH₃) (25%, 8 mL) was added to the mixture under nitrogen gas. The mixture waited at 70 °C for 15-30 minutes. Then the temperature of the mixture was cooled under 45° C. Black colored particles were collected with a magnet and washed with ethanol for 3 times. Particles were stored in ethanol at 4° C.

Coating of Fe₃O₄ Nanoparticles with Silica

Five mL tetra ethyl ortho silicate (TEOS) and NH₃ (10%, 5 mL) was added into the magnetic particle solution. The reaction was carried under at 40°C for 12 hours under magnetic stirring and was washed with methanol 3 times.

Amino Silane Conjugation of Silica Coated Fe₃O₄ Nanoparticles

Amino silane agent [N-(2-aminoetil)-3-aminopropil-trimetoksisilan] was added into the magnetic nanoparticles in ethanol and solution was kept in an ultrasonic bath for 5 minutes. After uniform dispersing, the reaction was carried out at 60 °C for 12 minutes and washed with ethanol 3 times. The resulting precipitates were collected, dried under vacuum and stored at 4°C.

Immobilization of TQ and TQG to Fe₃O₄ Nanoparticles (TQ-Fe₃O₄ and TQG-Fe₃O₄)

Twenty-five mg/mL of silanized Fe₃O₄ nanoparticles was washed with 0.1 M phosphate buffer solution (PBS pH=7.0 25°C). Then, nanoparticles were incubated with glutaraldehyde (2.5%) at 4°C in an ultrasonic bath for 4 hours. The suspension was centrifuged and washed with 0.1 M PBS. TQ (4 mg) and TQG (4 mg) were dissolved in 1 mL 0.1 M PBS, which contains 0.15 M NaCl and 0.005 M EDTA (pH=7.2). After 12 hours of incubation particles were washed with 0.1 M borate tampon which contains (pH=9.2) 0.5 mg/mL NaBH₄ and kept at 4°C for 30 minutes. Particles washed with 0.1 M PBS (pH=7.0 25°C) and resuspended in 1 mL 0.5M MES (pH=6.6).

Inactive iodination of TQG [Inactive iodine (¹²⁷I) labeled TQG (¹²⁷I-TQG)]

Cold-iodination of TQG was performed to gain insight about the molecular structure of radioiodinated TQG. With this purpose, TQG was iodinated within active iodine (¹²⁷I) by using stoichiometrically equivalent amounts of potassium iodide and oxidizing agent iodogen to prove the identity of the radiolabeled compound.

Quality Control Studies of TQ and TQG by using High Performance Liquid Chromatography (HPLC)

TQ and enzymatically glucuronidated TQG were analyzed with HPLC. A low-pressure gradient HPLC system (LC-10ATvp quaternary pump, SPD-M20A DAD detector, a syringe injector equipped with a 500 IL loop, CTO-10AS column oven, SIL 20A-HT auto sampler, FRC-10A fraction collector and 5μ C18-ODS column (250 x 4.6 mm ID) was used for HPLC analysis. 1mL/min was flow rate of the mobile phase and readings were collected at 254 nm. Mobile phase of analysis was water/methanol/isopropanol (50:45:5). HPLC chromatogram of TQ and TQG was shown in Figure 1.

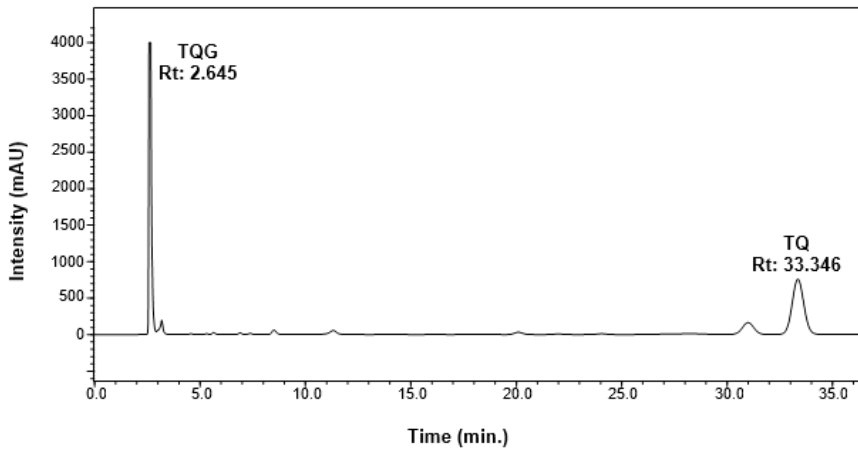
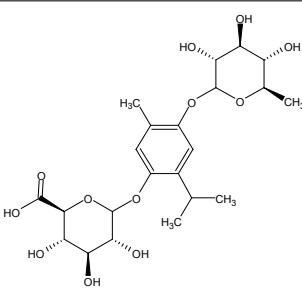
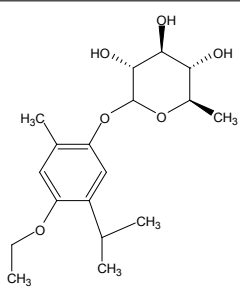
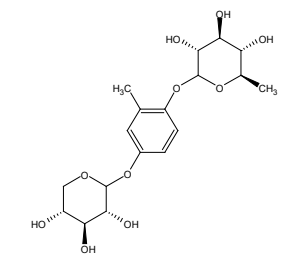
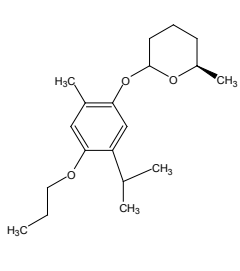
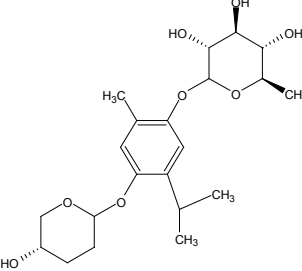
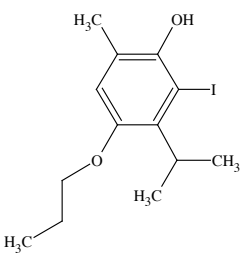
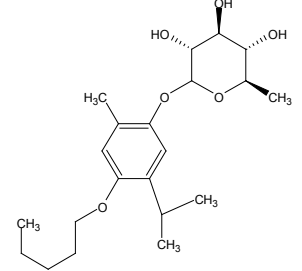
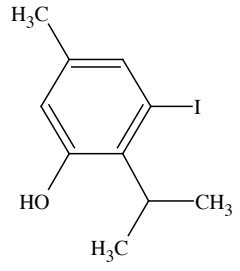


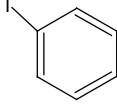
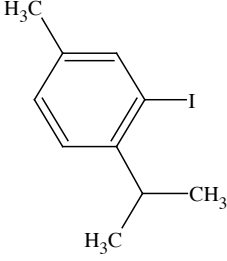
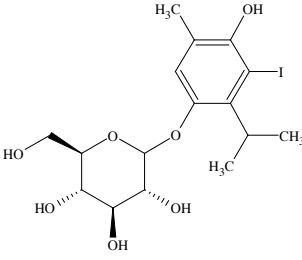
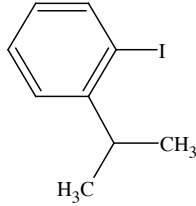
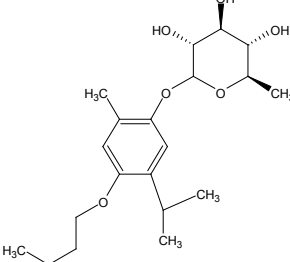
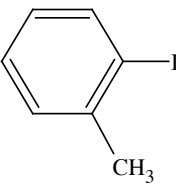
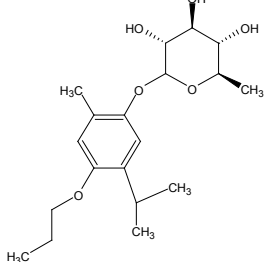
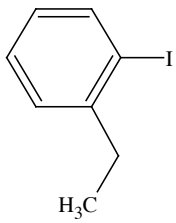
Figure 1. HPLC chromatogram of the TQ and TQG.

Structural Analysis of TQG and ¹²⁷I-TQG

Structural analysis of TQG and ¹²⁷I-TQG were performed by Liquid Chromatography-Mass Spectroscopy (LC-MS/MS) at the Laboratory of LC-MS at Ege University, Ege University, Center for Drug R&D and Pharmacokinetic Applications(ARGEFAR). m/z values of the TQG and ¹²⁷I-TQG, and also with other fragments were given in Table 1.

Table 1. LC-MS/MS m/z values of the TQG and ¹²⁷TQG compounds and some fragments.

	Fragment	m/z		Fragment	m/z
A		488.48	I		340.41
B		402.39	J		306.43
C		411.11	K		334.22
D		382.49	L		274.51

E		204.55	M		260.56
F		454.00	N		246
G		368.33	O		218
H		354.43	P		232

Characterization Studies

Characterization studies of Fe_3O_4 nanoparticles, silica coated Fe_3O_4 nanoparticles, silane conjugated Fe_3O_4 nanoparticles were done by using Dynamic Light Scattering Analysis, Transmission Electron Microscope (TEM) and Energy-dispersive X-ray Spectroscopy (EDX) methods (Figure 2).

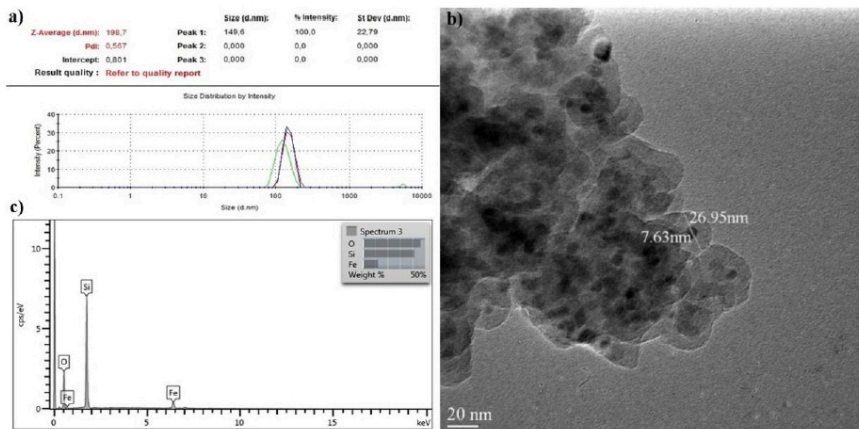


Figure 2. (a) DLS analysis diagram (b) EDX and (c) TEM image of silane conjugated Fe_3O_4 nanoparticles.

Radiolabeling with ^{125}I Procedure

Iodogen coated tubes were prepared as containing 250 μg of iodogen. The solvent was allowed to evaporate forming a thin solid layer on the wall of the reaction vial. Tubes were kept at 4 $^\circ\text{C}$. 50 μg of samples (TQ, TQG, TQ- Fe_3O_4 and TQG- Fe_3O_4) were added to prepared iodogen coated tubes and then 0.1 mCi/0.1 mL ^{125}I was added. The mixture was incubated for 30 min. at airtight conditions.

Quality control studies of radiolabeling compounds

The thin layer radio chromatography (TLRC) was used to determine the radiolabeling compounds (^{125}I -TQ, ^{125}I -TQG, ^{125}I -TQ- Fe_3O_4 and ^{125}I -TQG- Fe_3O_4).

10 cm \times 1.5 cm sized cellulose TLC strips were used as stable phase and 4 developing baths were used as mobile phase. The content of the developing baths is: n-butanol / bidistilled water / acetic acid (4:2:1) (TLRC1), n-butanol / ethyl alcohol / 0.2 N NH_4OH (5:2:1) (TLRC2), isopropanol / n-butanol / 0.2 N NH_4OH (4:2:1) (TLRC3) and isopropanol / n-butanol / 0.2 N NH_4OH (2:1:1) (TLRC4). Two μL of radio ligand was applied to Thin Layer Chromatography (TLC) strips and placed to the solutions. After mobile phase reached the end-

point, TLC strips were removed from bath solutions and left to dry. Radiochromatograms of TLC strips were obtained by Bioscan AR2000 TLRC scanner. R_f values of radiolabeled compounds and radiolabeling yields were calculated. Because of the higher separation efficiency TLRC1 developing bath was used in determining radiolabeling yield. R_f values of radioactive components were given in Table 2.

Table 2. R_f values of ^{125}I , Oxi. ^{125}I , ^{125}I -TQ, ^{125}I -TQG, ^{125}I -TQ- Fe_3O_4 and ^{125}I -TQG- Fe_3O_4 at TLRC1 solution.

	^{125}I	^{125}I -TQ	^{125}I -TQG	^{125}I -TQ- Fe_3O_4	^{125}I -TQG- Fe_3O_4
R_f	0.39	0.87	0.45	0.15	0.57
Cellulose TLC strips, n-butanol / bidistilled water / acetic acid (4:2:1) (TLRC 1)					

Cell Culture Studies

Human lung adenocarcinoma cells (A549) were grown in MEM supplemented with 10 % FBS, 2.0 mM glutamine, 0.1 mM nonessential amino acid, 1.5 g/L sodium bicarbonate and 1 mM sodium pyruvate and; normal human lung epithelial cells (BEAS-2B) were grown in Clonetics BEGM BulletKit. All cells were grown at 37 °C in a humidified incubator equilibrated with 5.0% CO_2 . The cells were maintained in exponential growth by sub-culturing with trypsin-EDTA (0.25% by w/v in Hank's balanced salt solution). The cells were then pelleted and re-suspended in cell medium. In cell culture studies, samples that are conjugated to magnetic nanoparticles were exposed to a constant magnetic field (1.17-1.21 Tesla) while studies. Control and other nonmagnetic samples were not treated with the external magnetic field.

Cytotoxicity Studies

Cytotoxicity studies of TQ, TQG, Fe_3O_4 , TQ- Fe_3O_4 , TQG- Fe_3O_4 , TQ- Fe_3O_4 (MF) and TQG- Fe_3O_4 (MF) were performed on A549 cells. Each parameter was performed in two different days and repeated three times. IC_{50} values of samples were calculated by WST-8 test as a colorimetric way. The cell suspension was prepared as 10^5 cells/ml for each well at 96-well plate. One hundred μL of cell suspension and 5 different concentrations of sample were added to each well. Cell and medium without reagent was used as negative control. Cells were incubated at 37 °C in a humidified incubator equilibrated with 5.0% CO_2 for 72 hours. After incubation 10 μL of WST solution was added to the wells and incubated for 4 hours. Absorbance values (OD) were obtained at 450 nm wavelength and 690 nm reference range by spectrophotometric method. Zero absorbance was ap-

plied as negative control. Cytotoxicity values (%) were calculated by using this formula;

$$\% \text{ Cytotoxicity} = (\text{measured optical density value} / \text{control value}) \times 100$$

Apoptosis Study

Apoptotic effects of samples were evaluated on A549 and BEAS-2B cells by using the Dead End Fluoro-metric TUNEL System (Promega) according to the manufacturer's instructions as described below. Minimum 300 cells were evaluated for each group. Cells were prepared on chamber slides. After 24 hours, mediums of cells were changed with mediums, which contain samples in IC_{50} concentrations. After 24 hours, medium of chamber slides was removed and washed with PBS 2 times. Slides with cells were incubated in PBS with paraformaldehyde (4%) (pH 7.4) solution at 4°C, for 25 minutes. Then the slides were incubated in PBS with Triton-X (0.2%) for 5 minutes to increase the cell permeability. Then the slides were washed with PBS 3 times for 5 minutes. One hundred μL of equilibration tampon was added to the slides and incubated for 10 minutes. During this time, rTdT incubation tampon was prepared: 90 μL equilibration tampon, 10 μL nucleotide mixture and 2 μL rTdT enzyme. After 5-10 minutes, liquid in the slides were removed and nucleotide mixture was added instead of this, then lamella was used. Samples were incubated at 37°C for 60 minutes. At room temperature, samples were incubated in 2XSSC for 15 minutes to stop the reaction. The slides were washed with PBS for 5 minutes and this process was repeated 3 times. The slides were incubated in propidium iodid solution (1 $\mu\text{g}/\text{mL}$) for 15 minutes. After the slides were dried, the cells were imaged by fluorescence microscope by using green (520 nm) and red (620 nm) filters.

Time Dependent Incorporation Study of ^{125}I Labeled Samples on Cells

Cells were grown to determine the optimum time parameter for incorporation of ^{125}I labeled TQ, TQG, $\text{TQ-Fe}_3\text{O}_4$, $\text{TQG-Fe}_3\text{O}_4$, $\text{TQ-Fe}_3\text{O}_4$ (MF) and $\text{TQG-Fe}_3\text{O}_4$ (MF) on cells. 24-well plates were prepared and time parameters specified as 30., 60., 120. and 240. minutes.

0.1 $\mu\text{g}/\text{mL}$ of sample and ^{125}I 1 $\mu\text{Ci}/\text{mL}$ were used for per well. 0.5 mL of ^{125}I labeled ligand was added to the wells. 1 $\mu\text{Ci}/\text{mL}$ of ^{125}I was used to determine the incorporation of unbound ^{125}I . Only medium was added to cells as a control. Cells were incubated at 37 °C. When incubation time was over, cells were washed with PBS two times and suspended by treating with 200 μL RIPA lyse buffer solution. After 30, 60, 120 and 240 minutes, the protein concentration of the lysed cell suspension (25 μL) was determined by the Bicinchoninic acid (BCA) kit. Also, 100 μL of lysed cell suspension was used to count the radioactivity by a liquid

scintillation counter (Packard TriCARB-1200). Radioactivity corresponding to per µg of protein was used in the calculation of incorporation values.

Statistical analysis

The statistical significance of cell culture studies was assessed by one-way ANOVA and linear regression using the Graph Pad (prism 2.01V) program. Probability values $P < 0.05$ were considered statistically significant for studies.

RESULTS AND DISCUSSION

Structural Analysis Studies of TQG and ^{127}I -TQG Compounds

Table 1 shows LC-MS/MS m/z values of the TQG and ^{127}TQG compounds and some other fragments. The identification of the TQG was performed using LC-MS/MS with positive mode $[\text{M}+\text{H}]$ allowed the detection of corresponding molecular ion at m/z 488.48. ^{127}TQG and some fragments were 454, 334.22, 274.51, 260.56, 246 respectively. It is seen that the glucuronidation occurred on hydroxyl groups by transforming the carbonyl group in quinone ring of molecule to quinol.

Characterization of Silane Conjugated Fe_3O_4 Nanoparticles

Dynamic Light Scattering (DLS): Dynamic Light Scattering analysis of silane conjugated Fe_3O_4 nanoparticles in ethanol was performed by Malvern Nano ZS equipment. The average dynamic size of the silanated nanoparticles is 200 nm (Figure 1).

TEM: When Figure 1 is examined, it is seen that there is an aggregation between nanoparticles and size of nanoparticles is ranging between 7.63-26.95 nm. Also, the resulting nanoparticles were found to be spherical in shape.

EDX: As seen in Figure 1, the amount of Fe, O and Si are compatible with the elemental structure according to EDX results of silane conjugated Fe_3O_4 nanoparticles. The results are appropriate with expected structure.

Quality Control Studies by Chromatographic Methods

High Performance Liquid Chromatography (HPLC): Retention time (R_t) values of some compounds are given in Figure 2, R_t value of TQ is determined as 2.65 min. while TQG's is 33.35 min R_t value.

This result shows that the reaction of glucuronidation was performed with yield of 69.16 ± 3.28 % ($n=3$). R_t values of radiolabeled compounds are given in Table 3.

Table 3. R_f values of ¹²⁵I, Oxi. ¹²⁵I, ¹²⁵I-TQ, ¹²⁵I-TQG, ¹²⁵I-TQ-Fe₃O₄ and ¹²⁵I-TQG-Fe₃O₄.

	¹²⁵ I	¹²⁵ I-TQ	¹²⁵ I-TQG	¹²⁵ I-TQ-Fe ₃ O ₄	¹²⁵ I-TQG-Fe ₃ O ₄
R _f	2.23	5.12	5.26	5.77	6.03

The thin layer radio chromatography (TLRC): R_f values of the radiolabeled components (¹²⁵I and Oxi. ¹²⁵I, ¹²⁵I-TQ, ¹²⁵I-TQG, ¹²⁵I-TQ-Fe₃O₄ and ¹²⁵I-TQG-Fe₃O₄) for TLRC1 developing bath are given in Table3. The separation between compound peaks was satisfactorily achieved and radiolabeling yields of all compounds (TQ, TQG, TQ-Fe₃O₄ and TQG-Fe₃O₄) were determined over 95%.

Cytotoxicity Studies

The cytotoxic effects of the samples were investigated on A549 cell lines via WST-8 cytotoxicity assay kit. Five different concentrations were tested after 24, 48 and 72h of incubation at 37 °C. The obtained results are summarized in Figure 3. Fe₃O₄ nanoparticle conjugated samples have a negligible cytotoxic effect on the cell line for 24h. IC₅₀ values of samples were calculated and given Table 4. The results show that neither Fe₃O₄ nor Fe₃O₄ nanoparticle conjugated samples are cytotoxic at the concentration studied until 12.5 µg/mL for 24h. The cell viability of A549 is more than 80% for concentrations < 6.25µg/mL until 48h. However, in all concentrations the cytotoxic effect of Fe₃O₄ nanoparticle conjugated samples was less than Fe₃O₄.

Figure 3. Viabilities of A549 cells after a) 24h b) 48h c) 72h incubation.

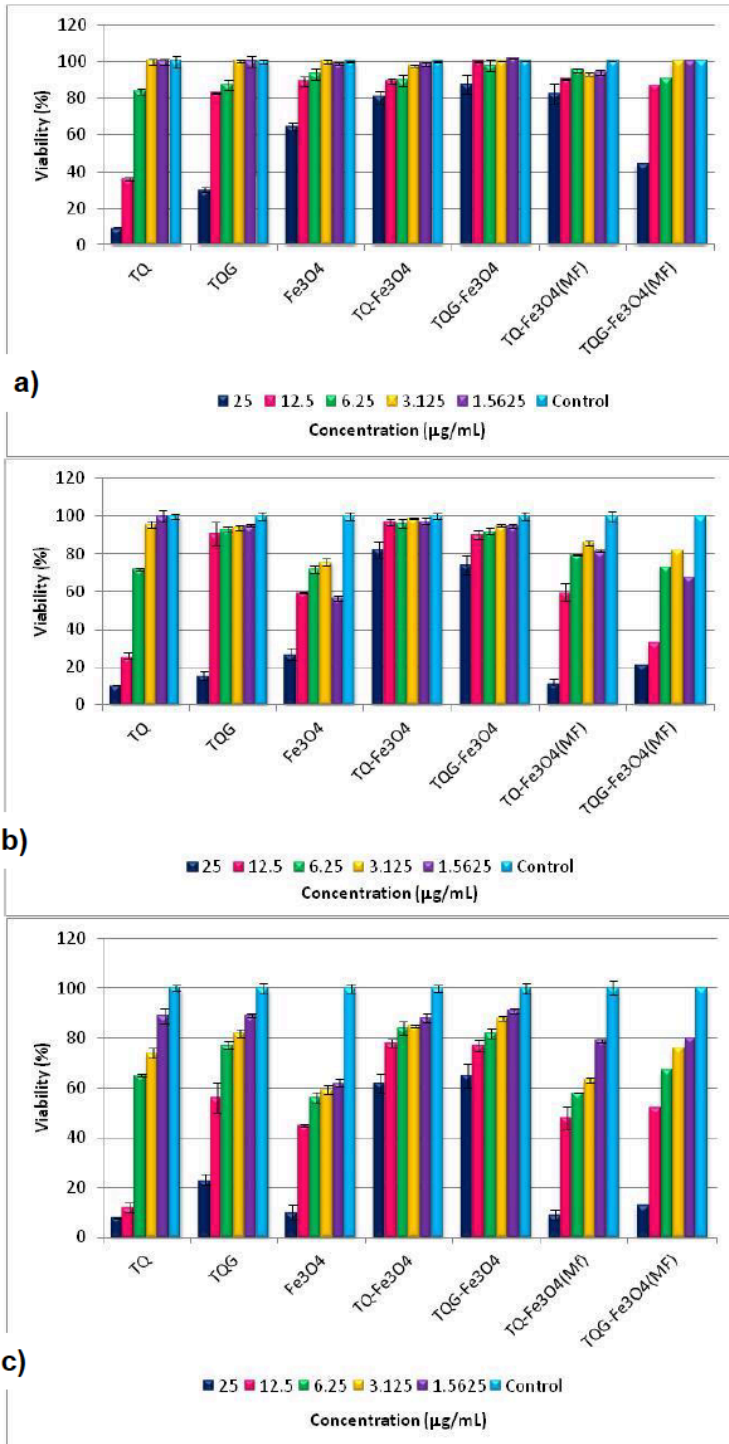


Table 4. IC₅₀ values of samples on A549 cells.

		A549					
		TQ	TQG	TQ-Fe ₃ O ₄	TQG-Fe ₃ O ₄	TQ-Fe ₃ O ₄ (MF) ⁴	TQ-G-Fe ₃ O ₄ (MF)
IC ₅₀ (µg/mL)	24 hours	10.58	19.39	15.63	27.31	16.10	23.45
	48 hours	8.81	17.51	14.97	18.68	12.71	10.78
	72 hours	6.59	15.62	12.40	11.88	7.04	9.579

Comparison of Incorporation Efficiency between A-549 and BEAS-2B cells

Comparison of incorporation efficiency of ¹²⁵I labeled samples on BEAS-2B and A549 cells is shown in Figure 4. After 2 hours, ¹²⁵I-TQ and ¹²⁵I-TQG were incorporated by healthy cells higher than carcinoma cells, and after conjugation of Fe₃O₄ affinity to carcinoma cells increased 2 times for ¹²⁵I-TQ-Fe₃O₄ and increased 3 times for ¹²⁵I-TQG-Fe₃O₄. This ratio increases 5-fold for ¹²⁵I-TQ-Fe₃O₄ and 6-fold for ¹²⁵I-TQG-Fe₃O₄ after magnetic field.

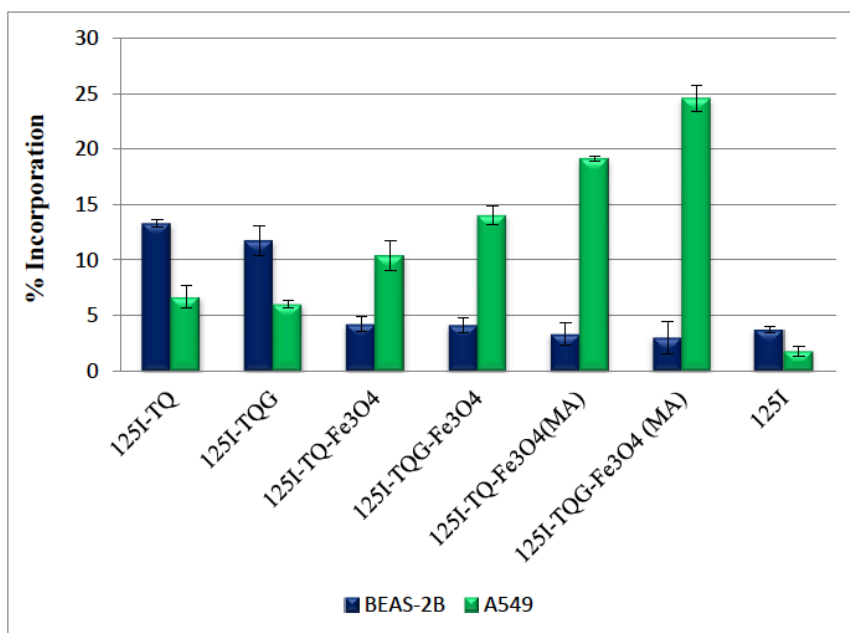


Figure 4. Comparison of time dependent incorporation ratios of the ¹²⁵I labeled samples on BEAS-2B and A549 cell lines (Dose: 1 µg ligand/1 µCi ¹²⁵I, Incubation time: 2h).

Apoptosis Study

According to results (Figure 5), there is no apoptotic effect of the samples on BEAS-2B cells was found. It is seen that magnetic nanoparticle conjugated TQG (TQG-Fe₃O₄), could inhibit the apoptosis on A549 cells. With magnetic field TQG-Fe₃O₄ could increase the apoptosis of the cells more than TQG-Fe₃O₄ and there is no inhibition of apoptosis for other samples.

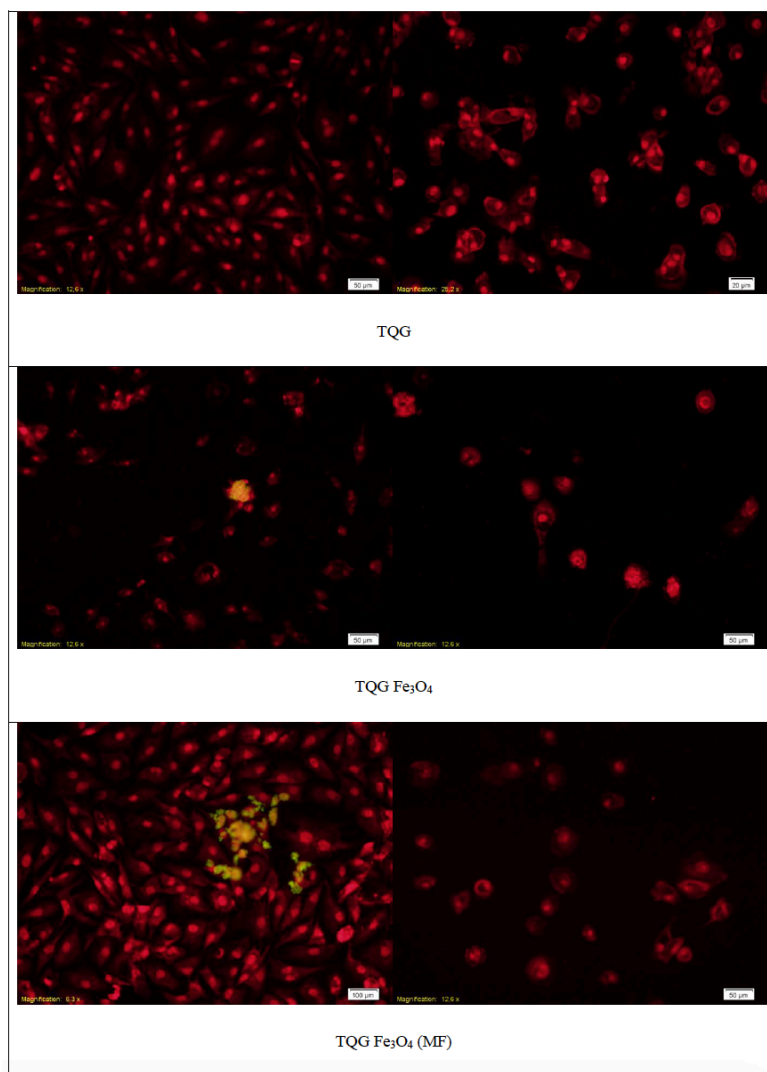


Figure 5. Apoptosis assay images of the TQG, TQG-Fe₃O₄ and TQG-Fe₃O₄(MF) on A549 and BEAS-2B cells (left images are for A-549 cells, right images are for BEAS-2B cells).

Time Dependent Incorporation Study

Results of time dependent incorporation study of ^{125}I labeled samples on A549 cells are given in Figure 6. Incorporation ratios of all samples increased by the time and the highest amount is determined for Fe_3O_4 conjugated TQG. The magnetic field has a dramatic effect on the incorporation ratios with the compounds loaded onto magnetic nanoparticles.

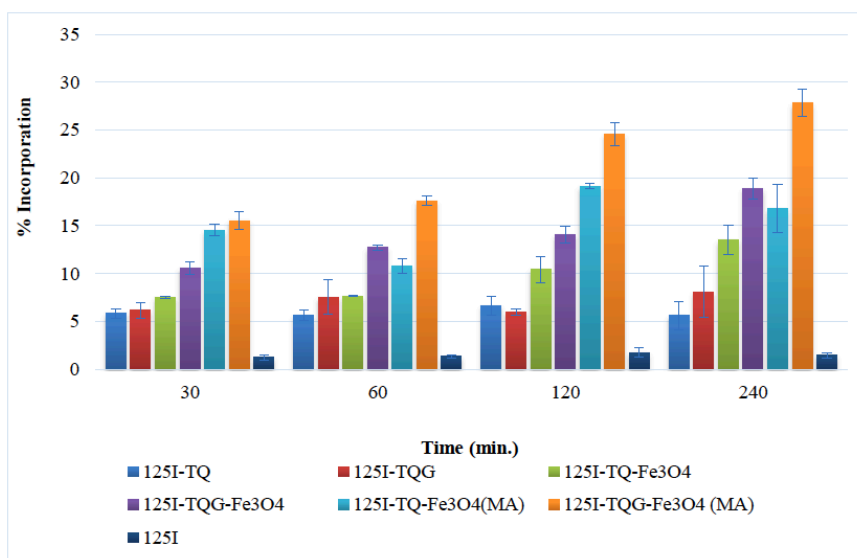


Figure 6. Time dependent incorporation ratios of the ^{125}I labeled samples on A549 cells.

Results show that magnetic nanoparticles could be used as efficient carriers for the bioactive molecules along with drugs, and these nanoparticles might be easily accommodated to the targeted for diagnosis and therapy applications¹⁶.

CONCLUSION

Preparation of TQ glucuronide derivatives, labeling of them with ^{131}I or with other radionuclides (^{125}I , ^{124}I , ^{123}I , other radiohalogenated isotopes and ^{211}At), conjugation with Fe_3O_4 nanoparticles and preparing radionuclide labeled TQG conjugated Fe_3O_4 nanoparticles of solid, semi-solid and liquid formulations, in which TQG's prepared using enzyme preparations prepared from human cancer cells in the synthesis, obtaining radionuclide labeled of them by attaching with radioiodine, preparing of them solid, semi-solid and liquid dosage forms.

TQ glucuronide preparation of derivatives ^{131}I or with other radionuclides (^{125}I , ^{124}I , ^{123}I , other radiohalogenated isotopes and ^{211}At) labeling, conjugating with Fe_3O_4 nanoparticles prepared TQG conjugated Fe_3O_4 nanoparticles of solid,

semi-solid and liquid form is the preparation of formulations, in which by molecules inserted radionuclide feature cancer Single Photon Emission Tomography (SPECT) and Positron Emission Tomography (PET) radionuclide labeled TQ of which enables the use of imaging TQ or TQG which is conjugated to Fe_3O_4 nanoparticles.

TQ glucuronide derivatives preparation of labeling with ^{131}I or with other radionuclides ^{125}I , ^{124}I , ^{123}I , other radiohalogenated isotopes and ^{211}At , conjugated with Fe_3O_4 nanoparticles prepared thymoquinone radionuclide labeled glucuronide (TQG) conjugated Fe_3O_4 nanoparticles of solid, semi-solid and liquid form is the preparation of formulations, in which MR which enables the use in imaging lymph node or tumor contains radionuclides or radionuclide transport marked the thymoquinone or thymoquinone glucuronide bound Fe_3O_4 nanoparticles.

TQ glucuronide derivatives of labeled with ^{131}I or with other radionuclides ^{125}I , ^{124}I , ^{123}I , other radiohalogenated isotopes and ^{211}At labeled, conjugated with Fe_3O_4 nanoparticles, prepared thymoquinone radionuclide labeled glucuronide (TQG) conjugated Fe_3O_4 nanoparticles of solid, semi-solid and liquid form is the preparation of formulations, in which according to the different cancer molecule attached radionuclide feature that can be used in diagnostic and therapeutic radionuclides or contains TQ marked TQG connected Fe_3O_4 nanoparticles.

Thymoquinone glucuronide preparation of derivatives ^{131}I or with other radionuclides (^{125}I , ^{124}I , ^{123}I , other radiohalogenated isotopes and ^{211}At) labeled, conjugated with Fe_3O_4 nanoparticles, prepared thymoquinone radionuclide labeled glucuronide conjugated Fe_3O_4 nanoparticles of solid, semi-solid and liquid form is the preparation of formulations, in which In the treatment of different cancer with hyperthermia and providing thymoquinone (TQ) be used to monitor therapy or thymoquinone glucuronide (TQG) which is connected Fe_3O_4 nanoparticles.

TQ glucuronide preparation of derivatives ^{131}I or with other radionuclides ^{125}I , ^{124}I , ^{123}I , other radiohalogenated isotopes and ^{211}At marking, conjugated to Fe_3O_4 nanoparticles, prepared thymoquinone radionuclide labeled glucuronide (TQG) conjugated Fe_3O_4 nanoparticles of solid, semi-solid and liquid form is the preparation of formulations, in which beta-glucuronidase rich in the enzymes that allow the use of different cancers in vitro diagnostic kit for the diagnosis of cancer TQ or TQG bound Fe_3O_4 nanoparticles it contains.

ACKNOWLEDGEMENT

This project was financially supported by Turkish Scientific Research Council- Health Sciences Research Support Group (TUBİTAK-SBAG; Project No: 113S922), Ankara, TURKEY.

REFERENCES

1. Aslan O., Biber Muftuler F. Z., Yurt Kilcar A., Ichedef C., Unak P., In vivo biological evaluation of ^{131}I radiolabeled-paclitaxel glucuronide (^{131}I -PAC-G), *Radiochimica Acta*, **2012**, *100*, 339-45.
2. Aşikoğlu M., Yurt F., Çağlayan O., Ünak P., Özkılıç H., Detecting inflammation with ^{131}I -labeled ornidazole, *Applied Radiation Isotopes*, **2000**, *53*, 3, 411-13.
3. Bicker U., Application of β -D-Glucuronides and Glucose Together Suggest A New Direction For Cancer Chemotherapy, *Nature*, **1974** *252*, 726-30.
4. Biber F. Z., Ünak P., Ertay T., Medine E. I., Zihnioglu F., Taşçı C., Durak H., Synthesis of an Estradiol Glucuronide Derivative and Investigation of its Radiopharmaceutical Potential, *Applied Radiation Isotopes*, **2006**, *64*, 7, 778-88.
5. Biber Muftuler F. Z., Unak P., Enginar H., Yolcular S., Yurt A., Acar Ç., Sakarya S., Synthesis, Radiolabelling and In Vivo Tissue Distribution of Anti Estrogen Glucuronide Compound: 99mTc-Toremifene-DTPA-Glucuronide, *Anticancer Research*, **2010**, *30*, 1243-9.
6. Biber Muftuler F. Z., Demir İ., Unak P., İçhedef Ç., Yurt Kilcar A., Bioavailability of 99mTc-paclitaxel-glucuronide (99mTc-PAC-G), *Radiochimica Acta*, **2011**, *99*, 5, 301-6.
7. Biber Muftuler F. Z., Unak P., İçhedef Ç., Demir İ., Synthesis of a Radioiodinated Antiestrogen Glucuronide Compound (Tam-G), *Journal of Radioanalytical and Nuclear Chemistry*, **2011**, *287*, 679-89.
8. Ediz M., Avcibasi U., Unak P., Muftuler Z., Medine I., Yurt Kilcar A., Demiroglu H., Gumuser F., Sakarya S., Investigation of Therapeutic Efficiency of Bleomycin and Bleomycin-Glucuronide Labeled with ^{131}I on the Cancer Cell Lines. *Cancer Biotherapy and Radiopharmaceuticals*, **2013**, *28*, 4, 310-9.
9. Enginar H., Ünak P., Biber Müftüler F. Z., Lambrecht F. Y., Medine E. İ., Yolcular S., Yurt A., Seyitoğlu B., Bulduk İ., Synthesis, Radiolabelling and In Vivo Tissue Distribution of Codeine Glucuronide, *INCS News*, **2009**, *6*, 2, 22, 46-56.
10. Ertay T., Ünak P., Tasci C., Biber F. Z., Zihnioglu F., Durak H., Scintigraphic imaging with a peptide glucuronide in rabbits: 99mTc- exorphin C glucuronide, *Applied Radiation Isotopes*, **2007**, *65*, 170-5.
11. Ertay T., Ünak P., Tasci C., Biber F. Z., Zihnioglu F., Medine E. İ., Durak H., 99mTc-Exorphin-glucuronide in tumor diagnosis: Preparation and Biodistribution Studies in Rats, *Journal of Radioanalytical and Nuclear Chemistry*, **2006**, *269*, 1, 21-8
12. Hafeli U.O., Sweeney S.M., Beresford B.A., Humm J.L., Macklis R.M., Effective Targeting of Magnetic Radioactive 90-Y-Microspheres to Tumor Cells by an Externally Applied Magnetic Field. Preliminary In Vitro and In Vivo Results, *Nuclear Medicine and Biology* **1995**, *22*, 2, 147-55.
13. Koçan F., Avcibaşı U., Ünak P., Biber Müftüler F. Z., İçhedef Ç. A., Demiroğlu H., Gümüşer F. G., Metabolic comparison of radiolabeled bleomycin (BLM) and bleomycin-glucuronide (BLMG) labeled with 99mTc, *Cancer Biotherapy and Radiopharmaceuticals*, **2011**, *26*, 5, 573-84.
14. Lubbe A. S., Alexiou C., Bergemann C., Clinical Applications of Magnetic Drug Targeting, *Journal of Surgical Research*, **2001**, *95*, 200-6.
15. Medine E. I., Unak P., Sakarya S., Toksöz F., Enzymatic Synthesis of Uracil Glucuronide, Labeling with $^{125/131}\text{I}$, and In vitro evaluation on Adenocarcinoma Cells, *Cancer Biotherapy & Radiopharmaceuticals*, **2010**, *25*, 3, 335-45.

16. Medine E. I., Unak P., Sakarya S., Ozkaya F., Investigation of in vitro efficiency of magnetic nanoparticle-conjugated ^{125}I -uracil glucuronides in adenocarcinoma cells, *Journal of Nanoparticle Research*, **2011**, *13*, 4703–15.
17. Miranda R. V. P. E., Pawar P., Gaikwad R. V. , Samad A., Jagtap A. G., Radiotracer Uptake Studies of Technetium Labeled Thymoquinone Using Gamma Scintigraphy Imaging Technique, *First AAPS-NUD-BCP-Regional Conference*, **2010**, *72*, 2, 272-5.
18. Mohapatra S., Mallick S.K., Skghosh T., Pramanik P., Synthesis of Highly Stable Folic Acid Conjugated Magnetite Nanoparticles for Targeting Cancer Cells, *Nanotechnology*, **2007**, *18*, 385102, 1-9.
19. Moritake S., Taira S., Ichianagi Y., Morone N., Song S., Hatanaka T., Yuasa S., Setou M., Functionalized Nano-Magnetic Particles For An In Vivo Delivery System, *Journal of Nanoscience And Nanotechnology*, **2007**, *7*, 3, 937-44.
20. Murdter T.E., Sperker B., Backman J. T., Friedel G., McClellan M., Fritz P. , Bossler K., Kromer H. K., Beta-Glucuronidase expression, activity, and localization of in human lung cancer: A base for drug targeting, *Naunyn-Schmiedebergs Archives of Pharmacology*, **1998**, *358*, 1, 2, R534- P4518,
21. Özdemir D., Ünak P., Study on Labeling conditions of ^{125}I -synkavit with iodogen method, *Journal of Radioanalytical and Nuclear Chemistry*, *187*, 4, 227-83, (1994).
22. Stachulski A. V., Meng X. L., Glucuronides from metabolites to medicines: a survey of the *in vivo* generation, chemical synthesis and properties of glucuronides, *Natural Product Reports*, **2013**, *30*, 6, 806-48,
23. Teksöz S., İchedef Ç. A., Özyüncü S., Biber Müftüler F. Z., Ünak P., Medine E. İ., Ertay T., Eren M. Ş., $^{99\text{mTc}}$ -D-Penicillamine-Glucuronide: Synthesis, Radiolabeling, In Vitro and in Vivo Evaluation, *Cancer Biotherapy and Radiopharmaceuticals*, **2011**, *26*, 5, 1-8.
24. Ünak P., Medine E. I., Sakarya S., Yürekli Y., Radyonüklid işaretli manyetik nanopartiküllerin sentezi ve terapötik potansiyellerinin hücre düzeyinde incelenmesi, (Tübitak projesi, 105S486), Nükleer Bilimler Enstitüsü, Ege Üniversitesi, (2008).
25. Ünak P., Radionuclide Labeled Glucuronide Prodrugs for Imaging and Targeting Therapy of Cancer, Ed: Gutierrez L. M., Neuro-Oncology and Cancer Targeted Therapy, *Cancer Etiology Diagnosis and Treatments*, **2010**, 239-48.
26. Ünak T., Ünak P., Direct Radioiodination of Metabolic 8-hydroxy-quinolyl-glucuronide, as a Potential Anti-Cancer Drug, *Applied Radiation Isotopes*, **1996**, *47*, 7, 645-7.
27. Ünak T., Ünak P., Ongun B., Synthesis and Iodine-125 Labelling of Glucuronide Compounds for Combined Chemo- and Radiotherapy of Cancer; *Applied Radiation Isotopes*, **1997**, *48*, 6, 777-83.
28. Woo C. C., Kumar A. P., Sethi G., Tan K. H., Thymoquinone: Potential cure for inflammatory disorders and cancer, *Biochemical Pharmacology* **2012**, *83*, 443-51.
29. Yeşilağaç R., Ünak P., Medine E. İ., İchedef Ç. A., Ertay T., Biber Müftüler F. Z., Enzymatical Synthesis of 8-Hydroxyquinoline Glucuronide, Labeling With ^{125}I , In Vitro Evaluation of Biological Influence on Cancer Cell Line, *Applied Radiation and Isotopes*, **2011**, *69*, 2, 299–307.
30. Yılmaz T., Unak P., Biber Muftuler F. Z., Medine E. I., Sakarya S., Acar İchedef C., Unak T., Diethylstilbestrol glucuronide (DESG): Synthesis, labeling with radioiodine and in vivo/in vitro evaluations, *Journal of Radioanalytical Nuclear Chemistry*, **2013**, *295*, 1395–1404.

The Effects of Maternal Omega-3 Fatty Acid Supplementation on Breast Milk Fatty Acid Composition

Ezgi Ay¹, Nihal Büyükuşlu^{1*}, Saime Batirel², Havvanur Yoldaş İlktaç³,
Muazzez Garipağaoğlu⁴

¹Department of Nutrition and Dietetics, School of Health Sciences, Istanbul Medipol University, Istanbul, Turkey.

²Department of Medical Biochemistry, Faculty of Medicine, Marmara University, Istanbul, Turkey.

³Department of Nutrition and Dietetics, School of Health Sciences, Istanbul Medeniyet University, Istanbul, Turkey.

⁴Department of Nutrition and Dietetics, School of Health Sciences, Fenerbahçe University, Istanbul, Turkey.

ABSTRACT

Breast milk is the first source of omega-3 fatty acids (FA) for infants. We hypothesized that maternal omega-3 FAs supplementation affects the FA composition of breast milk. Thirty-six women received 950 mg omega-3 polyunsaturated (PUFA) supplementation per day for 9 months from 22-24 weeks of pregnancy until the 6 months of lactation and 26 women were enrolled as controls. Demographic data and nutritional status were taken by a questionnaire. Breast milk samples were collected at just after birth and 6 months of lactation. Fatty acids were analyzed by gas chromatography mass spectrometry (GC-MS). Data was assessed using SPSS 22.0 software. The supplementation increased the level of docosahexaenoic acid (DHA) and eicosapentaenoic acid (EPA) while decreased the level of saturated fatty acids (SFA) in breast milk. The ratio of omega-6/omega-3 FAs was also decreased in the supplemented mothers' milk. In conclusion the maternal supplementation of omega-3 FAs improved the DHA and EPA levels.

Keywords: Docosahexaenoic acid (DHA); eicosapentaenoic acid (EPA); omega-3 fatty acids; omega supplement; breast milk.

INTRODUCTION

The lipid content of mature breast milk is 3.2-4.8%.¹ This amount of lipid provides approximately 40-50% of daily energy demand for infants. Nutritional status of mother is one of the major factors that affects the milk content.² There is a correlation between carbohydrate intake of mothers and fat content in breast milk.³ Diet rich in carbohydrates results in higher levels of saturated fatty acids.⁴ In addition, there are several studies showed the association between mother's diet and breast milk fat content.⁵⁻⁸

*Corresponding author: Nihal Büyükuşlu, e-mail: nbuyukuslu@medipol.edu.tr
(Received 22 January 2018, accepted 03 March 2018)

Human breast milk has the ideal composition for feeding infants to meet all necessary nutrients for growth and development. The fatty acid composition of breast milk varied in the mothers from different countries all around the world. For instance, milk samples from Spanish mothers contain high monounsaturated fatty acids (MUFAs) ($39.63 \pm 3.57\%$).⁹ On the other hand, milk samples from Nigerian mothers contain high saturated fatty acids (SFAs) (54.07%).¹⁰ In the mothers from Kenya the percentage of the SFAs ($\sim 16\%$) was significantly lower than the percent of the unsaturated fatty acids in breast milk.¹¹

Long chain polyunsaturated fatty acids (LC-PUFAs) contain two principal families: omega-6 PUFAs including linoleic acid (LA, 18:2n6), arachidonic acid (AA, 22:4n6), and omega-3 PUFAs including alpha linolenic acid (ALA, 18:3n3), eicosapentaenoic acid (EPA, 20:5n3), docosapentaenoic acid (DPA, 22:5n3) and docosahexaenoic acid (DHA, 22:6n3). LC-PUFAs are essential for normal neonatal mammalian development. Breast milk is the unique source of the LC-PUFAs for breastfed infants. The levels of DHA, EPA and AA are elevated in fetus brain and associated with the development of the central nervous and visual systems.^{12,13} The level of DHA in breast milk varies between 0.06% to 1.4% of total fatty acids with a mean of $0.32 \pm 0.22\%$ worldwide average.¹⁴ In a comparative study, it was shown that the DHA levels were $0.67 \pm 0.32\%$ in Asia (excluding China), $0.37 \pm 0.15\%$ in China, $0.34 \pm 0.14\%$ in Europe, $0.32 \pm 0.30\%$ in Africa and the lowest in America ($0.20 \pm 0.11\%$).¹⁵ The amount of DHA in the breast milk of the women who had high fish intake was higher than the ones who consumed less fish. The DHA levels in the milk of women from Surinam, St Lucia, Malaysia, Dominica and Curacao were found higher than the western style diet such as in USA and many European countries.¹⁶⁻²⁰

Since omega-3 FAs can only be obtained from the diet, the omega-3 rich foods and supplements should be advised to women during pregnancy and lactation. The major sources of omega-3 FAs are fish, flaxseed, canola and soybean oils. However, overconsumption of certain fish may cause high mercury intake and can cause toxicity.²¹ Therefore omega-3 FAs from vegetable sources and the supplements containing DHA and EPA are recommended to the mothers.^{22,23} The daily recommended DHA intake is an average of ≥ 200 mg/day in pregnancy and lactation.²⁴ We previously studied the impact of DHA+EPA supplementation during the last trimester of pregnancy and found an increase in cord blood.²⁵ We extended the study to investigate the further effect of omega-3 supplement in lactation for 6 months and hypothesized that maternal supplementation would enhance breast milk fatty acid composition. To our knowledge this is the first study to cover both pregnancy and lactation for a long term (nine months) omega-3 FA supplementation.

METHODOLOGY

Study population and design

This experimental study was conducted on 62 healthy, singleton voluntary pregnant women between September 2015 and December 2016 in Istanbul, Turkey. The mothers were informed about the study at 22-24 weeks of pregnancy during routine prenatal care visits in the hospital. Among the interviewees thirty-six pregnant women accepted to take the supplement daily during the last trimester of pregnancy and the 6 month of lactation period and this group was named as omega-3 group. Twenty-six women participated in the study without taking supplementation and this group was named as control group. They were asked to sign an informed consent form and to answer the questions in a survey including the demographic and anthropometric data, daily energy and fat consumption. Breast milk samples were taken twice: just after birth and 6 months of lactation. The pregnant women who gave preterm birth and had a history of chronic diseases and/or consumed omega-3 fatty acid supplements were excluded. Six to 10 mL of breast milk samples were collected from each subject in the morning between 9.00 and 11.00 am. The samples immediately were carried to the laboratory in an ice-cold package, filled in vials and stored at $-80\text{ }^{\circ}\text{C}$ until analysis.

All procedures and protocols received prior approval by the Istanbul Medipol University Ethics and Research Committee.

Supplementation

The participants were assigned to receive a softgel capsule/day as the supplement (Martek Biosciences Corporation, Solgar, Leonia, NJ, USA), starting from last trimester to the end of 6th month of lactation. One capsule provides 378 mg docosahexaenoic acid (DHA) and 504 mg eicosapentaenoic acid (EPA) in total 950 mg omega-3 PUFA. Control group had no supplement or placebo. No dietary instructions were given to both groups.

Analysis of fatty acids

The milk samples were thawed and lipids were extracted according to Bligh and Dyer method.²⁶ Fatty acid composition of extracted lipids was determined by conversion into fatty acid methyl esters (FAME). Trans-methylation was performed in methanolic-HCl (0.5 N) at $80\text{ }^{\circ}\text{C}$. The FAME were separated and analyzed by gas chromatography - mass spectrometry (GC-MS) (Shimadzu QP-2010, Kyoto, Japan). Thirty meters of fused-silica capillary column was used. Standardization was performed using a standard mixture involving 37 fatty acids. Their retention times were recorded and fatty acid library was maintained. Chromatograms were analysed in terms of % by weight of total fatty acids.

Statistical analyses

Statistical Package for Social Sciences version 22.0 (SPSS, Chicago, IL, USA) was used for statistical analyses. The results were presented as mean \pm SD. The Student's t test was applied for paired and independent values and their nonparametric equivalent to evaluate significant differences. Pearson coefficient of correlation was used to analyze relationships between numerical variables. Statistically significance accepted as the level of $p < 0.05$. Considering a 0.05 two-sided significance level and large effect size (0.80), the power was 0.80.

RESULTS

The baseline characteristics and nutritional status of the mothers

The demographic characteristics of mothers were shown in Table 1. The mean ages of women in omega-3 group and control group were 31.8 ± 4.3 years and 30.4 ± 3.9 years respectively. BMI values of women at pre-pregnancy were 22.9 ± 3.1 kg/m² (omega-3 group, n=36) and 23.0 ± 2.5 kg/m² (control group, n=26). There was no significance for each parameter indicating the homogeneity of the pregnant participants in the study.

Table 1. Demographic characteristics of women*

	Control group	Omega-3 group	P
N	26	36	
Age (year)	30.4 ± 3.9	31.8 ± 4.3	0.168
Pre-pregnancy BMI (kg/m ²)	23.0 ± 2.5	22.9 ± 3.1	0.550

*Data recorded at 22-24 weeks of pregnancy

During lactation period, the daily energy and fat intake was recorded once at the 3rd month and results were shown in Table 2. The comparison of two groups revealed no significance in the daily intake of energy, carbohydrate, protein and fat. There were no significant differences in daily MUFA and PUFA intakes between two groups ($p < 0.05$) but the daily SFA intake was found significantly different ($p > 0.05$).

Table 2. Daily energy and fat intakes at the 3rd month of lactation

	Control group	Omega-3 group	P
Energy (kcal)	1789.0±439.1	1804.7±614.7	0.865
Fat (g)	80.1±24.7	86.0±33.1	0.594
Fat (%)	41.3±7.7	42.6±5.7	0.515
SFA (g)	27.5±7.4	33.5±12.4	0.038*
MUFA (g)	30.0±11	32.7±13.9	0.541
PUFA (g)	16.2±9.3	13.6±9.1	0.234

*Statistical significance at $p < 0.05$ level

Fatty acid distribution in breast milk

The effect of omega-3 supplementation during pregnancy and lactation on FA composition of breast milk was demonstrated in Table 3. The omega-3 FA supplementation decreased total SFA in colostrum and mature milk. However, the only significant difference was in mature milk ($p < 0.05$). Total MUFAs was higher in colostrum but slightly lower in mature milk at 6 months with no significance in omega-3 supplemented group. Total PUFAs were increased in both milk sampling occasions. The only significant difference was in colostrum ($p < 0.05$).

Table 3. Fatty acid composition of mothers' milk

	Colostrum			Mature milk (6 months)		
	Control group (n=26)	Omega-3 group (n=28)	P	Control group (n=18)	Omega-3 group (n=26)	P
Total SFA	44.84±3.93	43.15±6.27	0.059	44.42±4.72	41.50±6.25	0.038*
Total MUFA	35.21±3.40	36.52±6.43	0.144	35.34±1.71	35.25±4.16	0.148
Total PUFA	19.08±3.56	21.35±4.66	0.047*	20.20±4.66	22.46±5.41	0.080
Total omega-3	1.32±0.32	1.58±0.38	0.083	1.26±0.31	1.65±0.71	0.142
DHA 22:6n3	0.36±0.10	0.51±0.18	0.000**	0.22±0.10	0.31±0.23	0.000**
EPA 20:5n3	0.09±0.04	0.16±0.07	0.000**	0.08±0.03	0.14±0.08	0.232
Total omega-6	17.80±3.59	19.77±4.52	0.034*	18.93±4.69	20.81±5.26	0.094
Omega-6/ Omega-3	14.31±4.72	12.97±3.62	0.723	16.32±8.13	13.79±4.16	0.872

The fatty acids were given % by weight of total fats

*Statistical significance at $p < 0.05$ level; ** Statistical significance at $p < 0.000$ level

Total omega-3 FAs levels were higher in colostrum and 6th month milk. Among omega-3 FAs the levels of DHA and EPA were significantly increased in colostrum. Both DHA and EPA levels in mature milk at 6 months were higher in supplemented groups with the only significance at DHA level. The levels of total omega-6 FAs were higher in colostrum ($p < 0.05$) and mature milk ($p > 0.05$) samples from supplemented mothers.

The ratio of omega-6 FAs to omega-3 FAs was lower in colostrum and at 6 months from supplemented mothers. The omega-6/omega-3 ratios in both colostrum and 6th month samples were lower in the supplemented mother milks. None of the differences were significant.

The levels of DHA and EPA in breast milk

Omega-3 supplementation increased the levels of DHA and EPA in both colostrum and mature milk. The differences between control and supplemented groups were significant for DHA levels for colostrum ($p < 0.001$) and mature milk ($p < 0.001$) but EPA levels were significant in colostrum ($p < 0.001$) but not in mature milk ($p > 0.05$). The total omega-6 FAs of supplemented mothers were higher in colostrum ($p < 0.05$) and mature milk ($p > 0.05$) than the control mothers had. The rate of omega-6 to omega-3 was affected by the omega-3 FAs supplementation. The ratios decreased in colostrum (from 14.31 ± 4.72 to 12.97 ± 3.62) and at 6th months milk (from 16.32 ± 8.13 to 13.79 ± 4.16) depending on the increased amounts of omega-3 FAs indicating the beneficial influence of maternal omega-3 supplementation on omega-3 FAs quality of mother milk.

DISCUSSION

This study was designed to compare the levels of fatty acids in breast milk samples between control and omega supplemented groups during the last trimester of their pregnancy and 6 months of lactation period. Within our knowledge this is the longest omega-3 supplementation for mothers during lactation.²⁷ There are several studies indicate that the composition of fatty acids in breast milk changes through the lactation period. The content of human milk is affected by nutritional habits, cultural and social differences, maternal and environmental factors.¹ A study on the prediction of cognitive test performance associated with the fatty acid content included the level of fatty acids in different countries. In mentioned study, the mean levels of fatty acids were $43.32 \pm 9.56\%$ SFAs (33 countries), $35.69 \pm 6.45\%$ MUFAs (34 countries), $14.53 \pm 3.82\%$ PUFAs (33 countries) and $0.73 \pm 0.38\%$ LC omega-3 FAs (30 countries). The concentrations of omega-3 fatty acids were reported as $0.38 \pm 0.23\%$ DHA (50 countries), $0.19 \pm 0.09\%$ DPA (33 countries) and $0.13 \pm 0.09\%$ EPA (36 countries).²⁸ As the content of breast milk is highly related to mother's diet, daily intake of DHA-rich

foods as much as foods containing industrial trans fatty acid, supplements, processed foods and meats would be the major indicators of the distribution of fatty acids in milk.²⁹ The FAs composition of mature breast milk of Israeli women was analysed and it was found that the contents of total SFAs, total MUFAs and total PUFAs were $42\pm 7\%$, $33\pm 5\%$ and $24\pm 4\%$ of total FAs respectively.³⁰ In a study on Turkish women, Aydın et al. showed higher level of SFA in total FAs of breast milk (46.57% at 7 days, 51.56% at 28 days of lactation) than predicted in the control group of current study ($44.84\pm 3.93\%$ in colostrum and $44.42\pm 4.72\%$ at 15 days of lactation).³¹ Omega-3 supplementation further reduced the values. The fluctuations between the fatty acid levels in different countries might arise from the cultural habits, regional and seasonal differences in nutritional behaviours. In a study by Lopez-Lopez the omega-6/omega-3 FAs ratios in breast milk of Spanish women were very similar the ratios in our study.⁹ This similarity may reflect the Mediterranean style nutrition in both Spain and Turkey.

Linoleic acid and ALA are the precursors of LC-PUFAs. The conversion of these precursors into AA, EPA and DHA is low.^{32,33} As the beneficial effects of omega-3 fatty acids for infant development are inevitable, any touch to increase omega-3 FAs level in breast milk is appreciable. The reported average concentration of DHA in human milk Worldwide is $0.32\pm 0.22\%$. In the current study, Turkish women had the level of DHA min. $0.22\pm 0.10\%$ (6th month) and max. 0.36 ± 0.10 (colostrum). After DHA+EPA supplementation during pregnancy and lactation the levels increased to 0.31 ± 0.23 (6th month) and 0.51 ± 0.18 (colostrum).

There are several studies which demonstrate that omega-3 supplementation to mothers during lactation may influence its concentration in human breast milk. Bortolozza et al measured the DHA and EPA levels after a daily supplementation with fish oil capsules that corresponded to a daily intake of 315 mg of DHA and 80 mg of EPA during the third trimester of pregnancy and the first three months postpartum. They found that the milk of women taking fish oil had higher DHA levels after delivery (0.324% at 30th day, 0.207% at 90th day) comparing with the DHA levels of control mothers' milk (0.104% at 30th day, 0.030% at 90th day). The EPA levels at 30 and 90 days were 0.109% and 0.107% in omega group and 0.084% and 0.050% in control group in the same study.³⁴ Smit et al investigated that DHA status of malnourished children was strongly dependent on the omega-3 fatty acid intake from breast milk.³⁵ In the present study, we also found an increase of DHA and EPA levels in colostrum and in mature milk samples from the supplemented mothers. In colostrum, the DHA and EPA differences between the groups were statistically significant at the level of $p=0.000$ indicating the improving effect of the omega fatty acid supplementation on the amount of DHA and EPA in human milk. In addition, it was observed that supplementation had

more influence on colostrum than mature milk at 6 months. The rise in omega-3 fatty acids is beneficial in case of the aid in development of infant. Similarly, Jensen et al determined that DHA supplementation (170-260 mg/day) of breastfeeding mothers increased the DHA contents of breast milk. They also found the strong positive correlations between maternal plasma-phospholipid DHA and EPA and the contents of these fatty acids in breast milk supporting the idea that of supplementation of lactating women with DHA might be the most reliable means of increasing breast-milk DHA.³⁶ The effects of DHA supplementation on the fatty acid composition of breast milk in lactating women were investigated in a study by Sherry et al. They found that saturated fatty acids were the most abundant in breast milk at baseline. After low (200 mg/day) and high dose (400 mg/day) of DHA supplementation for 6 weeks, the level of DHA in breast milk was significantly higher compared with placebo. The levels of DHA were elevated from $6.98 \pm 0.94\%$ to $8.83 \pm 1.03\%$ for low dose and from $5.14 \pm 0.51\%$ to $13.08 \pm 1.69\%$ for high dose supplementation.³⁷ The results support our findings that DHA supplementation in lactation period increase the DHA level and decrease SFAs in breast milk. Moreover, Much et al reported that the DHA levels at 6th and 16th weeks postpartum were $0.28 \pm 0.14\%$ and $0.24 \pm 0.13\%$ respectively. After diet intervention, they increased to $1.34 \pm 0.67\%$ and $1.12 \pm 0.39\%$ pointing out the efficiency of DHA supplementation specifically at early times of lactation in a similarity to our results.³⁸

In our daily life, the consumption of n-6 fatty acids are increased compared to the traditional diet due to widely used industrially processed fat.³⁹ We defined that the ratios of omega-6/omega-3 were between 10.7 and 14.2 for omega supplemented mothers and between 11.9 and 15.0 for control mothers. That means that the supplementation of omega-3 FAs lowers the ratio of omega-6 to omega-3 FAs in the breast milk in comparison with control mothers.

This study has some limitations. The numbers of mothers for each group were not equal because of elimination of mothers for several reasons such as being away from city, diseases of mothers or babies at one or more stages of the study. The questionnaire used for evaluation of demographic and nutritional status was based on self-report. The nutritional status was reported once at 3rd month of lactation. Omega-3 supplementation was voluntarily performed. Although there were a good correlation between the numbers of the supplement packages and the days that the mothers took the supplements, nine months period was quite long time for mothers to follow daily requirements for supplement. However, all participants verbally declared that they took one capsule omega in a day.

In conclusion, the supplementation of omega-3 FAs for nine months starting from the beginning of the last trimester to the 6th month of lactation improves the DHA and EPA levels significantly in colostrum and the mature milk and decreases the ratio of omega-6/omega-3 FAs and saturated fatty acid concentrations of breast milk. Further studies need to be proceeded on the factors affecting FAs composition of breast milk for omega-3 supplemented mothers and optimize the concentration of omega-3 FAs intaken during lactation for better development of infants.

CONFLICT OF INTEREST

The authors declare no conflict of interest.

REFERENCES

1. Ballard, O.; Morrow, A.L. Human milk composition: Nutrients and bioactive factors. *Pediatr. Clin. North. Am.* **2013**, *60*, 49-74.
2. Martin, M.A.; Lassek, W.D.; Gaulin, S.J.C.; Evans, R.W.; Woo, J.G.; Geraghty, S.R.; et al., Fatty acid composition in the mature milk of Bolivian forager-horticulturalists: Controlled comparisons with a US sample. *Matern. Child Nutr.* **2012**, *8*, 404-418.
3. Nikniaz, L.; Mahdavi, R.; Arefhosesseini, S.R.; Khiabani, M. S. Association between fat content of breast milk and maternal nutritional status and infants' weight in Tabriz. *Iran. Malays. J. Nutr.* **2009**, *15*, 37-44.
4. Delplanque, B.; Gibson, R.; Koletzko, B.; Lapillonne, A.; Strandvik, B. Lipid quality in infant nutrition: Current knowledge and future opportunities. *J. Pediatr. Gastroenterol. Nutr. Discipline.* **2015**, *61*, 8-17.
5. Kelishadi, R.; Hadi, B.; Iranpour, R.; Khosravi-Darani, K.; Mirmoghtadaee, P.; Farajian S. et al., A study on lipid content and fatty acid of breast milk and its association with mother's diet composition. *J. Res. Med. Sci.* **2012**, *9*, 824-827.
6. Villalpando, S.; del Prado, M. Interrelation among dietary energy and fat intake, maternal body fatness and milk total lipids in humans. *J. Mammary Gland. Biol. Neoplasia.* **1999**, *4*, 285-295.
7. Peng, Y.; Zhou, T.; Wang, Q.; Liu, P.; Zhang, T.; Zetterström, R. et al., Fatty acid composition of diet, cord blood and breast milk in Chinese mothers with different dietary habits. *PLEFA*, **2009**, *81*, 325-330.
8. Michaelsen, K.F.; Larsen, P.S.; Thomsen, B.L.; Samuelson, G. The Copenhagen cohort study on infant nutrition and growth: Breast-milk intake, human milk macronutrient content, and influencing factors. *Am. J. Clin. Nutr.* **1994**, *59*, 600-611.
9. Lopez-Lopez, A.; Lopez-Sabater, M.C.; Campoy-Folgozo, C.; Rivero-Urgell, M.; Castellote-Bargallo, A.I. Fatty acid and sn-2 fatty acid composition in human milk from Granada (Spain) and in infant formulas. *Eur. J. Clin. Nutr.* **2002**, *56*, 1242-1254.
10. Koletzko, B.; Thiel, I.; Abiodun, P.O. Fatty acid composition of mature human milk in Nigeria. *Zernahrungwiss.* **1991**, *30*, 289-297.

11. Kiprop, J.V.; Girard, A.W.; Gogo, L.A.; Omwamba, M.N.; Mahungu, S. M. Determination of the fatty acid profile of breast milk from nursing mothers in Bungoma County, Kenya. *Food Nutr. Sci.* **2016**, *7*, 661-670.
12. Bernardi, J.R.; Escobar, R.S.; Ferreira, C.F.; Silveira, P.P. Fetal and neonatal levels of omega-3: Effects on neurodevelopment, nutrition, and growth. *Scientific World Journal.* **2012**, *2012*: 202473.
13. Lauritzen, L.; Brambilla, P.; Mazzocchi, A.; Harslof, L.B.; Ciappolino, V.; Agostoni, C. DHA effects in brain development and function. *Nutrients* **2016**, *8*, 6. doi:10.3390/nu8010006.
14. Brenna, J.T.; Varamini, B.; Jensen, R.G.; Diersen-Schade, D.A.; Boettcher, J.A.; Arterburn, L.M. Docosahexaenoic and arachidonic acid concentrations in human breast milk worldwide. *Am. J. Clin. Nutr.* **2007**, *85*, 1457-1464.
15. Li, S.Y.; Dong, X.L.; Wong, W.S.V.; Su, Y.X.; Wong, M.S. Long-chain polyunsaturated fatty acid concentrations in breast milk from Chinese mothers: Comparison with other regions. *Int. J. Child Health Nutr.* **2015**, *4*, 230-239.
16. Muskiet, F.A.; Hutter, N.H.; Martini, I.A.; Jonxis, J.H.; Offringa, P.J.; Boersma, E.R. Comparison of the fatty acid composition of human milk from mothers in Tanzania, Curacao and Surinam. *Hum. Nutr. Clin. Nutr.* **1987**, *41*, 149-159.
17. Boersma, E.R.; Offringa, P.J.; Muskiet, F.A.; Chase, W.M.; Simmons, I.J. Vitamin E, lipid fractions, and fatty acid composition of colostrum, transitional milk, and mature milk: an international comparative study. *Am. J. Clin. Nutr.* **1991**, *53*, 1197-1204.
18. Kneebone, G.M.; Kneebone, R.; Gibson, R.A. Fatty acid composition of breast milk from three racial groups from Penang, Malaysia. *Am. J. Clin. Nutr.* **1985**, *41*, 765-769.
19. Koletzko, B.; Thiel, I.; Abiodun, P.O. The fatty acid composition of human milk in Europe and Africa. *J. Pediatr.* **1992**, *120*, S62-70.
20. Salamon, Sz.; Csapo, J. Composition of the mother's milk II. Fat contents, fatty acid composition. A review. *Acta Univ. Sapientiae, Alimentaria.* **2009**, *2*, 196-234.
21. WHO, Preventing disease through healthy environments. Exposure to mercury: A major public health concern. **2007**. Geneva, *World Health Organization*.
22. Coletta, J.M.; Bell, S.J.; Roman, A.S. Omega-3 fatty acids and pregnancy. *Rev. Obstet. Gynecol.* **2010**, *3*, 163-171.
23. Greenberg, J.A.; Bell, S.J.; Van Ausdal, W. Omega-3 fatty acid supplementation during pregnancy. *Rev. Obstet. Gynecol.* **2008**, *1*, 162-169.
24. FAO, Fats and fatty acids in human nutrition. Report of an expert consultation. *FAO Food Nutr. Pap.* **2008**, *91*, 63-76.
25. Büyükkuslu, N.; Ovalı, S.; Altuntaş, Ş.L.; Batrel, S.; Yiğit, P.; Garipağaoğlu, M. Supplementation of docosahexaenoic acid (DHA) / Eicosapentaenoic acid (EPA) in a ratio of 1 / 1.3 during last trimester of pregnancy results in EPA accumulation in cord blood. *PLEFA.* **2017**, *125*(1), 32-36.
26. Blich, E.G.; Dyer, W.J. A rapid method of total lipid extraction and purification. *Can. J. Biochem. Physiol.* **1959**, *37*, 911-917.
27. Li G, Chen H, Zhang W, Tong Q, Yan Y. Effects of maternal omega-3 fatty acids supplementation during pregnancy/lactation on body composition of the offspring: A systematic review and meta-analysis. *Clin.Nutr.* **2017**, 1-12.

28. Lassek, W.D.; Gaulin, S.J.C. Linoleic and docosahexaenoic acids in human milk have opposite relationships with cognitive test performance in a sample of 28 countries. *PLEFA*. **2014**, *91*, 195-201.
29. Bradbury, J. Docosahexaenoic Acid (DHA): An ancient nutrient for the modern human brain. *Nutrients*. **2011**, *3*, 529-554.
30. Saphier, O.; Blumenfeld, J.; Silberstein, T.; Tzor, T.; Burg, A. Fatty acid composition of breastmilk of Israeli mothers. *Indian Pediatr*. **2013**, *50*, 1044-1046.
31. Aydın, I.; Turan, O.; Aydın, F.N.; Koç, E.; Hirfanoğlu, I.M.; Akyol, M. et al., Comparing the fatty acid levels of preterm and term breast milk in Turkish women. *Turk J. Med. Sci*. **2014**, *44*, 305-310.
32. Burdge, G.C.; Jones, A.E.; Wootton, S.A. Eicosapentaenoic and docosapentaenoic acids are the principal products of α -linolenic acid metabolism in young men. *Br. J. Nutr*. **2002**, *88*, 355-364.
33. Burdge, G.C.; Wootton, S.A. Conversion of α -linolenic acid to eicosapentaenoic, docosapentaenoic and docosahexaenoic acids in young women. *Br. J. Nutr*. **2002**, *88*, 411-420.
34. Bortolozzo, E.A.F.Q.; E. Sauer, Supplementation with the omega-3 docosahexaenoic acid: Influence on the lipid composition and fatty acid profile of human milk. *Rev. Nutr. Campinas*. **2013**, *26*, 27-36.
35. Smit, E.N.; Oelen, E.A.; Seerat, E.; Muskiet, F.A.J.; Boersma, E.R. Breast milk docosahexaenoic acid (DHA) correlates with DHA status of malnourished infants. *Arch. Dis. Child*. **2000**, *82*, 493-494.
36. Jensen, C.L.; Maude, M.; Anderson, R.E.; Heird, W.C. Effect of docosahexaenoic acid supplementation of lactating women on the fatty acid composition of breast milk lipids and maternal and infant plasma phospholipids. *Am. J. Clin. Nutr*. **2000**, *71*, 292S-299S.
37. Sherry, C.L.; Oliver, J.S.; Marriage, B.J. Docosahexaenoic acid supplementation in lactating women increases breast milk and plasma docosahexaenoic acid concentrations and alters infant omega 6:3 fatty acid ratio. *PLEFA*. **2015**, *95*, 63-69.
38. Much, D.; Brunner, S.; Vollhardt, C.; Schmid, D.; Sedlmeier, E.M.; Bruder, M. et al. Breast milk fatty acid profile in relation to infant growth and body composition: results from the INFAT study. *Pediatr. Res*. **2013**, *74*, 230-237.
39. Simopoulos, A. P. An increase in the omega-6/omega-3 fatty acid ratio increases the risk for obesity. *Nutrients*. **2016**, *8*, 128-145.



IN VITRO FERTILIZATION AND REPRODUCTIVE HEALTH CENTER

The end of longing...

We promise outstanding success rate in IVF treatment owing to increasing knowledge and advanced technologies.

Keep in mind,
Infertility,
Polycystic Ovary Syndrome,
Endometriosis,
Ovulation Problem,
Tubal factor and
Sperm related problems
are not irremediable.



Synthesis, characterization and evaluation of antifungal activity of seven-membered heterocycles

Rasim Farraj Muslim^{1*}, Hiba Mahir Tawfeeq², Mustafa Nadhim Owaied³ Obaid Hasan Abid⁴

¹Department of Ecology, College of Applied Sciences, University of Anbar, Hit 31007, Anbar, Iraq

²Department of Chemistry, College of Education for Pure Sciences, Ramadi 31001, University of Anbar, Anbar, Iraq

³Department of Heet Education, General Directorate of Education in Anbar, Ministry of Education, Hit, Anbar 31007, Iraq

⁴Department of Scientific Affairs and Graduate Studies, University of Fallujah, Anbar, Iraq

ABSTRACT

This research includes synthesis of new heterocyclic derivatives of disubstituted 1,3-oxazepine-5-one. Azomethine compounds (N1-N5) were synthesized by the reaction of aromatic aldehydes with primary aromatic amines, in the presence of glacial acetic acid as a catalyst in absolute ethanol. The synthesized compounds were identified via spectral methods viz., FT-IR, ¹H-NMR, and ¹³C-NMR and measurements of some physical properties. The prepared oxazepine compounds (N6-N10) were obtained from treatment of azomethine compounds with phthalide. N9 and N7 derivatives have recorded the higher zone of inhibition 15 mm against *Candida guilliermondii* and *Candida zeylanoides* respectively. The lower zone of inhibition was 8.0 mm and 9.3 mm by N7 toward the growth of *Candida albicans* and *Candida guilliermondii* respectively. Slight variation in the structure of those derivatives can show the very dramatic effect on the efficiency of these compounds in their bio-activity and may be helpful in designing more antifungal agents for therapeutic use in future.

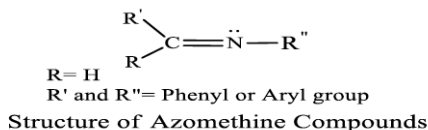
Keywords: Azomethine, anti-candidal activity, NMR, phthalide, oxazepine.

INTRODUCTION

Azomethine compounds are class of compounds containing the group (C=N) (Scheme 1), usually prepared by the condensation of a primary aromatic amino group with an active carbonyl aromatic aldehyde. They are versatile precursors in the synthesis of organic, bio-organic, organometallic and industrial compounds via ring closure, cycloaddition, and replacement reactions.¹⁻³

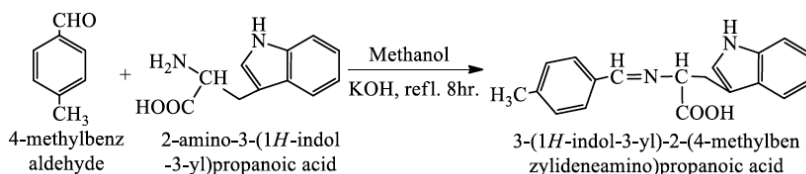
*Corresponding author: Rasim Farraj Muslim, e-mail: dr.rasim92hmts@gmail.com
(Received 13 February 2018, accepted 03 March 2018)

A German chemist discovered azomethine compounds, Nobel Prize winner, Hugo Schiff in 1864⁴, and structurally, an analog of a ketone or aldehyde in which azomethine group has replaced the carbonyl group (C=O), as shown in Scheme 1.⁵



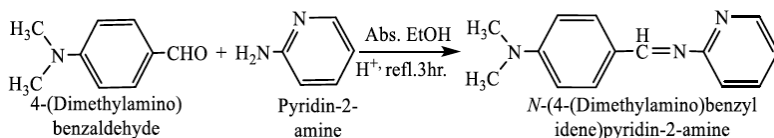
Scheme 1. Structure of azomethine compounds

Initially, the classical synthetic route for azomethine compounds involves condensation of ammonia, primary amines and amino acids with carbonyl compounds under azeotropic distillation with the simultaneous removal of water⁶⁻⁸, see Scheme 2.



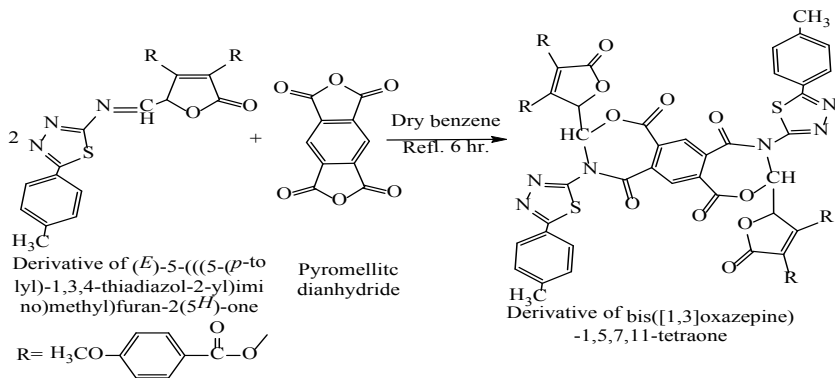
Scheme 2. The effect of KOH on azomethine synthesis

The reaction of pyridine-2-amine with 4-(dimethylamino) benzaldehyde produces the azomethine compound (Scheme 3).⁹



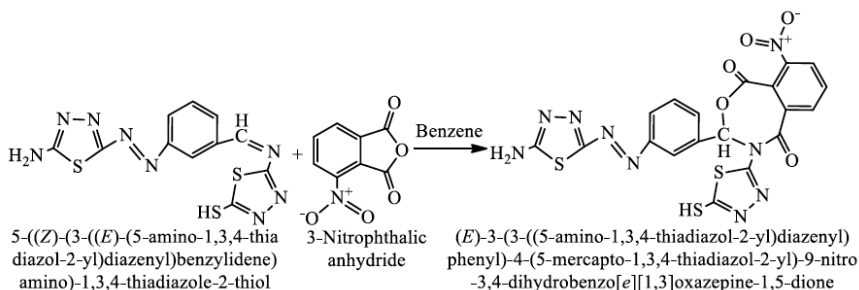
Scheme 3 The prepared azomethine compound presence glacial acetic acid

Oxazepines are class of heterocyclic compounds of the seven-membered ring with two heteroatoms (O and N). The oxygen atom is located at position 1 and a nitrogen atom in positions -2,-3 or -4. Example of one of oxazepine compound is the product of the reaction between azomethine compounds and pyromellitic dianhydride (Scheme 4).¹⁰



Scheme 4 Using dry benzene as a solvent to prepare oxazepine derivatives

Reaction of azomethine compound (2-Amino-1,3,4 -thiadiazole-5-thiol) with 3-Nitrophthalic anhydride gave oxazepine compounds in efficient yields, see Scheme 5.¹¹



Scheme 5 Effect of nitro group on product efficiency of the prepared oxazepine compound

The aim of this work is preparing azomethine compounds from aromatic aldehyde reaction with primary aromatic amines to interfere with the preparation of oxazepine compounds from the reaction of azomethine compounds prepared with phthalide compound. Oxazepine compounds were tested against some pathogenic yeasts *in vitro*.

METHODOLOGY

Melting points were recorded on Electrothermal Melting point Apparatus (uncorrected). FT-IR spectra were recorded at room temperature from 4000-400 cm⁻¹ with KBr disc on Infrared Spectrophotometer Model Tensor 27 Bruker Co., Germany. The ¹H-NMR and ¹³C-NMR spectra were recorded on Bruker Ac-300MHz spectrometer.

General Procedure for synthesis of azomethine compounds N₁-N₅

Equimolar mixtures 0.02 mol of aldehydes and aromatic amines and trace of glacial acetic acid dissolved in 25 ml absolute ethanol was placed in a 100-ml round-bottom flask equipped with condenser and stirrer bar. The mixture was allowed to react at reflux temperature for 4 hour, and then let to cool down to the room temperature, whereby a crystalline solid was separated out. The solid product was recrystallized twice from ethanol. The structural formula, names, melting points, colors, and percentage of yields for the synthesized azomethine compounds are recorded.¹²⁻¹⁹

General procedure for synthesis of oxazepine compounds N₆-N₁₀

Equimolar mixtures 0.01 mol of azomethine compounds and phthalide compound dissolved in 30 ml of tetrahydrofuran was placed in a 100-ml round-bottom flask equipped with condenser and stirrer bar presence trace of glacial acetic acid as a catalyst was added. The reaction mixture was refluxed for 3 hour, and left to stand for 24 hour and then solid product was precipitated. The solid product was filtered off and recrystallized from ethanol. The structural formula, names, melting points, colors, and percentage of yields for the prepared oxazepine compounds are recorded.²⁰⁻²⁵

Antifungal activity

This test was archived *in vitro* to investigate inhibitory effects of the prepared oxazepine compounds using well diffusion method on Muller-Hinton agar. This experiment was done as mentioned by Owaied et al. Four milligrams of the prepared oxazepine compounds were dissolved in absolute methanol and applied separately in 6 mm-well, while methanol was used as a control.²⁶ After 18 hr of incubation at 37 °C, the zone of inhibition was taken using the ruler in millimeters.

RESULTS AND DISCUSSION

Tables 1 and 2 exhibited structural formula, nomenclature, the percentage of yield, melting point, and their color. The best yield of the prepared azomethine compounds was 90% for compounds N₃ and N₄ while the lower yield was 80% for compounds N₂. The higher melting point was 250-252 °C for compound N₂. The lower melting point was 60-62 °C for compound N₁. The best yield of the prepared oxazepine compounds was 91% for compounds N₉ while N₈ compound given lower yield reaches 75%. The higher melting point was 243-245 °C for compound N₈. The lower melting point was 76-78 °C for compound N₆. The different colors and melting points between the raw material and products are initial evidence to take place the chemical reaction.

Table 1. Structural formulas, nomenclature, melting points, colors and % yields of azomethine compounds N₁-N₅

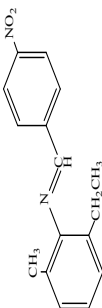
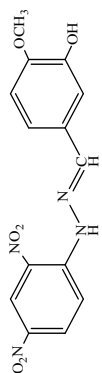
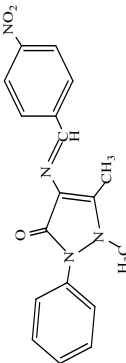
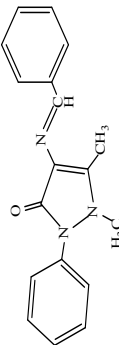
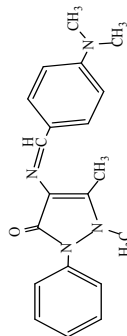
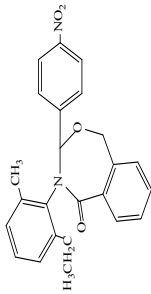
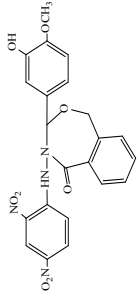
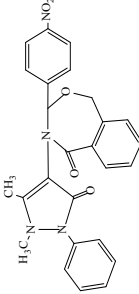
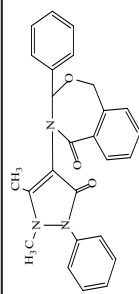
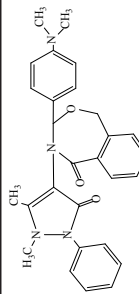
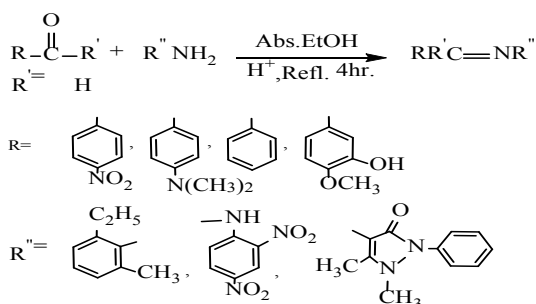
Comp. Code	Structural formula	Nomenclature	Yield %	m.p. °C	Color
N ₁		(E)-2-ethyl-6-methyl-N-(4-nitrobenzylidene)aniline	83%	60-62	Bright golden
N ₂		(E)-5-(2-(2,4-dinitro phenyl)hydrazone)methyl)-2-methoxyphenol	80%	250-252	Dark red
N ₃		(E)-1,5-dimethyl-4-(4-nitrobenzylideneamino)-2-phenyl-1H-pyrazol-3(2H)-one	90%	220-222	Orange
N ₄		(E)-4-(benzylideneamino)-1,5-dimethyl-2-phenyl-1H-pyrazol-3(2H)-one	90%	130-132	Bright yellow
N ₅		4-(4-(dimethylamino) benzylideneamino)-1,5-dimethyl-2-phenyl-1H-pyrazol-3(2H)-one	88%	178-180	Bright Pale yellow

Table 2. Structural formulas, nomenclature, melting points, colors and % yields of the prepared oxazepine compounds N₆-N₁₀

Comp. Code	Structural formula	Nomenclature	Yield %	m.p. °C	Color
N₆		4-(2-ethyl-6-methyl phenyl)-3-(4-nitrophenyl)-3,4-dihydrobenzo[e][1,3] oxazepine-5(1H)-one	89%	76-78	Bright yellow
N₇		4-(2,4-dinitrophenylamino)-3-(3-hydroxy-4-methoxyphenyl)-3,4-dihydro benzo[e][1,3]oxazepine-5(1H)-one	85%	218-220	Red
N₈		4-(1,5-dimethyl-3-oxo-2-phenyl-2,3-dihydro-1H-pyrazol-4-yl)-3-(4-nitrophenyl)-3,4-dihydro benzo[e][1,3]oxazepine-5(1H)-one	75%	243-245	Orange
N₉		4-(1,5-dimethyl-3-oxo-2-phenyl-2,3-dihydro-1H-pyrazol-4-yl)-3-phenyl-3,4-dihydrobenzo[e][1,3] oxazepine-5(1H)-one	91%	100-102	Orange
N₁₀		4-(1,5-dimethyl-3-oxo-2-phenyl-2,3-dihydro-1H-pyrazol-4-yl)-3-(4-(dimethylamino)phenyl)-3,4-dihydrobenzo[e][1,3] oxazepine-5(1H)-one	78%	208-210	Bright Pale yellow

Azomethine compounds were synthesized from commercially available aromatic aldehydes and primary aromatic amines and identified by their melting points and FT-IR.

FT-IR spectra showed the disappearance of the stretching absorption bands of carbonyl group (C=O) of the aldehydes at 1700-1715 cm^{-1} and the appearance of the stretching absorption bands of azomethine group (C=N) at 1549-1642 cm^{-1} indicative of the formation of the resulting imines beside the characteristic bands of the residual groups in the structure (Scheme 6). It was observed that the aromatic amine which contains electrophoresis group in at para position when condensing with aromatic aldehyde; it has less reaction speed. While the reaction speed increases when the same group and the same site on the aromatic aldehyde ring. Glacial acid is used as a catalyst to increase the electrophile of the carbonyl group to accelerate the reaction and increase the percentage yield, see Table 3 and Figures 1 and 2.²⁷



Scheme 6. Structure of the prepared azomethine compounds

Table 3. FTIR of azomethine compounds N₁-N₅

Comp. Code	FT-IR, $\nu(\text{cm}^{-1})$						Others
	C=N	C=C Aromatic	C-H		C-H Ali.		
			Aromatic	Alkene	Asym.	sym.	
N ₁	1642	1599	3066	3101	2963	2874	NO ₂ 1519, 1341
N ₂	1609	1580	3042	3113	2972	2945	NO ₂ 1500, 1328 O-H 3491, NH 3278
N ₃	1549	1481	3043	3070	2962	2886	C=O 1640 NO ₂ 1511, 1334
N ₄	1592	1562	3042	3088	2984	2874	C=O 1645
N ₅	1607	1580	3042	3101	2987	2891	C=O 1642

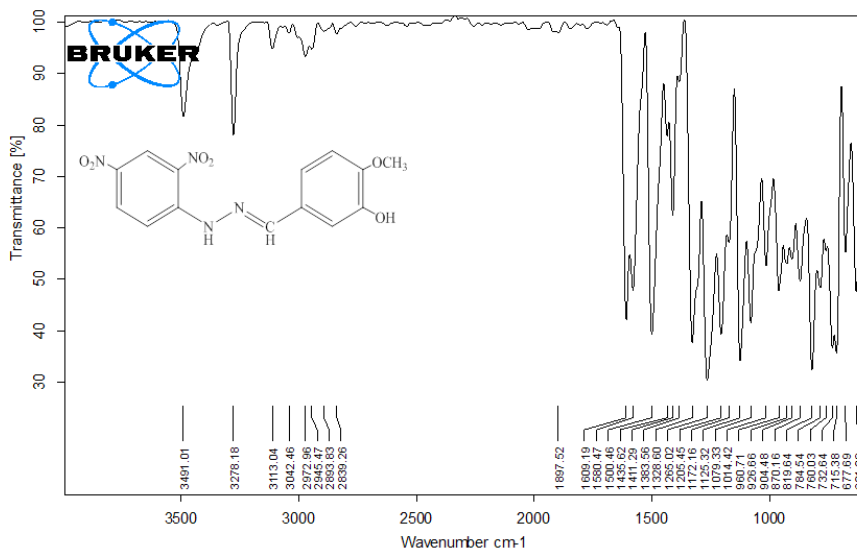


Figure 1. FT-IR spectra of N_2

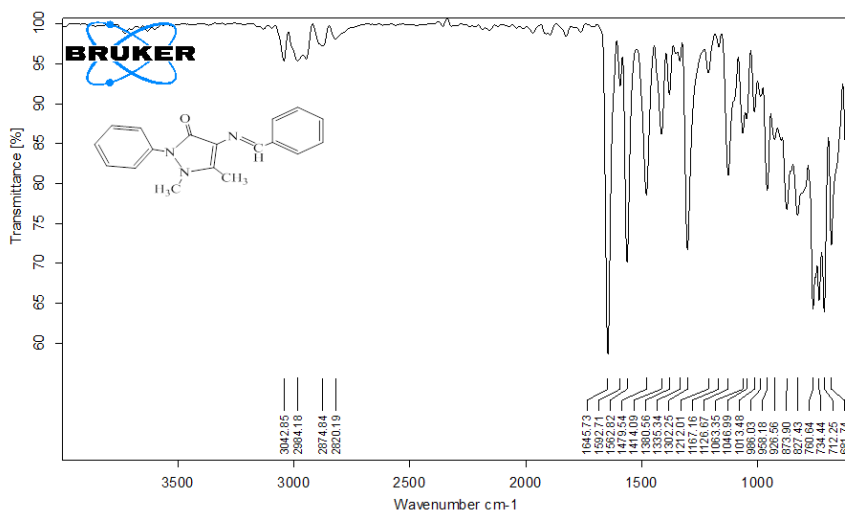
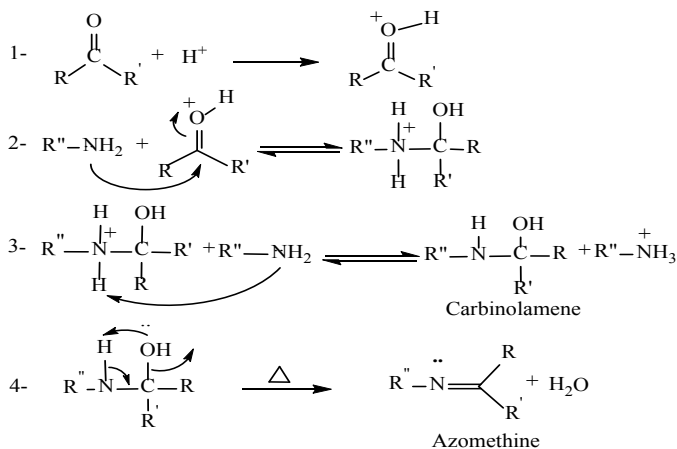


Figure 2. FT-IR spectra of N_4

The mechanism of azomethine compounds formation was established by literature as given by Scheme 7. The reaction involves a nucleophile attack of the double-electronic of the NH_2 group on the carbonyl group $C=O$ of aldehydes to form a hemiaminal N-substituted medium that loses a water molecule to give the stable compound (azomethine). The reaction is believed to occur in the following mechanism²⁸:



Scheme 7. Mechanism of azomethine compounds formation

The synthesis of oxazepine compounds was achieved by the reaction of imines and phthalide. The resulted products were identified by their melting points, FT-IR spectra (Table 4) and both $^1\text{H-NMR}$ and $^{13}\text{C-NMR}$ spectral data (Table 5 & 6). The FT-IR spectra of the products showed the disappearance of the stretching absorption bands of the group (C=N) of the azomethine compounds and the stretching absorption bands phthalide compound and showed the appearance of the stretching absorption bands at $1614\text{-}1650\text{ cm}^{-1}$ indicative of lactam bond (C=O) formation beside the characteristic bands of the residual groups in the structure, see Table 4 and Figure 3 and 4).²⁷

Table 4. FT-IR of the prepared oxazepine compounds $\text{N}_6\text{-N}_{10}$

Comp. Code	FT-IR $\nu(\text{cm}^{-1})$							Others
	C=O Lactam	C-O Lactam	C-N Lactam	C=C Arom	C-H Arom	C-H Ali.		
						Asym.	Sym.	
N_6	1647	1112	1181	1603	3066	2962	2876	NO_2 1523, 1347
N_7	1614	1134	1211	1586	3109	2987	2877	O-H 3497 N-H 3281 NO_2 1509, 1340
N_8	1647	1108	1167	1576	3069	2943	2847	NO_2 1520, 1341
N_9	1650	1130	1307	1567	3038	2944	2863	--
N_{10}	1643	1129	1289	1580	3042	2987	2890	--

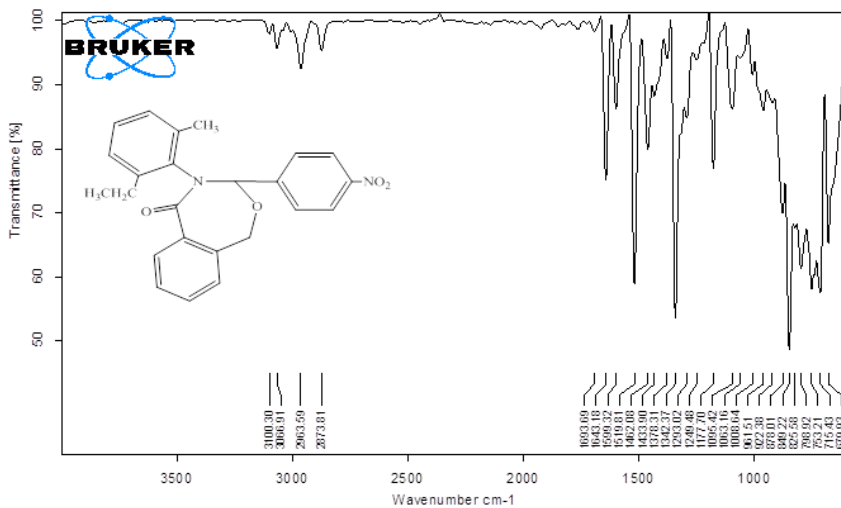


Figure 3. FT-IR spectra of N_6

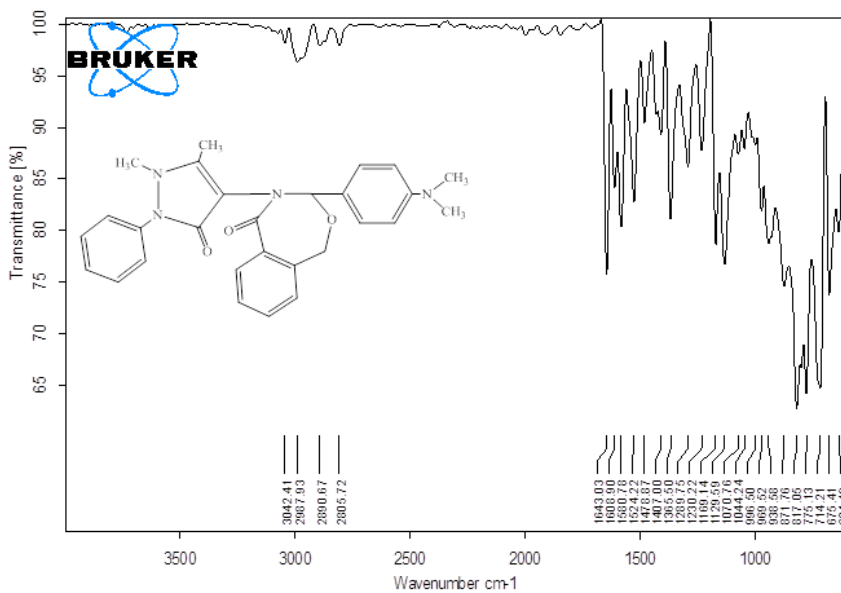


Figure 4. FT-IR spectra of N_{10}

The $^1\text{H-NMR}$ spectrum of compound N_6 in solvent DMSO (Figure 5) showed chemical shifts, $\delta(\text{ppm})$, triplet in 1.06 (3H, $\text{CH}_2\text{-CH}_3$), singlet in 2.07 (3H, C-CH_3), quartet in 2.44 (2H, $\text{CH}_3\text{-CH}_2$), singlet in 3.18 (2H, O-CH_2), singlet in 8.55 (H, N-CH), multiplet and doublet of doublet in 8.42-6.98 (11H, aromatic protons) and spectrum of compound N_7 (Figure 6) showed chemical shifts, $\delta(\text{ppm})$ at: singlet in 3.31 (3H, O-CH_3), singlet in 3.83 (2H, O-CH_2), singlet in 5.43 (1H, -NH), singlet in 9.33 (2H, N-CH), singlet in 11.57 (1H, -OH), multiplet in 8.87-7.00 (13H, aromatic protons).²⁸ Other chemical shifts, $\delta(\text{ppm})$ of compounds $\text{N}_8\text{-N}_{10}$, are given in Table 5.

Table 5. The $^1\text{H-NMR}$ Spectra of the prepared oxazepine compounds $\text{N}_6\text{-N}_{10}$ in DMSO

Comp. code	Chemical Shift δ ppm
N_6	Triplet in 1.06 (3H, $\text{CH}_2\text{-CH}_3$), singlet in 2.07 (3H, C-CH_3), quartet in 2.44 (2H, $\text{CH}_3\text{-CH}_2$), singlet in 3.18 (2H, O-CH_2), singlet in 8.55 (H, N-CH), multiplet and doublet of doublet in 8.42-6.98 (11H, aromatic protons).
N_7	Singlet in 3.31 (3H, O-CH_3), singlet in 3.83 (2H, O-CH_2), singlet in 5.43 (1H, -NH), singlet in 9.33 (H, N-CH), singlet in 11.57 (1H, -OH), multiplet in 8.87-7.00 (13H, aromatic protons).
N_8	Singlet in 1.18 (3H, N-CH_3), singlet in 2.51 (3H, =C-CH_3), singlet in 3.39 (2H, O-CH_2), singlet in 9.67 (H, N-CH), multiplet and doublet of doublet in 8.31-7.37 (13H, aromatic protons).
N_9	Singlet in 1.24 (3H, N-CH_3), singlet in 2.47 (3H, =C-CH_3), singlet in 3.19 (2H, O-CH_2), singlet in 9.59 (H, N-CH), multiplet in 7.83-7.36 (14H, aromatic protons)
N_{10}	Singlet in 1.23 (6H, $\text{-N(CH}_3)_2$), singlet in 2.41 (3H, N-N-CH_3), singlet in 2.98 (3H, =C-CH_3), singlet in 3.11 (2H, O-CH_2), singlet in 9.34 (H, N-CH), multiplet and doublet of doublet in 7.64-6.74 (13H, aromatic protons).

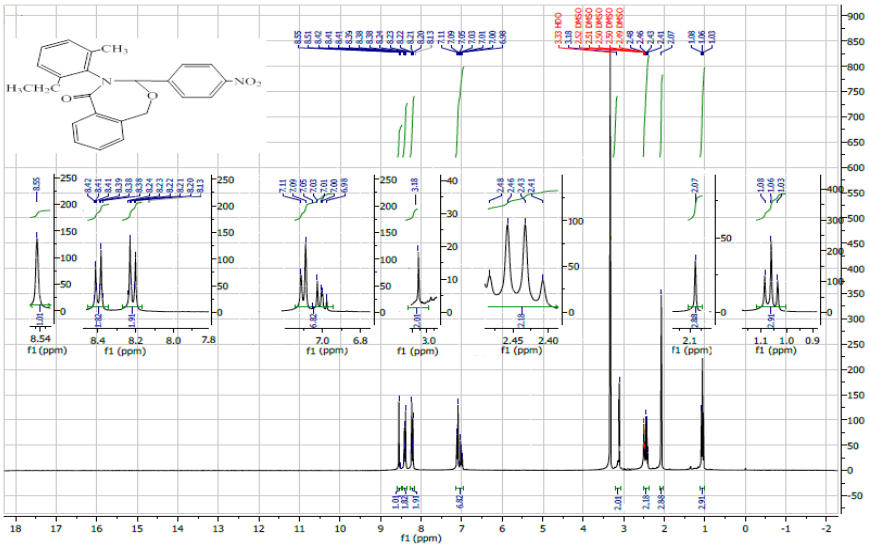


Figure 5. ¹H-NMR Spectra of N₆

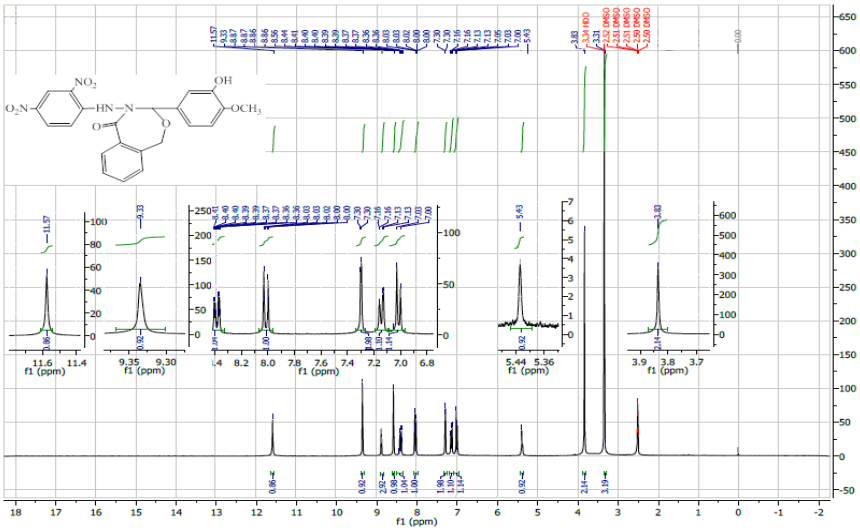


Figure 6. ¹H-NMR Spectra of N₇

The ^{13}C -NMR spectrum of compound N_6 in solvent DMSO (Figure 7) showed chemical shifts, $\delta(\text{ppm})$, 14.92 ($\text{C}-\underline{\text{C}}\text{H}_3$), 18.45 ($\text{CH}_2-\underline{\text{C}}\text{H}_3$), 24.60 ($\underline{\text{C}}\text{H}_2-\text{CH}_3$), 92.12 ($\text{O}-\underline{\text{C}}\text{H}_2$), 150.36 ($\text{N}-\underline{\text{C}}\text{H}$), 162.20 ($\text{N}-\underline{\text{C}}\text{O}$), 124.56-141.59 (aromatic carbons) and spectrum of compound N_7 (Figure 8) showed chemical shifts, $\delta(\text{ppm})$, 25.58 ($\text{O}-\underline{\text{C}}\text{H}_3$), 72.11 ($\text{O}-\underline{\text{C}}\text{H}_2$), 147.35 ($\text{N}-\underline{\text{C}}\text{H}$), 150.73 ($\text{N}-\underline{\text{C}}\text{O}$), 112.34-137.04 (aromatic carbons)²⁹. Other chemical shifts, $\delta(\text{ppm})$ of compounds N_8 - N_{10} , are given in Table 6.

Table 6. The ^{13}C -NMR Spectra of the prepared oxazepine compounds N_6 - N_{10} in DMSO

Comp. code	Chemical Shift δ ppm
N_6	14.92 ($\text{C}-\underline{\text{C}}\text{H}_3$), 18.45 ($\text{CH}_2-\underline{\text{C}}\text{H}_3$), 24.60 ($\underline{\text{C}}\text{H}_2-\text{CH}_3$), 92.12 ($\text{O}-\underline{\text{C}}\text{H}_2$), 150.36 ($\text{N}-\underline{\text{C}}\text{H}$), 162.20 ($\text{N}-\underline{\text{C}}\text{O}$), 124.56-141.59 (Aromatic Carbons).
N_7	25.58 ($\text{O}-\underline{\text{C}}\text{H}_3$), 72.11 ($\text{O}-\underline{\text{C}}\text{H}_2$), 147.35 ($\text{N}-\underline{\text{C}}\text{H}$), 150.73 ($\text{N}-\underline{\text{C}}\text{O}$), 112.34-137.04 (Aromatic Carbons).
N_8	10.17 ($\text{N}-\underline{\text{C}}\text{H}_3$), 35.41 ($=\text{C}-\underline{\text{C}}\text{H}_3$), 99.14 ($\text{O}-\underline{\text{C}}\text{H}_2$), 144.03 ($\text{N}-\underline{\text{C}}\text{H}$), 148.21 ($\text{CH}_3-\underline{\text{C}}\equiv$), 151.22 ($\text{CO}-\underline{\text{C}}\equiv$), 152.83 ($\text{N}-\underline{\text{C}}\text{O}$ in the five-membered ring), 159.41 ($\text{N}-\underline{\text{C}}\text{O}$ in the seven-membered ring), 116.05-129.69 (Aromatic Carbons).
N_9	10.24 ($\text{N}-\underline{\text{C}}\text{H}_3$), 35.83 ($=\text{C}-\underline{\text{C}}\text{H}_3$), 93.62 ($\text{O}-\underline{\text{C}}\text{H}_2$), 145.04 ($\text{N}-\underline{\text{C}}\text{H}$), 147.99 ($\text{CH}_3-\underline{\text{C}}\equiv$), 152.69 ($\text{CO}-\underline{\text{C}}\equiv$), 154.80 ($\text{N}-\underline{\text{C}}\text{O}$ in the five-membered ring), 160.07 ($\text{N}-\underline{\text{C}}\text{O}$ in the seven-membered ring), 116.60-130.63 (Aromatic Carbons).
N_{10}	singlet in 10.31 ($-\text{N}(\text{CH}_3)_2$), singlet in 36.26 ($\text{N}-\text{N}-\text{CH}_3$), 38.08 ($=\text{C}-\text{CH}_3$), 98.12 ($\text{O}-\text{CH}_2$), 135.11 ($\text{N}-\text{CH}$), 151.77 ($\text{CH}_3-\text{C}=\text{C}$), 152.19 ($\text{CO}-\text{C}=\text{C}$), 155.87 ($\text{N}-\text{CO}$ in the five-membered ring), 160.07 ($\text{N}-\text{CO}$ in the seven-membered ring), 118.05-129.52 (Aromatic Carbons).

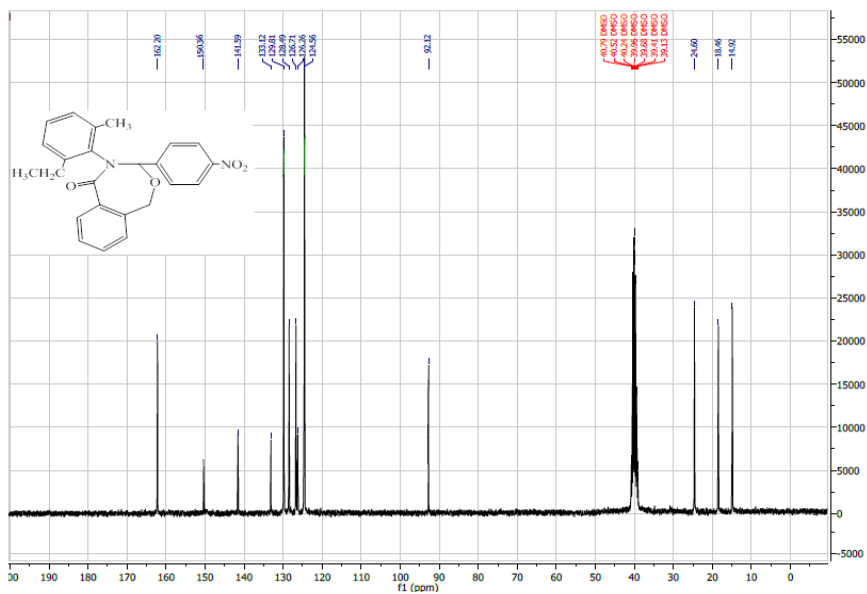


Figure 7. ^{13}C -NMR Spectra of N_6

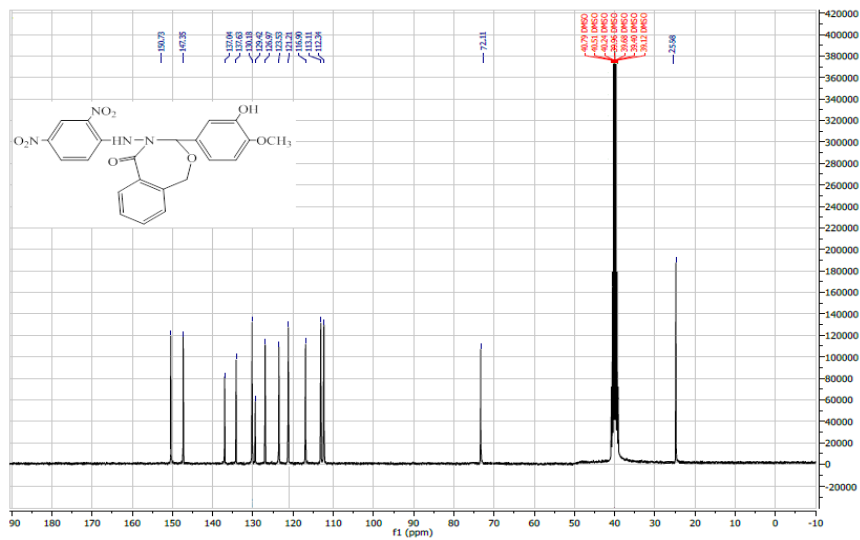
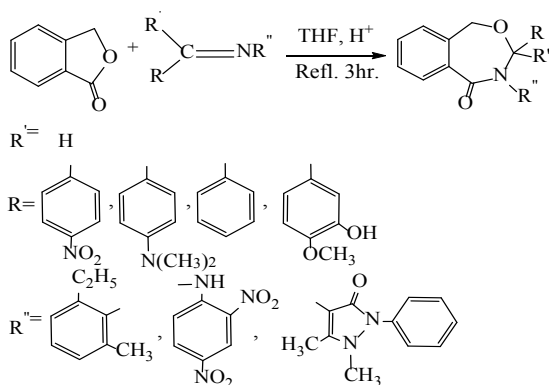


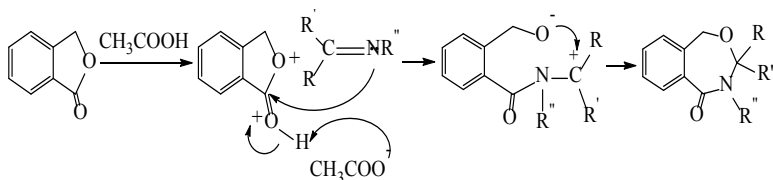
Figure 8. ^{13}C -NMR Spectra of N_7

The reaction of the prepared azomethine compounds with phthalide is given in the following equation (Scheme 8). Glacial acid is used as a catalyst to increase the electrophile of the carbonyl group of phthalide compound to accelerate the reaction and direct the reaction toward the carbon of carbonyl in the five-membered ring of phthalide compound rather than toward the methylene group (CH₂) at the same ring of phthalide compound.³⁰



Scheme 8. Structure of the prepared oxazepine compounds

It may be concluded that the reaction takes place via concerted (5+2) dipolar cycloaddition mechanism as represented in the reaction Scheme 9.^{30,31}



Scheme 9. Mechanism of oxazepine compounds formation

The reaction involves a nucleophile attack of the double-electronic of the azomethine group at the electropositive carbon atom of the carbonyl group to give a dipolar intermediate and the target molecule of oxazepine compounds.

Antifungal activity

Zone of inhibition of some human pathogenic fungi was done well-diffusion method to test the potential of the prepared oxazepine compounds N₆-N₉ as shown in Figure 9. Generally, N₉ is the best derivative that has significantly ($p < 0.01$) recorded a stronger influence to inhibit the growth of *Candida* sp. at an average of the zone of inhibition 13.8 mm, while N₇ derivative has recorded the lowest inhibition 10.9 mm toward clinical fungal pathogens. From another hand, N₆ and N₇ derivatives have recorded the higher zone of inhibition 15 mm

against *Candida guilliermondii* and *Candida zeylanoides* respectively followed 14 mm by N₉ toward *Candida albicans*. N8 and N6 derivatives have shown inhibitory effects 13.3 mm and 13.0 mm against growth of *Candida krusei* and *Candida guilliermondii* respectively. The lower zone of inhibition was 8.0 mm and 9.3 mm by N₇ toward the growth of *Candida albicans* and *Candida guilliermondii* respectively (see Figure 10). Ahmed et al. studied antibacterial activity of 1,3-oxazepine and 1,3,4-oxadiazole³², while Sunil et al. studies role of oxazepine derivative as an anticancer agent against Human Colorectal Adenocarcinoma.³³ The resistance mechanisms depend on which specific pathways are inhibited by the drugs and the alternative ways available for those pathways that the organisms can modify to get a way around to survive.³⁴

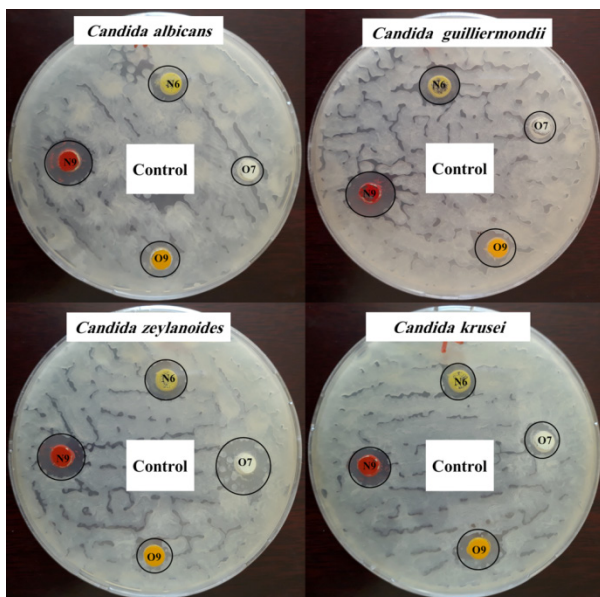


Figure 9. Antifungal activity of the prepared oxazepine compounds N₆-N₉ in methanol

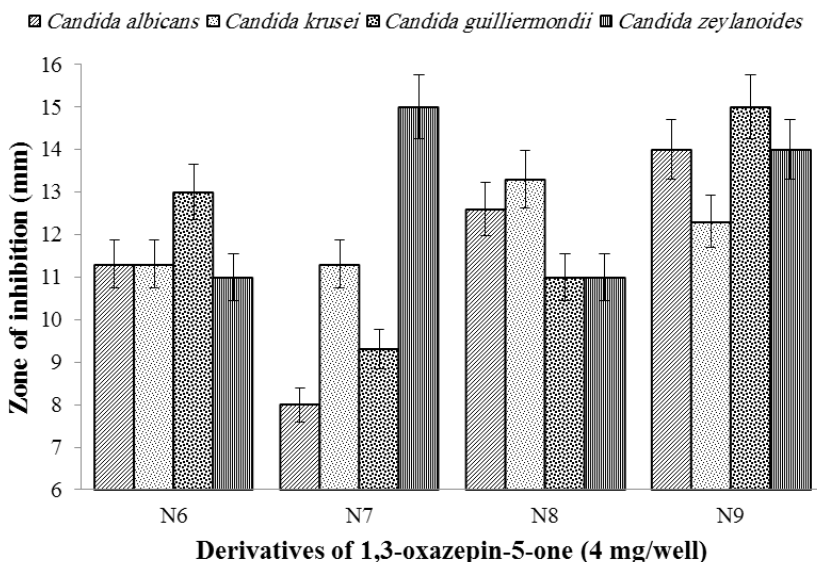


Figure 10. Zone of inhibition of *Candida* sp. using the prepared oxazepine compounds (mm)

CONCLUSION

The formation of stable 7th-membered 1,3-oxazepine ring has been achieved by (5+2) cycloaddition reaction of phthalic and azomethine group. The results of FT-IR, ^{13}C -NMR, and ^1H -NMR showed that the target molecules were formed due to the least obstructive effect in all preparation processes. Generally, N_9 is the best derivative that has significantly ($p < 0.01$) recorded a stronger influence to inhibit growth of *Candida* sp. at average of zone of inhibition 13.8 mm, while N_7 derivative has recorded the lowest inhibition to clinical fungal pathogens (10.9 mm). Slight variation in the structure of those derivatives can show the very dramatic effect on the efficiency of these compounds in their bio-activity. The present work may be helpful in designing more potential antibacterial and antifungal agents for therapeutic use in the future.

ACKNOWLEDGEMENTS

The authors are thanking staff of Department of Chemistry, College of Science, University of Anbar for achieving this work in well. Also, they are grateful for Al-Mustafa Laboratory in Hit, Iraq for helping to complete the bioactivity tests and for Dr. Rusol Al-Bahrani for obtaining the *Candida* isolates from College of Science, University of Baghdad, Iraq.

REFERENCES

1. K Brodowska and E Chruścińska. Schiff bases – interesting range of applications in various fields of science. *CHEMIK*, **2014**, 68, 129-134.
2. W Qin, S Long, M Panunzio and S Biondi. Schiff Bases: A Short Survey on an Evergreen Chemistry Tool. *Molecules* **2013**, 18, 12264-12289.
3. A Adabardakani, M Hakimi and H Kargar. Cinnamaldehyde Schiff Base Derivatives: A Short Review. *WA P journal* **2012**, 2, 472-476.
4. A Ashraf, K Mahmood and A Wajid. Synthesis, Characterization and Biological Activity of Schiff Bases. *IPCBE* **2011**, 10, 1-7.
5. Z Hussain, Z Fadhil, H Adil, M Khalaf, B Abdullah and E Yousif. Schiff's Bases Containing Sulphamethoxazole Nucleus. *RJPBCS* **2016**, 7(3), 1500-1510.
6. T Helal, G Abbas and F Mohammed. Synthesis and Identification of new 4-Aminophenazone derivatives containing azo group. *IJMRD* **2014**, 1, 41-45.
7. V Desai and R Shinde. Green Synthesis of Nicotinic Acid Hydrazone Schiff Bases And Its Biological Evaluation. *Int J Pharm.* **2015**, 5, 930-935.
8. Z Salim, I Hameed and A Hussein. Synthesis and Characterization of New Amino Acid-Schiff Bases and Studies their Effects on the Activity of ACP, PAP and NPA Enzymes (In Vitro). *EJCHEM*, **2102**, 9, 962-969.
9. N Al-Jamali, M Jameel and A Al-Haidari. Preparation And Invitigation Of Diazipene, Oxazipene Compounds Through Condensation Reaction. *Innovare Journal of Science* **2013**, 1, 13-15.
10. A Khan, I Raoof and H Essa. Synthesis, Characterization of Some New Azo Compounds Containing 1,3-Oxazepine, Anthraquinone Moieties and Studying Their Activity against Pathogenic Bacteria. *Journal of Natural Sciences Research*, **2015**, 5, 69-80.
11. R Haiwal. Synthesis of Novel 1, 3 -Oxazepine Compounds from New Azo Schiff bases Containing Thiadiazole Moiety. *Scientific Journal of Kerbala University* **2011**, 9, 96-111.
12. OH Abid, RF Muslim and KM Mohammed. Synthesis and Characterization of Novel 1,3,4,9a-Tetrahydrobenzo[e][1,3]oxazepin- 5(5aH)-one Derivatives via Cycloaddition Reactions of Schiff Bases. *Journal of University of Al-Anbar for Pure Science* **2016**, 10, 8-18.
13. A Younus and N Jaber. Synthesis and Characterization a New 1,3-Oxazepine Compounds from New Bis-4-Amino-3-mercapto-1,2,4-triazole Derivatives. *Organic Chemistry: An Indian Journal* **2016**, 12, 1-12.
14. H Sabah. Synthesis, spectroscopic characterization of schiff bases derived from 4,4'-methylene di aniline. *Der Pharma Chemica* **2014**, 6, 38-41.
15. R Al-Juburi. Synthesis and Characterization of Some Heterocyclic Compounds (Oxazepine, Tetrazole) Derived from Schiff Bases. *Journal of Al-Nahrain University* **2012**, 15, 60-67.
16. MY Nassar, IS Ahmed, HA Dessouki and SS Ali. Synthesis and characterization of some Schiff base complexes derived from 2, 5-dihydroxyacetophenone with transition metal ions and their biological activity. *Journal of Basic and Environmental Sciences* **2018**, 5, 60-71.
17. MM El-ajaily¹, AA Maihub, UK Mahanta, G Badhei, RK Mohapatra and PK Das. Mixed ligand complexes containing schiff bases and their biological activities: a short review. *Rasayan J. Chem.* **2018**, 11, 166-174.

18. C Nastasa, DC Vodnar, I Ionu, A Stana, D Benedec, R Tamaian, O Oniga and B Tiperciuc. Antibacterial Evaluation and Virtual Screening of New Thiazolyl-Triazole Schiff Bases as Potential DNA-Gyrase Inhibitors, *Int. J. Mol. Sci.* **2018**, *19*, 1-18.
19. JN Bavane and RB Mohod. Synthesis, characterization and electrochemical studies of symmetrical schiff base complexes of [1-(5 chloro-2-hydroxy-4-methyl- phenyl) ethanone-4-chloro (-3-trifluoro methyl) aniline]. *The Pharma Innovation Journal* **2018**, *7*, 149-152.
20. K Al-Sultani. Synthesis, identification and evaluation tha biological activity for some new heterocyclic compoundsderived from Schiff bases. *IOSR Journal of Applied Chemistry* **2016**, *9*, 01-11.
21. A Yasir and H Mohammed. Synthesis of New Heterocyclic Derivative [4-(2-Phenyl-2,3-Dihydrobenzo-1,3-Oxazipine-4,7-Dione)Benzaldehyde]. *Int. J. Adv. Res.* **2017**, *5*, 170-175.
22. H Sadiq. Synthesis And Characterization of Novel 1,3-Oxazepine Derivatives From Amino-pyrazine. *World Journal of Pharmacy and Pharmaceutical Sciences* **2017**, *6*, 186-198.
23. A Yasir. Synthesis of New Heterocyclic Derivative 1,3-Oxazepine From Schiff Base Benzyli-denehydrazine. *MJPS*, **2016**, *3*, 1-5.
24. K Mohammad, M Ahmed and M Mahmoud. Synthesis and characterization of some new (1,3-Oxazepine) derivative from 6-methyl 2-thiouracil and study their biological activity. *Tikrit Journal of Pure Science* **2017**, *22*, 67-81.
25. M Kadhim and H Ghanim, Synthesis And Identification 1-3 Diazepine From Ibuprofen, *International Journal of Scientific & Technology Research* **2014**, *3*, 213-217.
26. MN Owaid, J Raman, H Lakshmanan, SSS Al-Saeedi, V Sabaratnam and IAA Al-Assaffii. Mycosynthesis of silver nanoparticles from *Pleurotus cornucopiae* var. *citrinopileatus* and its inhibitory effects against *Candida* sp. *Materials Letters* **2015**, *153*, 186-190.
27. J Simek. *Organic Chemistry*. 8th edition, Pearson education, Inc., **2013**, p. 412-414.
28. R Silverstein, F Webster and D Kiemle. *Spectrometric identification of organic compounds*. 7th edition, John Wiley and sons, Inc., **2005**, p. 72-126.
29. B Mistry, *A Handbook of spectroscopic Data chemistry*. Oxford book company Jaipor India, Mehra Offset Printers, Delhi, **2009**, p. 99-127.
30. OH Abid, HM Tawfeeq and RF Muslim. Synthesis and Characterization of Novel 1,3-oxazepin-5(1H)-one Derivatives via Reaction of Imine Compounds with Isobenzofuran-1(3H)-one. *Acta Pharm. Sci.* **2017**, *55*, 43-55.
31. OH Abid, RF Muslim and KM Mohammed. Synthesis and Characterization of Novel 1,3-oxazepin-4-ones derivatives via Schiff Bases Reactions with Phthalide *J. of University of Al-Anbar for pure science* **2016**, *10*, 1-9.
32. A Ahmed, S Mahdi, A Hussein, A Hamed, E Yousif. Antibacterial Study of Some Oxazepine Derivatives. *Journal of Al-Nahrain University* **2015**, *18*, 22-26.
33. D Sunil, C Ranjitha, M Rama and Pai KSR. Oxazepine Derivative as an Antitumor Agent and Snail Inhibitor against Human Colorectal Adenocarcinoma. *International Journal of Innovative Research in Science, Engineering and Technology* **2014**, *3*, 15357-15363.
34. FC Tenover. Mechanisms of antimicrobial resistance in bacteria. *Am. J. Med.* **2006**, *119*, 3-10.



ADULT-PEDIATRIC BONE MARROW AND STEM CELL TRANSPLANTATION CENTER

Those who hold on to life...

A promising method of treatment by modern medicine:
Stem cell – bone marrow transplantation

BONE MARROW AND STEM CELL TRANSPLANTATION IS PERFORMED BY
OUR EXPERIENCED ACADEMIC STAFF IN OUR CENTER EQUIPPED WITH
LATEST-STATE OF THE ART TECHNOLOGY.

- ▶ MULTIPLE MYELOMA ▶ LYMPHOMA (HEMATOLOGIC LYMPH GLAND CANCER)
- ▶ ACUTE LEUKEMIA (BLOOD CANCER) ▶ CHRONIC LEUKEMIA ▶ BONE MARROW DEFICIENCY
- ▶ APLASTIC ANEMIA ▶ MDS - BONE MARROW DEFICIENCY IN THE ELDERLY



MEDIPOL
CALL
CENTER

+90 444 70 44

International WhatsApp Line:
+90 549 794 13 45

www.internationalmedipol.com



MEDIPOL
MEGA
MEDIPO
MEGA
HOSPITAL
COMPLEX



The Essential Oils of Two *Achillea* L. species from Turkey

Fatma Tosun¹, Mine Kürkçüoğlu^{2*}

¹Istanbul Medipol University, School of Pharmacy, Department of Pharmacognosy, 34810 Istanbul, Turkey.

²Anadolu University, Faculty of Pharmacy, Department of Pharmacognosy, 26470, Eskişehir, Turkey.

ABSTRACT

Chemical composition of the essential oils obtained by hydrodistillation from the aerial parts of *Achillea biebersteinii* Afan. and *A. wilhelmsii* C. Koch were analyzed by GC-FID and GC-MS. The essential oils of *A. biebersteinii* and *A. wilhelmsii* were characterized by the presence of a high percentage of oxygenated monoterpenes 72.9% and 49%, respectively. Sixty-four compounds were identified in the essential oil of aerial parts of *A. biebersteinii* representing 95.9 % of the essential oil. The main components of *A. biebersteinii* essential oil were 1,8-cineole (34.6%) and camphor (12.9%). Forty-two compounds were identified in the essential oil of aerial parts of *A. wilhelmsii* representing 88.2 % of the essential oil. Main component of the essential oil of *A. wilhelmsii* was determined as camphor (32.0%).

Keywords: *Achillea biebersteinii*, *Achillea wilhelmsii*, essential oil, GC-FID and GC-MS.

INTRODUCTION

Genus *Achillea* L. (Asteraceae) is represented by more than 140 species in all around the world. The genus is widespread in Europe, Asia, North America and Middle East¹. There are 59 taxa of *Achillea* found in Turkey which are divided into 6 sections *Ptarmica* (DC.) W. Koch, *Arthrolepis* Boiss., *Babounya* Boiss., *Santalinoidea* DC., *Millefolium* (DC.) W. Koch, and *Filipendulinae* (DC.) Boiss. Among them, 31 taxa are endemic to Turkey (%53)²⁻⁴. The essential oil composition of several *Achillea* spp. growing in Turkey have been studied⁵. Antioxidant, insecticidal and herbicidal activities of *A. biebersteinii* oils were reported⁶⁻¹³. The antimicrobial activity of *A. wilhelmsii* subsp. *wilhelmsii* essential oil was tested against several microorganisms and strong inhibitory activity was observed against *Enterobacter aerogenes*, *Proteus vulgaris* and *Alternaria brassicola*¹⁴ species.

*Corresponding author: Mine Kürkçüoğlu, e-mail: minekurkuoglu@gmail.com
(Received 14 March 2018, accepted 19 March 2018)

Biological activities of various *Achillea* species include angiogenic⁷, antifungal^{8,15}, antibacterial¹⁶, antimicrobial^{14,17}, hepatoprotective¹⁸, herbicidal⁸, insecticidal^{11,19}, antioxidant^{16,18} antiradical¹⁷ and protective effects against oxidative stress^{6,20}.

In the present work, chemical composition of the *Achillea biebersteinii* and *A. wilhelmsii* essential oils were analyzed by gas chromatography (GC) and gas chromatography-mass spectrometry (GC-MS) systems.

MATERIALS AND METHODS

Plant Materials

The aerial parts of *Achillea biebersteinii* Afan. and *A. wilhelmsii* C. Koch were collected while flowering in the vicinity of Adana and Kayseri, respectively. The plant species were identified by Prof. Mecit Vural and voucher specimens have been deposited at the Herbarium of the Istanbul University, Faculty of Pharmacy, Istanbul, Turkey. (Voucher specimens no: ISTE 115056 and ISTE 115058 resp.)

Isolation of the Essential Oils

The air-dried plant materials were hydrodistilled for 3 hours using a Clevenger-type apparatus. *A. biebersteinii* and *A. wilhelmsii* oils were dried over anhydrous sodium sulphate and stored at 4 °C in the dark until analysed. The yield of essential oils were calculated as 0.98 % and 0.18 %, v/w on dry weight basis, resp.

GC and GC/MS Conditions:

The oils were analyzed by capillary GC and GC/MS using an Agilent GC-MSD system.

GC/MS analysis

The GC/MS analysis was carried out with an Agilent 5975 GC-MSD system. Innowax FSC column (60m x 0.25mm, 0.25µm film thickness) was used with helium as carrier gas (0.8 mL/min.). GC oven temperature was kept at 60°C for 10 min and programmed to 220°C at a rate of 4°C/min, and kept constant at 220°C for 10 min and then programmed to 240°C at a rate of 1°C/min. Split ratio was adjusted 40:1. The injector temperature was at 250°C. MS were taken at 70 eV. Mass range was from m/z 35 to 450.

GC analysis

The GC analysis was carried out using an Agilent 6890N GC system. In order to obtain the same elution order with GC/MS, simultaneous injection was done by using the same column and appropriate operational conditions. FID temperature was 300°C.

Identification of Compounds

Identification of the essential oil components was carried out by comparison of their relative retention times with those of authentic samples or by comparison of their relative retention index (RRI) to series of *n*-alkanes²¹. Computer matching against commercial (Wiley GC/MS Library, MassFinder 3 Library)^{22,23} and in-house “Baser Library of Essential Oil Constituents” built up by genuine compounds and components of known oils, as well as MS literature data^{24,25} was used for the identification. Relative percentage amounts of the separated compounds were calculated from FID chromatograms. The results of analysis are shown in Table 1.

Table 1. Composition of the essential oils of *Achillea biebersteinii* and *A. wilhelmsii*

RRI	Compounds	A %	B %	IM
1014	Tricyclene	tr	-	MS
1032	α -Pinene	2.6	-	t_{R^*} MS
1035	α -Thujene	tr	-	MS
1076	Camphene	-	0.4	t_{R^*} MS
1118	β -Pinene	1.1	-	t_{R^*} MS
1132	Sabinene	1.1	0.4	t_{R^*} MS
1138	Thuja-2,4 (10)-dien	tr	-	MS
1188	α -Terpinene	2.5	-	t_{R^*} MS
1195	Dehydro-1,8-cineole	tr	-	t_{R^*} MS
1203	Limonene	0.2	0.2	t_{R^*} MS
1213	1,8-Cineole	34.6	3.3	t_{R^*} MS
1255	γ -Terpinene	0.5	-	t_{R^*} MS
1280	<i>p</i> -Cymene	3.4	0.6	t_{R^*} MS
1290	Terpinolene	0.1	-	t_{R^*} MS
1409	Rosefuran	tr	-	MS
1437	α -Thujone	0.2	-	MS
1445	Filifolone	0.3	-	MS
1451	β -Thujone	0.1	-	MS
1452	1-Octen-3-ol	tr	-	t_{R^*} MS
1474	trans-Sabinene hydrate	0.6	0.6	t_{R^*} MS
1483	Isonerol oxide	-	0.8	MS
1499	α -Campholene aldehyde	0.2	-	MS
1522	Chrysanthenone	2.4	-	MS
1532	Camphor	12.9	32.0	t_{R^*} MS
1538	trans-Chrysanthenyl acetate	2.3	-	MS
1544	Dihydroachillene	0.5	0.5	MS

1553	Linalool	0.2	0.7	t _R , MS
1556	cis-Sabinene hydrate	0.8	tr	t _R , MS
1571	trans-p-Menth-2-en-1-ol	0.5	-	MS
1582	cis-Chrysanthenyl acetate	0.1	-	MS
1586	Pinocarvone	0.7	0.5	MS
1591	Bornyl acetate	0.4	0.5	t _R , MS
1600	Chrysanthenyl propionate	tr	-	MS
1611	Terpinen-4-ol	1.7	tr	t _R , MS
1612	β-Caryophyllene	tr	0.8	t _R , MS
1617	Lavandulyl acetate	-	2.0	MS
1638	cis-p-Menth-2-en-1-ol	0.4	-	MS
1648	Myrtenal	0.3	-	MS
1651	Sabina ketone	0.2	-	MS
1670	trans-Pinocarveol	0.6	-	t _R , MS
1663	cis-Verbenol	0.6	-	MS
1683	trans-Verbenol	4.0	0.6	MS
1687	Lavandulol	-	4.1	t _R , MS
1706	α-Terpineol	3.6	1.2	t _R , MS
1719	Borneol	2.0	2.6	t _R , MS
1725	Verbenone	0.1	-	t _R , MS
1726	Germacrene D	0.1	2.3	MS
1742	β-Selinene	-	0.4	MS
1747	p-Mentha-1,5-dien-8-ol	0.3	-	MS
1748	Piperitone	0.8	-	t _R , MS
1751	Bicyclogermacrene	-	1.5	MS
1755	Terpinyl acetate	6.0	-	t _R , MS
1758	cis-Piperitol	tr	-	MS
1764	cis-Chrysanthenol	0.7	-	MS
1776	γ-Cadinene	-	0.6	MS
1804	Myrtenol	0.2	-	MS
1845	(E)-Anethole	-	tr	MS
1864	p-Cymer-8-ol	0.1	-	t _R , MS
1882	1-Isobutyl 4-isopropyl-2,2-dimethyl succinate	-	tr	MS
1889	Ascaridole	3.1	-	MS
1900	Isoshyobunone	-	tr	MS
1916	Shyobunone	-	1.5	MS
1969	cis-Jasmone	0.4	-	MS

2008	Caryophyllene oxide	0.3	3.5	t _R , MS
2057	13-Tetradecanolide	-	1.9	MS
2065	p-Mentha-1,4-dien-7-ol	0.2	-	MS
2113	Cumin alcohol	0.3	-	t _R , MS
2131	Hexahydrofarnesyl acetone	-	0.2	t _R , MS
2144	Spathulenol	0.1	3.7	t _R , MS
2273	(2E,6E)-Farnesyl acetate	-	0.9	MS
2191	T-Cadinol	-	2.2	MS
2192	Eugenol	0.4	-	t _R , MS
2198	Thymol	0.1	2.6	t _R , MS
2239	Carvacrol	0.2	-	t _R , MS
2257	β-Eudesmol	0.1	2.6	MS
2260	15-Hexadecanolide	0.2	1.0	MS
2300	Tricosane	tr	-	t _R , MS
2316	Caryophylladienol I	-	1.2	MS
2324	Caryophylladienol II	0.2	4.1	MS
2353	Caryophyllenol I	-	2.2	MS
2392	Caryophyllenol II	-	1.7	MS
2600	Hexacosane	0.1	-	MS
2607	Octadecanol	-	2.3	MS
2931	Hexadecanoic acid	0.2	-	MS
	Grouped compounds (%)			
	Monoterpene hydrocarbones	12.0	2.1	
	Oxygenated monoterpenes	72.9	49.0	
	Sesquiterpenes hydrocarbones	0.1	5.6	
	Oxygenated sesquiterpenes	0.7	22.7	
	Others	10.2	8.8	

RRI: Relative retention indices experimentally calculated against n-alkanes; %: calculated from FID data; IM: Identification Method: t_R, Identification based on comparison with co-injected with standards on a HP Innowax column; MS, identified on the basis of computer matching of the mass spectra with those of the in-house Baser Library of Essential Oil Constituents, Adams, MassFinder and Wiley libraries. A: *Achillea biebersteinii* Afan., B: *A. wilhelmsii* C. Koch.

RESULTS AND DISCUSSION

A. biebersteinii oils contained camphor and 1,8-cineole as main constituents⁶. In a sample of Ankara origin α -terpinyl acetate (7%) was also encountered in this oil⁹. A sample from Sivas contained 1,8-cineole (31%), camphor (14%) α -thujone (13%), p-cymene (5%), β -thujone (3%), borneol (3%) as other significant constituents^{6,10}.

Camphor (40%), artemisia alcohol (18%), yomogi alcohol (16%), and 1,8-cineole (7%) were reported as main constituents in *A. wilhelmsii* oil¹⁴. Camphor (41%) was also the main constituent in another study together with caryophylladienol II (6%), borneol (6%), camphene (6%)^{6,26}.

Previously, 1,8-cineole and camphor rich oils were reported by several authors from *Achillea* species growing outside Turkey⁶.

According to another study which reported the compositions of essential oils of several *Achillea* species, *A. biebersteinii* has been found to be rich in oxygenated monoterpenes. Piperitone, p-cymene, and camphor were found as main components in the oil of this plant sample, collected from a different locality.¹

In our present study, we examined chemical composition of essential oils obtained from the aerial parts of *A. biebersteinii* and *A. wilhelmsii* collected in the vicinity of Adana and Kayseri. Yield of essential oils obtained by hydrodistillation for *A. biebersteinii* and *A. wilhelmsii* were found to be 0.98% and 0.18%, respectively. Essential oil components of two *Achillea* species are seen at Table 1. *A. biebersteinii* and *A. wilhelmsii* oils were characterized by the presence of a high percentage of oxygenated monoterpenes (72.9% and 49%). Sixty-four compounds were identified in oil of the aerial parts representing 95.9 % of the *A. biebersteinii* oil. The main components of the *A. biebersteinii* oil were 1,8-cineole (34.6%) and camphor (12.9%). Forty-two compounds were identified in oil of the aerial parts representing 88.2 % of the *A. wilhelmsii* oil. Main component determined for *A. wilhelmsii* is camphor (32.0%). These compounds have also been previously reported in *Achillea* essential oils⁶.

ACKNOWLEDGMENT

We thank Prof. Mecit Vural for identification of the plant materials.

REFERENCES

1. Kose, Y. B.; B. Demirci and G. İscan. Volatile Oil Composition and Biological Activity of *Achillea biebersteinii* Afan. and *Achillea teretifolia* Willd., *Fresenius Environmental Bulletin*, **2017**, 26 (8), 5213-5218.
2. Arabacı T. *Achillea* L. In *A Checklist of the Flora of Turkey (Vascular Plants)*, Güner, A.; Aslan, S.; Ekim, T.; Vural, M. and Babaç M.T., Eds.; Nezahat Gokyigit Botanik Bahçesi ve Flora Araştırmaları Derneği Yayını, İstanbul, **2012**; 108-112.

3. Huber-Morath A. *Achillea* L. In *Flora of Turkey and the East Aegean Islands*, vol. 5. Davis P.H., Ed.; Edinburgh University Press, Edinburgh, **1975**; pp 224–252.
4. Tabanca, N.; Demirci, B.; Aytac, Z. and Baser K.H.C. Chemical composition of *Achillea schischkinii* Sosn., an endemic species from Turkey, *Nat. Volatiles & Essent. Oils*, **2016**, 3(4): 24-28.
5. Kürkçüoğlu, M.; Demirci, B.; Tabanca, N.; Özek, T. and Başer K.H.C. The Essential Oil of *Achillea falcata*, *Flavour Fragr. J.* **2003**, 18, 192-194.
6. Baser, K.H.C. Essential Oils of *Achillea* Species of Turkey, *Nat. Volatiles & Essent. Oils*, **2016**, 3(1), 1-14.
7. Demirci, F.; Kiyan, H. T.; Demirci, B. & Baser, K. H. C. The in vivo angiogenic evaluation of *Achillea biebersteinii* Afan. and *Achillea teretifolia* Willd. essential oils. *Planta Medica*, **2011**, 77(12), 1391-1391.
8. Kordali, S.; Cakir, A.; Akcin, T.A.; Mete, E.; Akcin, A.; Aydin, & T., Kilic. Antifungal and herbicidal properties of essential oils and n-hexane extracts of *Achillea gypsicola* Hub.-Mor. and *Achillea biebersteinii* Afan. (Asteraceae). *Ind. Crop. Prod.* **2009**, 29, 562-570.
9. Kusmenoglu, S.; Baser, K. H. C.; Ozek, T.; Harmandar, M. & Gokalp, Z. Constituents of the Essential Oil of *Achillea biebersteinii* Afan. *J. Essent. Oil Res.* **1995**, 7(5), 527-528.
10. Polatoglu, K.; Karakoc, O. C. & Goren, N. Phytotoxic, DPPH scavenging, insecticidal activities and essential oil composition of *Achillea vermicularis*, *A. teretifolia* and proposed chemotypes of *A. biebersteinii* (Asteraceae). *Industrial Crops and Products*, **2013**, 51, 35-45.
11. Tabanca, N.; Demirci, B.; Gurbuz, I., Demirci, F.; Becnel, J. J.; Wedge, D. E. & Baser, K. H. C. Essential Oil Composition of Five Collections of *Achillea biebersteinii* from Central Turkey and their Antifungal and Insecticidal Activity. *Natural Product Communications*, **2011**, 6(5), 701-706.
12. Techen, N.; Tabanca, N.; Demirci, B.; Gurbuz, I.; Pan, Z.; Khan, I. A.; Wedge, D.E. & Baser, K. H. C. Chemical Characterization and Genomic Profiling of *Achillea biebersteinii* from Various Localities in Central Turkey. *Planta Medica*, **2009**, 75(4), 416-416.
13. Toner, O.; Basbag, S.; Karaman, S.; Diraz, E. & Basbag, M. Chemical Composition of the Essential Oils of some *Achillea* Species Growing Wild in Turkey. *International Journal of Agriculture and Biology*, **2010**, 12(4), 527-530.
14. Azaz, A. D.; Arabaci, T.; Sangun, M. K. & Yildiz, B. Composition and the in vitro antimicrobial activities of the essential oils of *Achillea wilhelmsii* C. Koch. and *Achillea lycanica* Boiss & Heldr. *Asian Journal of Chemistry*, **2008**, 20(2), 1238-1244.
15. Amjad, L.; Mousavideh-mourdi, K.; Rezvani, Z. In vitro Study on Antifungal Activity of *Achillea wilhelmsii* Flower Essential Oil Against Twenty Strains of *Candida albicans*, *Chiang Mai Journal of Science*, **2014**, 14, 1058-1064.
16. Alfatehi, S.M.H.; Rad, J.S.; Rad, M.S.; Mohsenzadeh, S.; Teixeira da Silva, J.A. Chemical composition, antioxidant activity and in vitro antibacterial activity of *Achillea wilhelmsii* C. Koch essential oil on methicillin-susceptible and methicillin-resistant *Staphylococcus aureus* spp., *3 Biotech* **2015**, 5(1) 39-44.
17. Sokmen, A.; Sokmen, M.; Daferera, D.; Polissiou, M.; Candan, F.; Unlu, M. & Akpulat, H.A. The in vitro antioxidant and antimicrobial activities of the essential oil and methanol extracts of *Achillea biebersteinii* Afan. (Asteraceae). *Phytother. Res.* **2004**, 18, 451–456.

18. Al-Said, M.S.; Mothana, R.A.; Al-Yahya, M.M.; Rafatullah, S.; Al-Sohaibani, M.O.; Khaled, J.M.; Alatar, A.; Alharbi, N.S.; Kurkcuoglu, M. and Baser, K.H.C. GC-MS Analysis: *In Vivo* Hepatoprotective and antioxidant Activities of the Essential Oil of *Achillea biebersteinii* Afan. growing in Saudi Arabia, *Evidence-Based Comp and Alt Med*, **2016**, Article ID 1867048.
19. Khani, A.; Asghari, J. Insecticide activity of essential oils of *Mentha longifolia*, *Pulicaria gnaphalodes* and *Achillea wilhelmsii* against two stored product pests, the flour beetle, *Tribolium castaneum*, and the cowpea weevil, *Callosobruchus maculatus*. *J. Insect Sci.* **2012**, *12*, 73.
20. Dadkhah, A.; Fatemi, F.; Alipour, M.; Ghaderi, Z.; Zolfaghari, F. & Razdan, F. Protective effects of Iranian *Achillea wilhelmsii* essential oil on acetaminophen-induced oxidative stress in rat liver, *Pharm. Biol.* **2015**, *53*(2) 220-227.
21. Curvers, J.; Rijks, J.; Cramers, C. A. M. G.; Knauss, K. & Larson, P. Temperature programmed retention indices: Calculation from isothermal data. Part 1: Theory. *Journal of Separation Science*, **1985**, *8*(9), 607-610.
22. McLafferty, F. W.; Stauffer, D. B. *The Wiley/NBS Registry of Mass Spectral Data*; J. Wiley and Sons: New York, **1989**.
23. Koenig, W. A.; Joulain, D.; Hochmuth, D. H. Terpenoids and related constituents of essential oils. MassFinder 3. Hamburg, Germany: Hochmuth Scientific Consulting, **2004**
24. Joulain, D.; Koenig, W. A. *The Atlas of Spectra Data of Sesquiterpene Hydrocarbons*. E.B.-Verlag Hamburg, **1998**.
25. ESO 2000. *The Complete Database of Essential Oils. Boelens Aroma Chemical Information Service*: The Netherlands, **1999**.
26. Turkmenoglu, F.P.; Agar, O.T.; Akaydin, G.; Hayran, M.; Demirci, B. Characterization of volatile compounds of eleven *Achillea* species from Turkey and biological activities of essential oil and methanol extract of *A. hamzaoghui* Arabaci et Budak, *Molecules*. **2015**, *20*, 11432-11458.

Renoprotective and anti-oxidant effects of *Coleus forskohlii* against gentamicin induced nephrotoxicity in albino wistar rats

Nishat Fatima^{1*}, Ather Sultana¹

¹Shadan Womens College of Pharmacy, Department of Pharmacology, Hyderabad, India.

ABSTRACT

The aim of present study was to evaluate the protective effects of *Coleus forskohlii* against Gentamicin (GM)-induced nephrotoxicity in male albino wistar rats.

Thirty rats were divided into five groups (n=6). Control rats received normal saline. Nephrotoxicity was induced in rats by gentamicin (80mg/Kg, IP) and treated with Silymarin (100mg/Kg, p.o.), aqueous and ethanolic extracts of (500mg/Kg, p.o) *C. Forskohlii* respectively for 15days. Markers of renal function (urea, uric acid and Creatinine), antioxidant markers were evaluated along with histopathological investigation in all experimental groups.

GM-treated rats showed significant increase in serum levels of renal markers, TBARS and decrease in GSH, SOD, CAT. Histopathological examinations of GM-treated rats revealed degenerative changes in glomeruli and renal tubules. Administration of aqueous and ethanolic root extracts of *Coleus forskohlii*, protected the kidney tissues against toxic effects of gentamicin as evidenced by amelioration of histopathological changes and normalization of kidney biochemical parameters.

The results of present study confirm the nephroprotective and anti-oxidant activity of *C. forskohlii*.

Key words: *Coleus forskohlii*, gentamicin, nephrotoxicity, antioxidant activity.

INTRODUCTION

Gentamicin is one of the widely used aminoglycoside antibiotics in treating gram negative bacterial infections. Its use is limited due to ototoxicity and nephrotoxic effects. It has been shown that up to 20% of people receiving gentamicin treatment develop symptoms of nephrotoxicity. Aminoglycosides throughout the

*Corresponding author: Dr. Nishat Fatima, e-mail: nishat_fatima50004@yahoo.com
(Received 11 February 2018, accepted 18 March 2018)

endocytic pathway are taken up into the epithelial cells of the renal proximal tubules and stay there for a long time, which leads to nephrotoxicity. Acidic phospholipids, broadly distributed in the plasma membranes in various tissues, are considered to be the binding site of aminoglycosides in brush-border membrane of proximal tubular cell.^{1,2} Although the actual mechanism behind gentamicin induced nephrotoxicity is not clearly known, numerous studies have found involvement of different pathways, which includes, production of reactive oxygen species (ROS), reactive nitrogen species (RNS), and reduction in antioxidant defence. Activation of inflammatory processes, contraction of mesangial cells causing tubular necrosis and reduced glomerular filtration rates (GFR) are the other complications of chronic gentamicin administration.

Hydroxyl radicals play a vital role in the pathogenesis of gentamicin-induced nephrotoxicity, leading to suppression of Na(+)-K(+)-ATPase activity and DNA synthesis in rats proximal tubules causing renal injury. This injury may be relevant to reactive oxygen metabolites generated by gentamicin. Renal cortical mitochondria is the source of reactive oxygen metabolites, which induces renal damage.³

Plants produce large range of bioactive principles and constitutes a huge source of medicines.^{4,5} Being less expensive than synthetic drugs, herbal medicines are primarily used for treating mild or chronic ailments. In India 45,000 plant species have been identified and out of which 15-20 thousand plants are of good medicinal value. It is generally estimated that over 6000 traditional plants in India are in use as folk and herbal medicine, representing about 75% of the medicinal needs of the Third World countries.⁴ Literature suggests the use of compounds with antioxidant and anti-inflammatory properties and are capable of altering gentamicin-induced nephrotoxicity.³

Coleus forskohlii (CF) (Syn. *Plectranthus Barbitus*) is a medicinal plant belonging to family, Lamiaceae, with well-known efficacy in Ayurveda and Indian indigenous system of medicine. Different parts of the plant are documented in the treatment of various ailments such as heart diseases, respiratory disorders, asthma, bronchitis, constipation and epilepsy. *Forskolin*, is reported to be main active ingredient, which is a diterpene compound (7 β -acetoxy-8, 13-epoxy- 1 α , 6 β , 9 α -trihydroxy-labd-14-ene-11-one).⁶ Schaneberg et al., has successfully evaluated forskolin qualitatively and quantitatively from root and stem by using reversed-phase liquid chromatography.⁷ The roots are also useful in the treatment of worms, eczema and to alleviate burning in festering boils.^{8,9} However, so far, no scientific validity has been made to establish it as a nephro-protective agent. Hence, in the present study, an effort has been made to au-

thenticate its traditional use by using ethanolic and aqueous root extracts of CF against gentamicin-induced nephrotoxicity in albino wistar rats.

METHODOLOGY

Authentication of plant material

The plant under study was identified and authenticated by the botanist, Dr. K. Madhav Chetty department of Botany in Sri Venkateshwara University, Tirupati, A.P, India and a specimen (voucher No.1965) has been deposited.

Preparation of plant extracts:

The dried roots of *Coleus forskohlii* were subjected to soxhlet extraction using ethanol as the solvent. Aqueous extract was prepared by freshly boiling in water before dosing.

Preliminary phytochemical investigations

The preliminary phytochemical investigations were carried out with ethanolic and aqueous extracts of dried roots of *Coleus forskohlii* for qualitative identification of phytochemical constituents present with each extract. Tests were carried out by standard methods described in practical Pharmacognosy by K.R. Khandelwal and Dr. C.K. Kokate.¹⁰ All the chemicals and reagents used were of analytical grade.

Experimental Animals

The study protocol was approved by the Institutional Animals Ethics Committee (IAEC) of Committee for the purpose of Control and Supervision of Experiments on Animals (CPCSEA), Government of India, through its reference no. IAEC-01/SES/2017/101, Dated: 06/05/2017. Male and female wistar albino rats weighing 150-180 grams, were obtained from the animal house of Sainath Agencies, Hyderabad (282/PO/Bt/S/2000 CPCSEA). The animals were housed with free access to food and water for one week in an air-conditioned room (25°C) under a 12 hr light: dark cycle prior to the experiment. During the experimental study rats were fed with pellets obtained from (Pranav Agro Industries limited, rat feed, India). The rats received humane care according to the criteria outlined in CPCSEA guidelines 2003, Government of India.

Chemicals

a. Silymarin – 100mg/Kg

Silymarin Tablets – Silybon 140mg, Micro labs Pvt Ltd.

Solan, Himachal Pradesh, India, Batch no. SIBDOO51,

MFD Jan 2017, Expiry date DEC 2018.

b. Gentamicin - 80mg/Kg

Gentamicin Injection – Gentamicin Sulphate B.P,

80 mg in 2ml, Pfizer Laboratories Pvt Ltd.

Acute oral toxicity study

The acute toxicity studies for ethanolic and aqueous extracts of dried roots of *Coleus forskohlii* were done according to the OECD guidelines No. 423 using female albino wistar rats.¹¹ Each animal was administered with the ethanolic and aqueous extracts of the plant by oral route (2000 mg/Kg was used as starting dose). Animals were observed individually after dosing atleast once during the first 30 minutes. At regular intervals, they were observed during the first 24 hours, with special attention to the first four hours and thereafter daily for the next fourteen days.

Evaluation of Nephroprotective Activity

Male wistar albino rats were divided into five groups of six animals each. Group I Normal control rats were treated with isotonic saline; Group II, rats received gentamicin half an hour before administration of standard drug Silymarin 100 mg/Kg in distilled water p.o; Group III, rats received only Gentamicin 80mg/Kg in isotonic saline by intraperitoneal route, Group IV and V rats received gentamicin half an hour before administration of ethanolic and aqueous extracts of *Coleus forskohlii* (500mg/Kg) in aqueous solution respectively.

Grouping of Animals

Table 1. Grouping of animals.

Group	Treatment
I –Normal Control	Normal Saline 0.5ml p.o
II- Standard	Half an hour before administration of Silymarin 100mg/Kg orally, rats were injected with Gentamicin 80mg/Kg IP.
III-Gentamicin Control	Rats received only Gentamicin 80mg/Kg in isotonic saline by intraperitoneal route (IP).
IV –Ethanollic extract	Rats received gentamicin 80mg/Kg, IP half an hour before administration of ethanollic extracts of <i>Coleus forskohlii</i> (500 mg/Kg),p.o.
V- Aqueous extract	Rats received gentamicin 80mg/Kg, IP half an hour before administration of aqueous extracts of <i>Coleus forskohlii</i> (500 mg/Kg),p.o.

The same dosing schedule was continued as per the assigned groups for 15 days for studying the gentamicin-induced nephrotoxicity. ^{12,13}

Blood sampling

At the end of experimental period (15 days) and after overnight fasting, blood samples were collected by retro-orbital puncture using capillary tube and animals were sacrificed using anaesthesia and kidneys were collected. Blood samples were centrifuged for 10 minutes at 3000 rpm within an hour and the sera were obtained.

Determination of serum urea, creatinine, uric acid and histopathology of kidney tissues

The serum parameters were estimated using standard kits obtained from Span Diagnostics, India and analysed spectrophotometrically by using double beam UV Visible spectro-photometer (UV-Visible spectrophotometer). Kidneys from all five groups were fixed in 10% neutral buffered formalin and processed to paraffin wax. 5 microns Sections are stained with Haematoxyllin and Eosin, Massons trichrome, and Periodic Acid Schiff and are examined under light microscope at 100 and 400 magnifications.

Preparation of renal homogenate and determination of antioxidant markers

The kidneys were removed and dissected free from the surrounding fat and connective tissue. Each kidney was longitudinally sectioned, and renal cortex was separated and kept at -8°C. Subsequently, renal cortex was homogenized in cold potassium phosphate buffer (0.05 M, pH 7.4). The renal cortical homogenates were centrifuged at 5000 rpm for 10 min at 4°C. The resulting supernatant was used for the determination of superoxide dismutase (SOD),¹⁴ catalase (CAT),¹⁵ lipid peroxidation (TBARS)¹⁶ and glutathione (GSH)¹⁷ using colorimetric assay.

Statistical analysis

Data was analysed by applying one-way ANOVA followed by Tukey's multiple comparison test using Graphpad Prism 5 software, version 5.3 La Jolla, San Diego, California, USA. Significance level was set at $p < 0.05$. All values are expressed as Mean \pm SEM.

RESULTS

Preliminary phytochemical screening

The preliminary phytochemical investigations of ethanolic and aqueous extracts of dried roots of *Coleus forskohlii* showed the presence of carbohydrates, proteins, amino acids, terpenoids and steroids, flavonoids, tannins, saponins and glycosides. Percentage yield of ethanolic extract was 11.35 grams and aqueous being 14 grams.

Acute oral toxicity study

Acute oral toxicity studies revealed the non-toxic nature of ethanolic and aqueous extracts of dried roots of *Coleus forskohlii*. There was no lethality observed nor any profound toxic reactions found at a dose of 2000 mg/Kg p.o. which pronounces the safety profile of the plant extract. Therefore 500mg/Kg was selected for further study.

Gentamicin-induced nephrotoxicity study

The results demonstrated significant improvement in urea, uric acid and creatinine levels on treatment with Silymarin, ethanolic and aqueous extracts of dried roots of *Coleus forskohlii* respectively, as these renal markers were increased in animals treated with gentamicin alone indicating nephrotoxicity. When compared between the two extracts, aqueous extracts have produced more potent reduction in the renal function parameters compared to the ethanolic extract treated group. Results are tabulated in (Table 2). Mean percent decrease in renal markers compared to gentamicin control are depicted in Figure 1,2, and 3.

Table 2. Effect of treatments on Serum Urea, Uric acid and Creatinine.

Treatment Groups	Urea(mg/dl)	Uric acid(mg/dl)	Creatinine(mg/dl)
Normal Control, Saline 0.5ml p.o	22 ± 1.97	2.7 ± 0.07	0.46 ± 0.07
Silymarin100mg/Kg, p.o	28 ±1.16 ^a	3.1 ± 0.18 ^a	0.5 ± 0.08 ^a
Gentamicin Control 80 mg/Kg, IP	45 ± 1.58 ^b	6.7 ± 0.4 ^b	1.7 ± 0.09 ^b
Aqueous Extract (CF) 500 mg/Kg, p.o	29 ± 1.71 ^a	3.4 ± 0.2 ^a	0.6 ± 0.06 ^a
Ethanolic Extract (CF) 500mg/Kg, p.o	34 ± 1.24 ^a	4.6 ± 0.3 ^a	1.1 ±0.7 ^a

All values are expressed as Mean± SEM, (CF): *Coleus Forskohlii*

a : p<0.001 Compared to Normal Control

b: p<0.001 Compared to Gentamicin Control

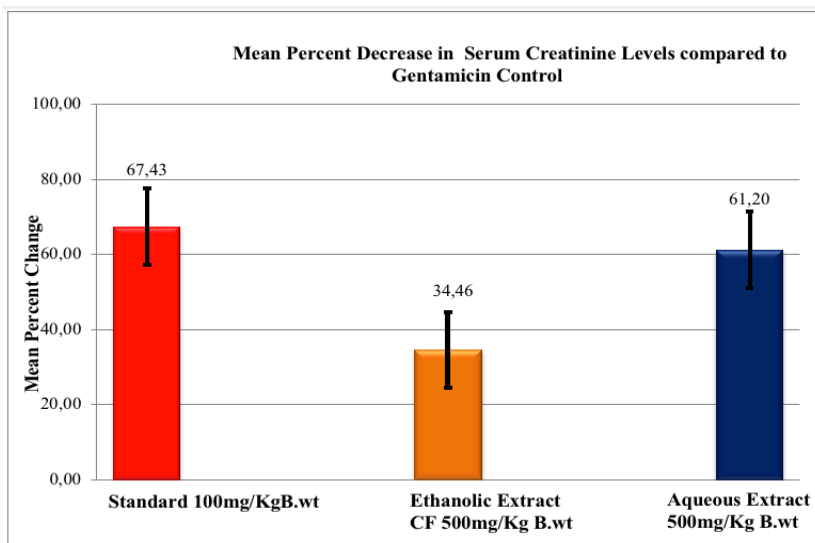


Figure 1. Mean percent decrease in serum creatinine levels compared to Gentamicin control.

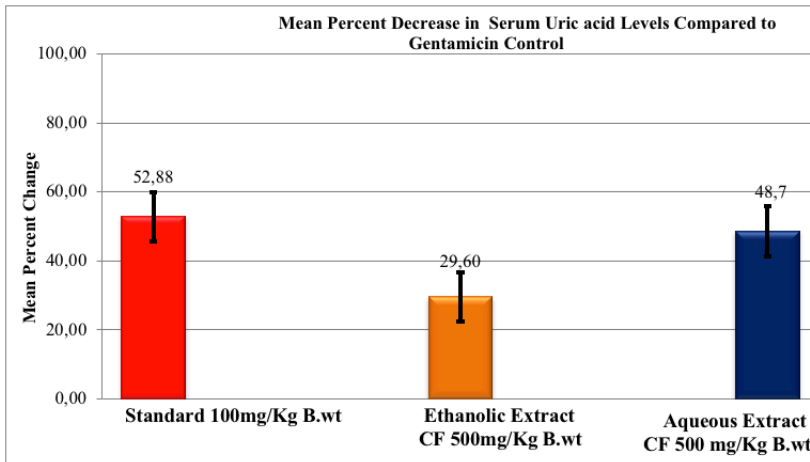


Figure 2. Mean percent decrease in serum uric acid levels compared to Gentamicin control.

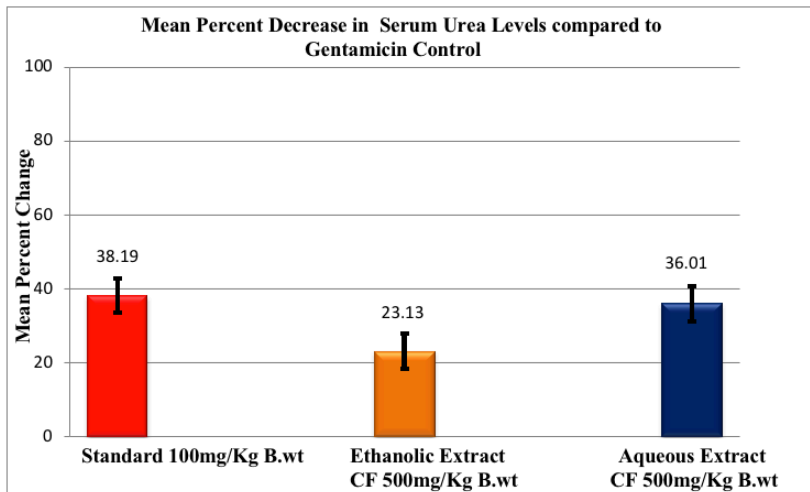


Figure 3. Mean percent decrease in serum urea levels compared to Gentamicin control.

Effect on body weights

The body weights were decreased in gentamicin treated animals compared to their initial body weights. Treatment with Silymarin, ethanolic and aqueous extracts of *Coleus forskohlii* improved the body weights compared to gentamicin control group but not statistically significant. Comparison of initial and final body weight between the groups is depicted in (Table 3).

Table 3. Comparison between initial and final body weights.

Treatment Groups	Initial Body Weight (grams)	Final Body Weight (grams)
Normal Control, Saline 0.5ml p.o	180 ± 0.9	200 ± 1.0
Silymarin100mg/Kg, p.o	152 ± 0.67	166 ± 2.44
Gentamicin Control 80 mg/Kg, IP	166 ± 1.47	157 ± 1.78
Ethanolic Extract (CF) 500 mg/Kg, p.o	156 ± 1.21	161 ± 2.56
Aqueous Extract(CF) 500 mg/Kg, p.o	164 ± 1.47	170 ± 2.33

All values are expressed as Mean± SEM, (CF): *Coleus Forskohlii*

Effect on kidney weight:

The kidney weights were increased in gentamicin treated groups compared to normal. Whereas treatment with Silymarin, ethanolic and aqueous extracts of *Coleus forskohlii* significantly reduced the relative kidney weights compared to the gentamicin control. Comparison of kidney weight between the groups is depicted in (Table 4).

Table 4. Effect treatments on kidney weight.

Treatment Groups	Kidney Weight (grams)
Normal Control Saline, 0.5ml p.o	0.66 ± 0.01
Silymarin100mg/Kg, p.o	0.74 ± 0.01
Gentamicin Control 80 mg/Kg, IP	0.86 ± 0.08
Aqueous Extract (CF)500 mg/Kg, p.o	0.65 ± 0.09 ^a
Ethanolic Extract (CF) 500 mg/Kg, p.o	0.76 ± 0.08 ^a

All values are expressed as Mean± SEM, (CF): *Coleus Forskohlii*

a: p<0.001 Compared to Gentamicin Control

Results of Histopathology

Group I- Treated with normal saline

The animals of Group I, were treated with only normal saline showed normal renal glomeruli with the intact bowman's capsule. Other structures like brush border cuboidal epithelium which lines the proximal convoluted tubules, simple cuboidal epithelium, which lines the distal convoluted tubules, and macula densa were very prominent. (Figure 4).

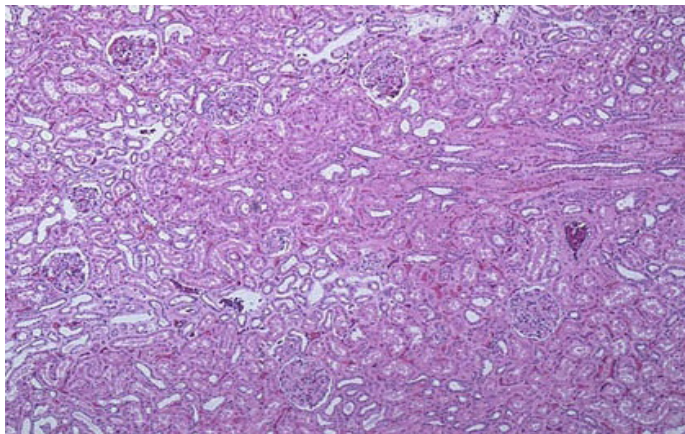


Figure 4. Photomicrograph of kidney of animals treated with normal saline.

Group II- Treated with Gentamicin+ Silymarin

Multifocal tubular inflammation in which infiltration of inflammatory cells are noticed. Glomerulus appeared normal, no degeneration nor inflammation was found. Only Moderate tubular degeneration was observed (Figure 5).

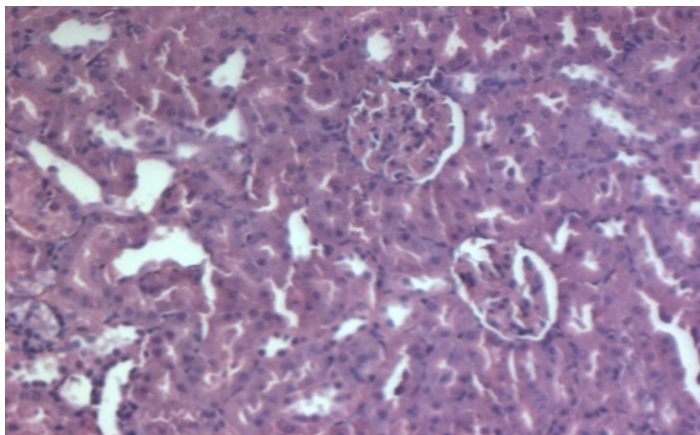


Figure 5. Photomicrograph of kidney of animals treated with Silymarin.

Group III- Treated with Gentamicin

Close examination of the sections at high magnification, revealed the appearance of cells with alterations typical of apoptosis (cell shrinkage and cytoplasm eosinophilia, presence of small and shrunken nucleus with chromatin condensation), break down of glomerular capillaries and vacuolar appearance in tubular lumen, glomerular congestion, disruption of glomerular capillaries, vacuolar degeneration of tubular epithelial cell is observed with hyaline cast formation. Atrophic glomeruli are present effecting half of the cortical region. (Figure 6).

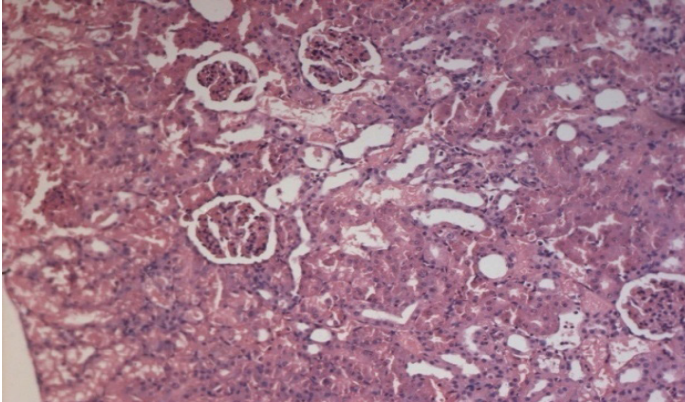


Figure 6. Photomicrograph of kidney of animals treated with Gentamicin

Group IV- Treated with ethanolic extract of *Coleus forskohlii* + Gentamicin

Treatment with Ethanolic extract of *Coleus forskohlii* reversed most of the histopathological alterations induced by Gentamicin as seen from the sections from gentamicin treated rats. Moderate tubular interstitial nephritis in which inflammation along with infiltration of inflammatory cells noticed in the interstitium between tubular region. Moderate tubular degeneration was also observed. (Figure 7).

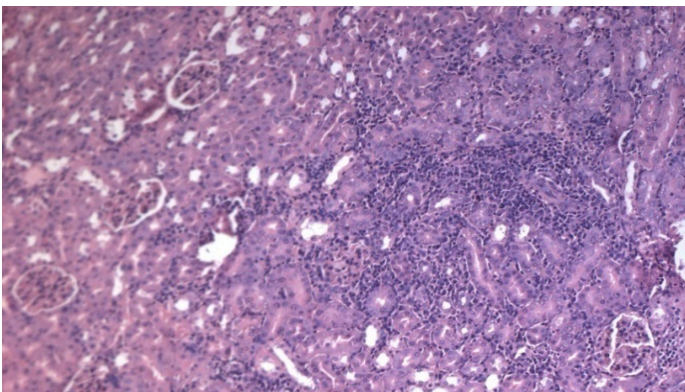


Figure 7. Photomicrographs of kidney of animals treated with ethanolic extract of *C. forskohlii* and Gentamicin.

Group V- Treated with aqueous extract of *C. forskohlii* + Gentamicin

Treatment with Ethanolic extract of *Coleus forskohlii* also reversed most of the histopathological alterations induced by Gentamicin. Photomicrographs of kidneys from this group revealed more prominent protection by showing normal glomeruli with absence of atrophy and hypertrophy. (Figure 8).

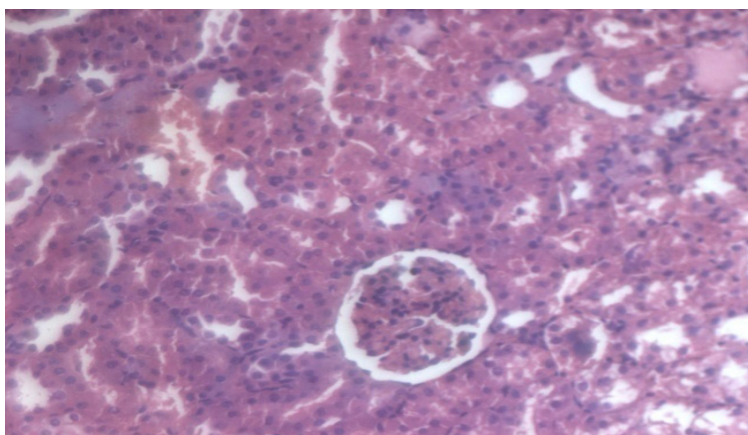


Figure 8. Kidney T.S. of animals treated with aqueous extract of *C. forskohlii* and Gentamicin.

Effect of treatments on antioxidant enzymes.

Treatment with gentamicin produced reduction in the superoxide dismutase levels compared to control. Whereas treatment with standard and extracts of *C. forskohlii* showed significant increase in superoxide dismutase levels compared to control indicating the antioxidant activity.

There was increase in malondialdehyde levels in gentamicin treated group compared to control, which suggests the nephrotoxic effect of gentamicin. However, two weeks of treatment with standard Silymarin and *C. forskohlii* showed significant decrease in thiobarbituric acid reactive substances i.e, malondialdehyde compared to control.

Treatment with standard, ethanolic and aqueous extract of *C. forskohlii* showed significant antioxidant effect, by producing increase in catalase levels compared to control. Gentamicin produced significant decrease in catalase levels compared to control, which explains the nephrotoxic effect of it.

Treatment with gentamicin showed significant decrease in glutathione levels, whereas two weeks of administration with Silymarin, ethanolic and aqueous extract of *C. forskohlii* produced significant increase in these levels compared to control. Results are shown in Table 5.

Table 5. Effect of treatments on antioxidant enzymes.

Treatment Groups	SODs (Units/ mg protein)	MDA (nanomoles/g tissue)	Catalase (Units/ mg protein)	Glutathione (Micromoles/g tissue)
Normal Control Saline, 0.5ml p.o	16.01 ± 0.46	10.37 ± 0.36	15.20 ± 0.42	14.27 ± 0.42
Silymarin100mg/ Kg, p.o	16.93 ± 0.31 ^b	8.49 ± 0.33 ^{ab}	17.11 ± 0.39 ^{ab}	16.26 ± 0.35 ^{ab}
Gentamicin Control 80 mg/ Kg, IP	8.88 ± 0.30 ^a	17.42 ± 0.42 ^a	6.93 ± 0.57 ^b	8.70 ± 0.33 ^b
Ethanollic Extract (CF) 500 mg/ Kg, p.o	11.14± 0.58 ^b	14.02 ± 0.30 ^{ab}	10.78±0.43 ^b	10.89 ± 0.50 ^{ab}
Aqueous Extract (CF) 500 mg/ Kg, p.o	15.55 ± 0.39 ^b	11.90 ± 0.32 ^b	13.19 ± 0.41 ^b	12.20 ± 0.61 ^{ab}

All Values expressed as Mean ±SEM, (CF): *Colueus Forskohlii*

SOD: Superoxide dismutase, MDA: Malondialdehyde

a: p<0.001 Compared to Normal Control

b: p<0.001 Compared to Gentamicin Control

DISCUSSION

Gentamicin is a promising bactericidal with less bacterial resistance properties. It is known for producing reversible and irreversible renal toxicity.¹⁸ The key pathological event in gentamicin-induced nephrotoxicity is through accumulation of drug and eventually resulting in renal dysfunction.¹⁹ It is a cation, which has a strong affinity towards negatively charged brush-border membrane components of proximal tubule where it can form drug receptor complex with megalin, a cationic drug receptor. The specificity of renal toxicity is apparently related to its preferential accumulation in the renal proximal convoluted tubules (50 to 100 times greater than serum). Then, pinocytosis translocates the drug to lysosomes, where phospholipidosis takes place to interrupt various intracellular renal functions leading to renal injury.^{20,21} This renal injury in turn manifests the migration of monocytes and macrophages to the site of injury by stimulating intercellular adhesion molecule-1 and monocyte chemoattractant protein.^{22,23} Kacew et al. and Aronoff et al.,²⁴⁻²⁷ demonstrated that the accumulation of the drug in specific target organelles in the renal cortex may be the critical step in

nephrotoxicity and it is generally agreed that gentamicin produces dose-dependent proximal renal tubular necrosis, which can be dissociated from intracellular accumulation. Papanikolaou et al,²⁸ reported that gentamicin is incorporated and accumulated in proximal tubule lysosomes which explain the gentamicin-induced nephrotoxicity.

GM induced nephrotoxicity is distinguished by elevated levels of urea and creatinine in plasma as well as urine, along with severe proximal tubular necrosis, resulting renal failure.²⁹ Similarly it is reported that treatment with only GM leads to significant increase in weight of kidney in rats.³⁰ Several days of treatment with aminoglycosides can cause defect in renal concentrating ability, which leads to mild proteinuria, reduction in glomerular filtration rate and appearance of hyaline and granular casts. Padmini et al, in their study reported that administration of 80 mg/Kg gentamicin dose in rats for ten days produced significant increase in serum creatinine, urea and uric acid.³¹ Similar pattern of changes were also observed in our study following GM treatment. Supplementation with aqueous and ethanolic extracts of roots of *C. forskohlii* in GM treated rats recorded decrement in levels of urea, uric acid and creatinine in serum which explains the worthwhile effect of this plant product on renal function. These observations indicate an improved renal function in form of effective clearance of urea and creatinine. Silymarin was also found to reduce the levels of renal markers similar to the plant extracts used in the study.

The release of oxygen-free radicals has been proposed as important mediator of GM-induced acute renal failure.³² These reactive oxygen species (ROS), lead to deficiency in intrinsic antioxidant enzymes.³³⁻³⁶ Its administration into rats induced impairment of renal function through liberation of oxygen free radical.³⁵ ROS have been suggested as a cause of death for many cells in different pathological states including various models of renal and cardiac diseases.³⁷ Several compounds with antioxidant activity has been successfully used to prevent or ameliorate gentamicin-induced nephrotoxicity. In the present study, the role of ROS in GM-induced nephrotoxicity was assessed by employing antioxidant agent, *C. forskohlii*, and further evaluation of alterations in the biochemical indicators of oxidative stress mainly GSH, TBARS levels, SOD and CAT.

It has been reported that under normal conditions, ROS, which are generated during cellular functions, are eliminated by intrinsic antioxidant enzymes like superoxide dismutase, catalase and glutathione peroxidase. Therefore, ROS scavengers and antioxidant molecules have the capacity to partially reduce or eliminate the deleterious effects induced by gentamicin. In the present study, the levels of lipid peroxidation stress markers significantly increased in GM

treated animals. Whereas treatment with *C. forskohlii*, demonstrated significant decrease in TBARS, indicating its anti-oxidant effect. Our study results are in accordance with the earlier published reports which explains the beneficial effect of *C. forskohlii* against reactive oxygen species.

Medicinal plants are important sources of natural products which differ widely in terms of their structures, biological properties and mechanisms of action. Various phytochemical components, especially polyphenols such as tannins, flavonoids, phenyl propanoids and phenolic acids, are known to have anti-oxidant and free radical scavenging efficacy. Polyphenols have various biological effects, which are mainly attributed to their antioxidant activities in scavenging free radicals, inhibition of lipid peroxidation and metal chelation. Polyphenols share the same general chemical pattern, with one or more phenolic groups which react as hydrogen donors and thus neutralize free radicals. The protective effect of this plant against gentamicin-induced nephrotoxicity can be attributed to the presence of phytoconstituents such as flavonoids, terpenoids and phenols. Forskolin being the major chemical constituent, herbal preparations of it act on various multiple pharmacological mechanisms. Forskolin was identified in shoot differentiating culture, micropropagated plants and root organ suspension by TLC and HPLC.³⁸ The blood pressure lowering and antispasmodic effects of extracts of *C. forskohlii* roots were reported by Dubey et al, based on the extensive screening of Indian plants for biological activity.³⁹ The principle mechanism by which forskolin exerts its hypotensive activity is by stimulation of adenylate cyclase and thereby increasing cellular concentrations of the secondary messenger cyclic AMP (cAMP).⁴⁰

Some investigators have demonstrated in their observations regarding the histopathological and structural changes in renal tissue post administration of GM.^{41,42} In our earlier study, we have reported the histopathological view of renal sections in GM treated group which showed degeneration, desquamation and necrosis in tubules and swelling in glomerulus, as compared to control group.¹³ Similarly, in the present work on histopathological examination we have observed damage in the structure of kidneys of gentamicin treated rats. Glomerular and tubular epithelial changes were considerably mild in the groups treated with aqueous and ethanolic extract of *C. forskohlii* along with restoration of normal histopathology. Two weeks of treatment with GM+ethanolic extract in the dose of 500mg/Kg showed moderate tubular epithelial changes while in case of animals treated with GM+aqueous showed regeneration in tubular epithelial cells. We expect that, morphological changes in kidneys were because of GM injection, but these changes were considerably mild in GM plus aqueous extract treatment. In summary, our data indicate that GM-induced nephrotoxicity might be related

to oxidative damage. Co-administration of *C. forskohlii* diminished the negative effects of GM-induced nephrotoxicity possibly by inhibiting free radical mediated process. Further investigation of these promising protective effects of *C. forskohlii* against GM-induced renal injury may have a considerable impact on developing clinically feasible strategies to treat patients with renal failure.

CONCLUSIONS

In conclusion, the results of the present study infer that the antioxidant activity and medicinal properties of *C. forskohlii* may be responsible for protection against GM-induced renal damage. When compared between the two extracts, aqueous extract showed more potent response in comparison to ethanolic. These findings also suggest the probable efficacy of *C. forskohlii* extract against oxidative deterioration and can be useful novel nephroprotective agent in the prevention of oxidative stress-related degenerative diseases. Further studies are warranted in pre-clinical and clinical set up, and for studying the structure of phytoconstituents in establishing pharmacological activities.

ACKNOWLEDGEMENTS

The authors thank Shadan Educational Society, Hyderabad, India, for providing necessary facilities for carrying out this research study. The authors are also thankful to Mr. M.A. Hafeeze Khan for assisting in study related procedures.

Funding: No funding sources

Conflict of interest: None declared

REFERENCES

1. Nagai, J. Molecular mechanisms underlying renal accumulation of aminoglycoside antibiotics and mechanism-based approach for developing non-nephrotoxic aminoglycoside therapy. *Yakugaku Zasshi*. **2006**, 126 (5), 327-35.
2. Abdel, Rahman.; R.S. Protective effect of apocynin against gentamicin induces nephrotoxicity in rats. *Human & Experimental Toxicology*. **2017**, 37(1), 27-37.
3. Mohammed, A.M.; Salwa I.A.; Entesar FA, Maha Y. K, Rehab A R, Magdy KH. Sildenafil Ameliorates Gentamicin-Induced Nephrotoxicity in Rats. Role of iNOS and eNOS. *Journal of Toxicology*. **2014**, 4893, 82.
4. Zeynab, M. Y.; Najafi, H.; Hamid, S.M. Protective of crocin on gentamicin induced nephrotoxicity in rats. *Iranian Journal of Basic Medical Sciences*. **2016**, 19(3), 337-343.
5. Al, asbahi, R.H.; Melziq, M.F. *Plectranthus barbatus*: A Review of photochemistry. ethanobotanical uses and pharmacology-part 1. *Planta Med*. **2010**, 76 (7), 653-61.
6. Kambham, V.N.; Devanna, K.B; Chandrasekhar. Preliminary phytochemical screening of roots of *Coleus forskohlii*. *International Journal of Current Trends In Pharmaceutical Research*. **2014**, 2 (6), 703-708.

7. Schaneberg, B.T.; Khan, I.A. Quantitative analysis of forskolin in *Coleus forskohlii* (Lamiaceae) by reversed-phase liquid chromatography. *JAOAC Int.* **2003**, *86*, 467–470.
8. Sharma, Y.; Vasundhara, M. Coleus (Plectranthus Barbatus) – A Multipurpose Medicinal Herb. *International Research Journal of Pharmacy.* **2011**, *2* (3), 47-58.
9. Malarvizhi, A.; Sivangami, S. Antioxidant potential of roots of *Coleus Forskohlii* in Balb/C Mice with DLA tumour. *International Journal of Pharmaceutical Sciences and Research.* **2015**, *31*(1), 38-41.
10. Khandelwal, K.R.; Kokate, C.K.; Gokhale, S.R. Practical Pharmacognosy Techniques and Experiments. Pune: Nirali Prakashan Publications; **1996**, 104-106.
11. OECD Guideline for Testing of Chemicals. Acute Oral Toxicity – Fixed Dose Procedure. 423 Adopted: 17th December; **2001**.
12. Ramesh, K.; Sudha, A.; Manimaran, A.; Saravanan, D.; Natrajan, E. Beneficial Effect of *Bacopa Monniera* Extract on Gentamicin Induced Nephrotoxicity and Oxidative stress in Albino Rats. *International Journal of Pharmacy and Pharmaceutical Sciences.* **2011**, *3*(5), 144-148.
13. Nishat, F.; Hajera, S. Evaluation of protective effect of *Terminalia Bellarica* against gentamicin induced nephrotoxicity in albino rats. *Pharmaceutical and Biological Evaluations.* **2016**, *3* (5), 486-494.
14. Caraway, W.T. Uric acid. In: Standard methods of clinical chemistry. Vol. 4. New York, **1963**: 239.
15. Habig, W.H.; Pabst, M.J.; Jakoby, W.B. Glutathione-S-transferase the first enzymatic step in mercapturic acid formation. *J Biol Chem.* **1974**, *249*(7), 130-139.
16. Aebi, H. Catalase In: Methods in enzymatic analysis. Bergmeyer. H.U. (Eds.). Academic Press. New York; **1983**, 276-286.
17. Rao, K.S.; Recknagel, R.O. Early onset of lipid peroxidation in rat liver after carbon tetrachloride administration. *Exp Mol Pathol.* **1968**, *9*, 271-278.
18. Appel, G.B. Aminoglycoside nephrotoxicity. *Am J Med.* **1990**, *88*,165-205.
19. Hori, R.; Inui, K. Cellular basis of aminoglycoside nephrotoxicity. *Physiology.* **1989**, *4*, 181–184.
20. Laurent, G.; Carlier, M.B.; Rollman, B.; Van, Hoof, F.; Tulkens, P. Mechanism of aminoglycoside-induced lysosomal phospholipidosis: *In vitro* and *in vivo* studies with gentamicin and amikacin. *Biochem Pharmacol.* **1982**, *31*, 3861–3870.
21. Sandhu, J.S.; Sehgal, A.; Gupta, O.; Singh, A. Aminoglycoside nephrotoxicity revisited. *J Indian Acad Clin Med.* **2007**, *8*, 331–333.
22. Wahl, S.M.; Hunt, D.A.; Wakefield, L.M.; McCartney-Francis, N.; Wahl, L.M.; Roberts. A.B.; et al. Transforming growth factor type beta induces monocyte chemotaxis and growth factor production. *Proc Natl Acad Sci.* **1987**, *84*, 5788–5792.
23. Feng, L.; Mathison, J.C.; Wilson, C.B. Cytokine expression, upregulation of intercellular adhesion molecule-1, and leukocyte infiltration in experimental tubulointerstitial nephritis. *Lab Invest.* **1994**, *70*, 631–638.
24. Kacew, S.; Bergeron, M.G. Pathogenic factors in aminoglycoside-induced nephrotoxicity. *Toxicol Letters.* **1990**, *51*, 241-59.
25. Aronoff, G.R.; Pottratz, S.T.; Brier, M.E.; Walker, N.E.; Fineberg, N.S.; Glant, M.D.; Luft,

F.C. Aminoglycosides accumulation kinetics in rat renal parenchyma. *Antimicrob Agents Chemother.* **1983**, *23*, 74-78.

26. Patel, V.; Luft, F.C.; Yum, M.N.; Patel, B.; Zeman, W.; Kleit, S.A. Enzymuria in gentamicin induced kidney damage. *Antimicrobial Agents Chemotherapy.* **1975**, *7*, 364-369.

27. Bennet, W.M.; Elliott, W.C.; Houghton, D.C.; Gilbert, D.N.; Defehr, J.; McCarran, D.A. Reduction of experimental gentamicin nephrotoxicity in rats by dietary calcium loading. *Antimicrob Agents. Chemother.* **1982**, *22*, 508-512.

28. Papanikolaou, N.; Peros, G.P.; Morphake, P.; Gkikas, G.; Maraghianne, D.; Tsipas, G.; et al. Does gentamicin induce acute renal failure by increasing renal TX₂ synthesis in rats. Prostaglandins. *Leukotrienes and Essential Fatty Acids.* **1992**, *45*, 131-136.

29. Laskshmi, B.V.S.; Sudhakar, M. Protective effect of *Zingiber officinale* on gentamicin-induced nephrotoxicity in rats. *Int J Pharmacol.* **2010**, *6*, 58-62.

30. Gilbert, D.N.; Wood, C.A.; Kohlhepp, S.; Kohnen, P.W.; Houghton, D.C.; Finkbener, H.C.; et al. Polyaspartic acid prevents experimental aminoglycoside nephrotoxicity. *J Infect Dis.* **1989**, *159*, 945-53.

31. Padmini, P.M.; Kumar, V.J. A Histopathological Study on Gentamicin Induced Nephrotoxicity in Experimental Albino Rats. *Journal of Dental and Medical Sciences.* **2012**, *1*, 14-17.

32. Baliga, R.; Ueda, N.; Walker, P.D.; Shah, S.V. Oxidant mechanisms in toxic acute renal failure. *Drug Metab Rev.* **1999**, *31*, 971-997.

33. Morales, A.I.; Buitrago, J.M.; Santiago, J.M.; Fernández, T. M.; López-Novoa, J.M.; Pérez, B.F. *Antioxid. Redox Signal.* **2002**, *4*, 893-898.

34. Yanagida, C.; Ito, K.; Komiya, I.; Horie, T. Protective effect of fosfomycin on gentamicin-induced lipid peroxidation of rat renal tissue. *Chem Biol Interact.* **2004**, *148*, 139-147.

35. Maldonado, P.D.; Barrera, D.; Medina-Campos, O.N.; Hernández- Pando, R.; Ibarra-Rubio, M.E.; Pedrazza-Chaverri J. Aged garlic extract attenuates gentamicin induced renal damage and oxidative stress in rats. *Life Sci.* **2003**, *73(20)*, 2543-2556.

36. Heibashy, M.I.A.; Abdel, Moneim A.E. Kidney and liver function tests after late Dimethyl sulfoxide (DMSO) administration in rats with gentamicin induced acute renal failure. *J Egypt Ger Soc Zool.* **1999**, *30*, 35-48.

37. Pedraza, J.C.; Barrera, D.; Hernández, P.R.; Medina, O.N.; Cruz, C.F., Murguía, F.; et al. Soy protein diet ameliorates renal nitrotyrosine formation and chronic nephropathy induced by puromycin aminonucleoside. *Life Sci.* **2004**, *74*, 987-999.

38. Sen, J.; Sharma, A.K.; Sahu, N.P.; Mahato, S.B.; Production of forskolin in in vitro cultures of *Coleus forskohlii*. *Planta Med.* **1992**, *58*, 324-332

39. Dubey, M.P.; Srimal RC, Patnaik GK, Dhawan BN. Blood pressure lowering and antispasmodic effects of *C. forskohlii* Briq. *Indian J. Pharm.* **1974**, *6*, 15.

40. Seamon, K.B.; Daly, J.W. Forskolin: a unique diterpene activator of cyclic AMP-generating systems. *J. Cyclic Nucleotide Res.* **1981**, *7*, 204-224.

41. Soumya, P.S.; Poornima, K.; Ravikumar, G.; Kalaiselvi, M.; Gomathi, D.; Uma; C. *Journal of Pharmacy Research.* **2011**, *4(8)*, 2474-2476.

42. Sodimbaku, V.; Pujari, L.; Mullangi, R.; Marri, S. Carrot (*Daucus carota* L.): Nephroprotective against gentamicin-induced nephrotoxicity in rats. *Indian J Pharmacol.* **2016**, *48 (2)*, 122-127.

Polyamine Metabolism and Obesity: Polyamine Metabolic Enzymes Involved in Obesity

Nihal Büyükuslu^{1*}, Rabia İclal Öztürk¹

¹Department of Nutrition and Dietetics, School of Health Sciences, Istanbul Medipol University, Istanbul, Turkey

ABSTRACT

The natural polyamines, putrescine, spermidine and spermine are distributed widely in all cells including adipocytes. They are involved in several physiological processes involving gene expression and cell proliferation. The body pool of polyamines is maintained by endogenous biosynthesis, intestinal microorganisms and the diet. A correlation between fat metabolism and polyamine metabolism has been reported in several studies. It was shown that the inhibition of polyamine metabolism enzymes had been associated with increased adipose tissue and weight gain in human and animal models. Ornithine decarboxylase (ODC) and S-adenosylmethionine decarboxylase (AdoMetDC) are anabolic enzymes; and spermidine/spermine N1-acetyltransferase (SSAT) and polyamine oxidase (PAO) are catabolic enzymes which regulate polyamine homeostasis. Genetically altered polyamine metabolic enzymes resulted in higher tissue adipose content and weight gain indicating potential links between obesity and polyamine metabolism. This review aims to provide details on previously reported sources of data published on polyamine metabolism and obesity.

Key words: Polyamine, obesity, ornithine decarboxylase, S-adenosylmethionine decarboxylase, spermidine/spermine N1-acetyltransferase, polyamine oxidase

INTRODUCTION

Putrescine, spermidine and spermine are the natural amines distributed widely in all cells including adipocytes. They are involved in several physiological processes such as DNA stabilization, regulation of gene expression, ion channel function and cell proliferation.¹ The aim of this review is to evaluate the relationship between polyamine metabolic enzymes and lipid metabolism to shed light on the treatment of obesity.

*Corresponding author: Nihal Büyükuslu, e-mail: nbuyukuslu@medipol.edu.tr
(Received 06 March 2018, accepted 28 March 2018)

Polyamines and metabolism

Polyamine homeostasis is regulated by synthesis, degradation and membrane transport of polyamines in mammalian cells (Figure 1).² Ornithine decarboxylase (ODC) and S-adenosyl-L-methionine decarboxylase (AdoMetDC) are the two key enzymes in the polyamine biosynthetic pathway. They are strongly regulated by feedback mechanisms at transcriptional, translational and posttranslational levels. Spermidine/spermine N1-acetyltransferase (SSAT) and polyamine oxidase (PAO) control the catabolism of polyamines in the polyamine metabolism. An increase in cellular polyamines rapidly induces SSAT, resulting in increased degradation/efflux of the polyamines. In addition, the active transport of extracellular polyamines into the cell associates with cellular polyamine homeostasis. In cytoplasm, the rate-limiting enzyme, SSAT acetylates the spermidine and spermine using acetyl-coenzyme A (CoA) to form N-acetylspermidine and N-acetylspermine. Then acetylated forms of polyamines are oxidized by PAO and converted into putrescine and spermidine, respectively.^{3,4} SSAT is a key metabolic regulator in polyamine homeostasis.⁵ The overexpression of polyamine-acetylating enzyme SSAT significantly increases biosynthesis and metabolic flux through the polyamine pathway.⁶ Via acetylation, the net positive charge of the polyamines declines and increased anionic character of polyamines alters the binding activity with biological molecules.³ The acetyl derivatives can be removed from the cells by transport and catabolism. Since SSAT is sensitive to cellular environment it rapidly alters its activity. SSAT basal activity is very low but increases quickly when polyamines are in excess.⁷ The short half-life of SSAT (20 min.) is also important to allow the cell to rapidly change the enzyme and polyamine levels.⁸ Two decarboxylase enzymes (ODC and AdoMetDC), the cytosolic acetyl-CoA:spermidine/spermine N1-acetyltransferase and a polyamine transport system are required for the regulation of cellular polyamine metabolism.

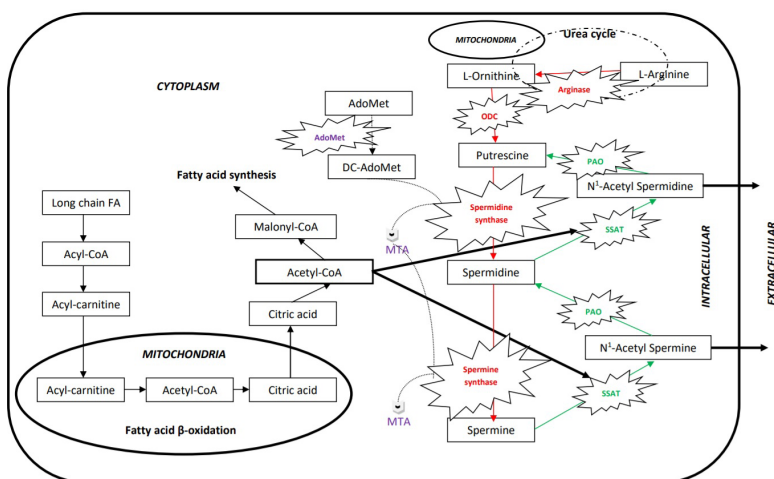


Figure 1. Metabolic pathways of polyamines and long chain fatty acids. AdoMet: S-Adenosyl methionine, AdoMetDC: Adenosylmethionine decarboxylase, DC-AdoMet: Decarboxylated S-adenosylmethionine, MTA: 5'-methylthioadenosine, ODC: Ornithine decarboxylase, PAO: *Polyamine oxidase*, SSAT: Spermidine/spermine N-1 acetyl transferase.

The levels of spermidine and spermine in cell are depended on polyamine homeostasis. Arginase catalysis the transformation of arginine to ornithine which is transformed to putrescine via ODC. Spermidine and spermine synthases catalyze the biosynthesis of spermidine from putrescine and spermine from spermidine respectively. The biosynthetic enzyme spermidine synthase uses DCAdoMet and putrescine to make spermidine and 5'-deoxy-5'-methylthioadenosine as a byproduct. The anabolic enzyme PAO deacetylates the N-Acetyl spermine and N-Acetyl spermidine to keep polyamines in cell for required processes. Long chain FAs are oxidized to yield Acetyl-CoA in mitochondrial matrix via beta oxidation. Then, acetyl-CoA can be degraded to CO₂ and H₂O via the Krebs Cycle in mitochondria or used for fatty acid synthesis through Malonyl-CoA in cytoplasm. In other pathway, acetyl-CoA can be used for activation of SSAT which catalysis the formation of acetylated spermidine and spermine before taken out of the cell.

Polyamine metabolism in obesity

Obesity is a growing health problem worldwide and associated with many diseases such as type II diabetes, stroke, cardiovascular disease, and cancer.⁹⁻¹¹ In obesity, positive caloric intake causes excess fat stored in adipocytes which are increased by their size (hyperplasia) and number (hypertrophy). Increasing in fat tissue rise energy expenditure, so that higher energy intake is needed to maintain energy balance. Thus, body weight can be regulated by energy intake and energy expenditure.

Adipose tissue is an active endocrine organ and a main energy store of the body. Excess fat accumulation leads the release of free fatty acids into the circulation from adipocytes. The major energy reserve in higher eukaryotes is triacylglycerol in white adipose tissue (WAT). In case of energy deprivation or changes in nutritional state, lipolysis in adipocytes regulating through hormonal and biochemical signals proceeds.

Indeed, the rates of fuel utilization and fuel storage have been regulated by acetyl- and malonyl-CoA pools. In case of limited fuel, glycogen is broken down into glucose and glycolysis is up-regulated through the AMP-*activated* protein kinase (AMPK) activation. When the level of glucose increased, acetyl-CoA accumulation can quickly be remedied by increased polyamine acetylation. One cycle of polyamine flux utilizes two acetyl-CoA moieties. These moieties can be used for polyamine acetylation. Acetylated forms of polyamines are excreted into the urine thus acetyl-CoA cannot be used for storing excess energy as fat. Any lost in energy is noteworthy since 2 acetyl-CoA molecules have the equivalent of 24 ATP molecules. Moreover, increased polyamine acetylation decreases the availability of acetyl-CoA for malonyl-CoA synthesis and increases fatty acid oxidation.

Excessive body weight associates with physiological mechanisms relating to control of fat deposition/mobilization. It has long been known that polyamines, specifically spermine and spermidine, stimulate adipose triacylglycerol formation by activation of several enzymes including sn-glycerol-3-phosphate acyltransferase, Mg²⁺-dependent phosphatidate phosphohydrolase and diacylglycerol acyl transferase.¹² In addition, at physiological concentrations, both spermine and spermidine have been shown to inhibit lipolysis by suppressing cyclic AMP levels and to facilitate glucose transport, which is accompanied by up-regulated conversion of glucose into triacylglycerols in adipocytes of Zucker obese rats.¹³ A comparison of lean and obese Zucker rats showed rising concentration of spermine and spermidine which was accompanied by increasing in the activities of various triacylglycerol synthetic enzymes.¹⁴ The inhibition of ODC, the enzyme producing putrescine and a limiting step in polyamine biosynthesis, by an irreversible inhibitor alpha-difluoromethylornithine (DFMO) prevented the differentiation of 3T3-L1 fibroblasts into adipocytes. In a recent paper, regulatory role of polyamines in adipogenesis was examined and it was shown that polyamines are required early in the adipogenic process.¹⁵

Polyamine flux is controlled by ODC, SSAT and PAO and has a role in energy metabolism.^{16,17} It was reported that perturbations of polyamine pathway flux were associated with obesity resistance or sensitivity in several mouse models.^{18,19} Nicotinamide N-methyltransferase (NNMT) methylates nicotinamide which is a precursor of NAD⁺ using S-adenosylmethionine (SAM). It was shown that an increase in spermidine was also accompanied by reduced levels of NNMT which is associated with obesity resistance.¹⁸ Additionally, the increase in spermidine in *Maf1*^{-/-} mice was accompanied by reduced levels of NNMT, which promotes polyamine synthesis, enables nicotinamide salvage to regenerate NAD⁺ and is associated with obesity resistance.²⁰ Therefore, it seems that targeting NNMT could be a promising approach for treating obesity and type 2 diabetes.

Regarding the proposed role of polyamines in hormone action, in a study by Grassi et al, it was suggested that polyamines may play a pivotal role in hormone responsiveness of hypothalamic-hypophyseal axis which was shown to contribute to the sympatho excitation of obesity.²¹ In obese and normal weight children luteinizing hormone (LH) values significantly increased after stimulation with acute gonadotropin-releasing hormone (GnRH) injection but reached higher peaks in normal children than in obese ones. On the contrary, polyamine levels increased significantly only in the normal weight children.²²

Genetic studies revealed a strong connection between SSAT activity and control of lipid metabolism. In transgenic mice, tissues were characterized by increased

N1-acetyltransferase activity, a marked elevation in tissue and urinary acetylated polyamines, a compensatory increase in polyamine biosynthetic enzyme activity, and an increase in metabolic flux through the polyamine pathway. SSAT-deficient mice developed insulin resistance at old age, possibly indicating that polyamine catabolism has a role in the regulation of glucose and energy metabolism.¹⁷ Male Gyro (Gy) mice with profound spermine deficiency due to the extensive disruption of both phosphate regulating endopeptidase and spermine synthase gene, exhibit the features of smaller size and lower weight than normal mice, whereas spermine synthase overexpressing mice are slightly larger than normal mice.^{23,24} In a study by Ishii et al, to explore the possible function of spermidine and spermine in adipogenesis, it was examined the effect of polyamine biosynthesis inhibitors, namely trans-4-methylcyclohexylamine (MCHA) and N-(3-aminopropyl)-cyclohexylamine (APCHA), on adipocyte differentiation and lipid accumulation of 3T3-L1 cells. They found that MCHA and APCHA have their own specific effects on both preadipocytes and mature adipocytes with the changes in SSAT activity suggesting that the control of polyamine metabolic enzyme activity could regulate adipogenesis.²⁵ Moreover, there has been a close link between the disturbances of cellular metabolism and mitochondrial dysfunction. Mitochondrial abnormalities may cause to the development of common metabolic disorders such as type 2 diabetes and obesity.²⁶ The activation of PGC-1 α , the master regulator of mitochondrial biogenesis and energy expenditure, in the WAT and liver of mice resulted that WAT-specific SSAT over expression was sufficient to increase the number of mitochondria, reduce WAT mass and protect the mice from high-fat diet-induced obesity.²⁷ Proteomics study on the liver tissues of SSAT-tg mice revealed changes in 23 proteins associated with polyamine catabolism.²⁸

In conclusion the polyamine metabolism enzymes modulate the acetyl-CoA flux associated with the lipolysis, energy metabolism and calorie loss influencing the accumulation of body fat. Any destruction on enzymes mainly SSAT, ODC, PAO and AdoMetDC reveals an alteration in the polyamine levels which may be associated with obesity. Therefore, in the future, polyamine metabolism should be considered as a valuable tool for research on lipid metabolism and drug development for obesity and related diseases.

CONFLICT OF INTEREST

Authors declare that there is no conflict of interest.

REFERENCES

1. Pegg, A.E. Functions of polyamines in mammals. *J. Biol. Chem.* **2016**, *291*, 14904–14912.
2. Persson, L. Polyamine homeostasis. *Essays Biochem.* **2009**, *46*, 11-24.
3. Wallace, H.M.; Fraser, A.V.; Hughes, A. A perspective of polyamine metabolism. *Biochem J.* **2003**, *376*, 1-14.
4. Perez-Leal, O.; Barrero, C.A.; Clarkson, A.B.; Merali, S. Polyamine-regulated translation of spermidine/spermine-N1-acetyltransferase. *Mol. Cell Biol.* **2012**, *32*(8), 1453-1467.
5. Pegg, A.E. Spermidine/spermine-N(1)-acetyltransferase: A key metabolic regulator. *Am. J. Physiol. Endocrinol. Metab.* **2008**, *294*, E995-1010.
6. Kramer, D.L.; Diegelman, P.; Jell, J.; Vujcic, S.; Merali, S.; Porter, C.W. Polyamine acetylation modulates polyamine metabolic flux, a prelude to broader metabolic consequences. *J. Biol. Chem.* **2008**, *283*, 4241-4251.
7. Casero, R.A.; Pegg, A.E. Polyamine catabolism and disease. *Biochem. J.* **2009**, *421*, 323-338.
8. McCloskey, D.E.; Pegg, A.E. Properties of the spermidine/spermine N1-acetyltransferase mutant L156F that decreases cellular sensitivity to the polyamine analogue N1,N11-bis(ethyl) norspermine. *J. Biol. Chem.* **2003**, *278*, 13881-13887.
9. Pearson-Stuttard, J.; Zhou, B.; Kontis, V.; Bentham, J.; Gunter, M.J.; Ezzati, M. Worldwide burden of cancer attributable to diabetes and high body-mass index: a comparative risk assessment. *Lancet Diabetes Endocrinol.* **2018**, *6*(2), 95-104.
10. Agha, M.; Agha, R. The rising prevalence of obesity: part A: Impact on public health. *Int. J. Surg. Oncol.* **2017**, *2*(7):e17.
11. Bhupathiraju, S.N.; Hu, F.B. Obesity, diabetes, and cardiovascular diseases Compendium. Epidemiology of obesity and diabetes and their cardiovascular complications. *Circ. Res.* **2016**, *118*, 1723-1735.
12. Jamdar, S.C.; Osborne, L.J. Glycerolipid biosynthesis in rat adipose tissue: II. Effects of polyamines on Mg²⁺-dependent phosphatidate phosphohydrolase. *Biochim. Biophys. Acta.* **1983**, *752*, 79-88.
13. Lockwood, D.H.; East, L.E. Studies of the insulin-like actions of polyamines on lipid and glucose metabolism in adipose tissue cells. *J. Biol. Chem.* **1974**, *249*, 7717-7722.
14. Jamdar, S.C.; Cao, W.F.; Samaniego, E. Relationship between adipose polyamine concentrations and triacylglycerol synthetic enzymes in lean and obese Zucker rats. *Enzyme Protein.* **1996**, *49*, 222-230.
15. Brenner, S.; Bercovich, Z.; Feiler, Y.; Keshet, R.; Kahana, C. Dual regulatory role of polyamines in adipogenesis. *J. Biol. Chem.* **2015**, *290*, 27384-27392.
16. Jell, J.; Merali, S.; Hensen, M.L.; Mazurchuk, R.; Spornyak, J.A.; Diegelman, P. et al., Genetically altered expression of spermidine/spermine N1-acetyltransferase affects fat metabolism in mice via acetyl-CoA. *J. Biol. Chem.* **2007**, *282*, 8404-8413.

17. Pirinen, E.; Kuulasmaa, T.; Pietila, M.; Heikkinen, S.; Tusa, M.; Itkonen, P. et al., Enhanced polyamine catabolism alters homeostatic control of white adipose tissue mass, energy expenditure, and glucose metabolism. *Mol. Cell Biol.* **2007**, *27*(13), 4953-4967.
18. Kraus, D.; Yang, Q.; Kong, D.; Banks, A.S.; Zhang, L.; Rodgers, J.T. et al., Nicotinamide N-methyltransferase knockdown protects against diet-induced obesity. *Nature.* **2014**, *508*, 258-262.
19. Liu, C.; Leal, O.P.; Barrero, C.; Zahedi, K.; Soleimani, M.; Porter, C.; et al., Modulation of polyamine metabolic flux in adipose tissue alters the accumulation of body fat by affecting glucose homeostasis. *Amino Acids.* **2014**, *46*, 701-715.
20. Bonhoure, N.; Brynes, A.; Moir, R.D.; Hodroj, W.; Preitner, F.; Praz, V. et al., Loss of the RNA polymerase III repressor MAF1 confers obesity resistance. *Genes Dev.* **2015**, *29*, 934-947.
21. Grassi, G.; Seravalle, G.; Dell'Oro, R.; Turri, C.; Pasqualinotto, L.; Colombo, M. et al., Participation of the hypothalamus-hypophysis axis in the sympathetic activation of human obesity. *Hypertension.* **2001**, *38*, 1316-1320.
22. Bernasconi, S.; Orlandini, G.; Reali, N.; Guarneri, G.; Soldi, M.E.; Bacciottini, F. et al., Effect of GnRH administration on blood polyamines and LH levels in normal and obese children. *Horm. Metab. Res.* **1988**, *20*, 648-651.
23. Meyer, R.A.; Henley, C.M.; Meyer, M.H.; Morgan, P.L.; McDonald, A.G.; Mills, C. et al., Partial deletion of both the spermine synthase gene and the Pex gene in the X-linked hypophosphatemic, gyro (Gy) mouse. *Genomics.* **1998**, *48*, 289-295.
24. Wang, X.; Ikeguchi, Y.; McCloskey, D.E.; Nelson, P.; Pegg, A.E. Spermine synthesis is required for normal viability, growth, and fertility in the mouse. *J. Biol. Chem.* **2004**, *279*, 51370-51375.
25. Ishii, I.; Ikeguchi, Y.; Mano, H.; Wada, M.; Pegg, A.E.; Shirahata, A. Polyamine metabolism is involved in adipogenesis of 3T3-L1 cells. *Amino Acids.* **2012**, *42*, 619-626.
26. Auwerx, J. Improving metabolisms by increasing energy expenditure. *Nat. Med.* **2006**, *12*, 44-45.
27. Koponen, T.; Cerrada-Gimenez, M.; Pirinen, E.; Hohtola, E.; Paananen, J.; Vuohelainen, S. et al., The activation of hepatic and muscle polyamine catabolism improves glucose homeostasis. *Amino Acids.* **2012**, *42*(2-3), 427-440.
28. Cerrada-Gimenez, M.; Hayrinen, J.; Juutinen, S.; Reponen, T.; Janne, J.; Alhonen, L. Proteomic analysis of livers from a transgenic mouse line with activated polyamine catabolism. *Amino Acids.* **2010**, *38*, 613-622.



M E D I P O L M E G A U N I V E R S I T Y H O S P I T A L
O R G A N T R A N S P L A N T C E N T E R

Donate an organ and
give a second life.

MEDIPOL
CALL
CENTER
+90 444 70 44
International WhatsApp Line:
+90 549 794 13 45
www.internationalmedipol.com

 MEDIPOL
MEGA
MEDIPOL
MEGA
HOSPITAL
COMPLEX

UNIVERSITY
HOSPITAL

 [medipolsaglik](https://www.instagram.com/medipolsaglik)

 [medipolsaglik](https://www.facebook.com/medipolsaglik)

 [medipolsaglik](https://www.twitter.com/medipolsaglik)

 [MedipolSaglikGrubu](https://www.youtube.com/MedipolSaglikGrubu)

Comparison of 3 Doses of *Aloe vera* and Burn Drugs in Market on Burnt Rat Models

Çağlar Macit^{1*}, M. Eşref Tatlıpınar², Emre Şefik Çağlar³, Neda Taner⁴, Senanur Turgut⁵, Elif Görkem Sarıkaya⁵

¹ İstanbul Medipol University, School of Pharmacy, Department of Pharmacology, İstanbul, Turkey.

² İstanbul Medipol University, School of Pharmacy, Department of Pharmaceutical Toxicology, İstanbul, Turkey.

³ İstanbul Medipol University, School of Pharmacy, Department of Pharmaceutical Technology, İstanbul, Turkey.

⁴ İstanbul Medipol University, School of Pharmacy, Department of Clinical Pharmacy, İstanbul, Turkey.

⁵ İstanbul Medipol University, School of Pharmacy, İstanbul, Turkey.

ABSTRACT

Burn injuries are an incident that can have serious traumatic consequences. Degree of tissue damage depends on height of heat and duration of contact. It can be classified as 4 different burn degrees. Herbal treatments can be applied for alleviating the symptoms alongside with pharmacological treatments in clinic. *Aloe vera* are used for burn cases for so many years because of its antiinflammatory, antiviral, antifungal, antibacterial, antidiabetic and rapid burn wound healing effects. Our aim in this study is to compare different doses of *Aloe vera* gel with burn medications in market. 48 female Sprague-Dawley rats divided into 8 groups (negative control, positive control, Silverdin®, Bepanthol®, Sudocrem®, *Aloe vera* 30 mg, *Aloe vera* 60 mg, *Aloe vera* 90 mg). For burn modelling, back of the rats were exposed to 90°C hot water which in the 1,5 cm diameter falcon tube for 10 seconds (burnt area: 7,069 cm²). After the modelling, serum physiologic was applied to each rat. Their treatments were always given at the same time. Experimental study was carried out with 14 numbered approval of İstanbul Medipol University Animal Experiments Local Ethical Committee. Obtained data were evaluated with SPSS v21 programme. After 15 days treatment, 30 mg of *Aloe vera* was more effective than Silverdin® cream (*Aloe vera* decreased burnt area: 3,064 cm², Silverdin® decreased burnt area: 3,731 cm²). The most effective drug among these medications is Sudocrem® with decreased burnt area 2,302 cm². Consequently, it can be seen that Sudocrem® is the most effective drug when comparing with these medications for burn treatment, and 30 mg dose of *Aloe vera* is better than Silverdin® cream.

Keywords: Burn, *aloe vera*, Sudocrem®, Silverdin®

INTRODUCTION

As a natural result of invention of fire, humanity encounters burn wounds since then. These wounds bring along injuries and deaths with them. Especially because of burn wounds, severe defects and also death may occur, according to its grade.

*Corresponding author: Çağlar Macit, e-mail: cmacit@medipol.edu.tr
(Received 01 March 2018, accepted 30 March 2018)

Extent of tissue damage depends on heat temperature and duration of contact. The severity of an injury is determined by measuring depth and width of the wound. Wound depth is identified mostly by clinical observation. Even the most experienced physicians can be misled when doing wound depth determination. There are several methods for wound depth determining but these are not generally accepted by experts.¹

Evaluation of burnt patient is done in two steps which are primary (first) and secondary (reexamination) evaluation.^{2,3} In the primary evaluation, life-threatening conditions are determined with rapid and systematic approaches. Urgent intervention and first aid operations are done in this step. Airway, breathing, circulation controls and immobilization of neck vertebrates are done, respectively. More detailed evaluation is taken part in second step and then patient transport is carried out and wound and maintenance treatment come after shock treatment.⁴

In the treatment of burn wound, wound depth determination is done after the clearance of wound. Wounds that has partial thickness are healed spontaneously. In first degree burns, 4-7 days are needed to recovery and 2-4 weeks for second degree burns. In this period, burn wound is protected from the outside by closing the wound.⁵

In recent years, nonpharmacological approaches with some plants for wound healing became popular and one of them is *Aloe vera*. Aloe has been used as a folk medicine because it has several important therapeutic properties.⁶ It can fight against fungal, viral and bacterial disease. Additionally, it has analgesic and antidiabetic effects. Beside these, Aloe forces and supports immune system of people.^{7,8}

In this study, we aimed to compare burn medicines in market with 3 different doses of *Aloe vera* preparations in rats that were formed as model of burn.

METHODOLOGY

Devices

We used various laboratory equipment such as fridge/deep frost, homogenizer, hot water bath, 50 mL falcon tube, surgical scissors, pliers, lancet, bistouries, surgical gloves, 5-10 mL syringes and ruler.

Chemical Substances and Drugs

For anesthesia; isoflurane (Forane-Abbott) and ketamine/xylazine (90/10 mg/kg) were used. For treatment; we used silver sulfadiazine (Silverdin®, Deva), dexpanthenol (Bepanthol®, Bayer), zinc oxide (Sudocrem®, MA Holder & Manufacturer) and Carbopol 934, triethanolamine, isopropyl alcohol and glycerin for preparation of *Aloe vera* gels. Silverdin, Bepanthol and Sudocrem were obtained from community pharmacies. Medicinal *Aloe vera* plant was purchased from Albanian Gardens greenhouse and gel was obtained by cutting of its

leaves. Finally, formulation was prepared at Istanbul Medipol University, School of Pharmacy, Department of Pharmaceutical Technology.

Formulation of *Aloe vera* Gel

Gel was prepared before addition of *Aloe vera*. Gel formulation is;

- Carbopol 934 1 g
- Triethanolamine 3,5 g
- Isopropyl alcohol 20 g
- Glycerin 7 g
- Distilled water q.s. 100 g

Preparation: Carbopol 934 and glycerin were mixed with each other, this mixture was homogenized by adding 50 grams of water. Homogenized isopropyl alcohol and water mixture was added into first mixture. Then, triethanolamine was dissolved in water and added into mixture dropwise. This mixture was stirred until the completion of gelation. Then, the mixture completed with water to the desired weight.

Animal Supply and Care Conditions

In this study, 48 female Sprague-Dawley rats which ranging in weight from 150 to 200 grams were used. Experimental study was carried out with 14 numbered approval of Istanbul Medipol University Animal Experiments Local Ethical Committee. Rats were obtained from Istanbul Medipol University. During the quarantine, rats were kept at a stable temperature ($23 \pm 1^\circ\text{C}$) for 12 hours. Also, they were kept for 12 hours in light and for 12 hours in dark. They were fed with standard rat food and allowed to reach water (tap water/*ad libitum*) (Figure 1).



Figure 1. Sprague-Dawley rats and experimental groups.

Burn Damage and Experimental Modelling

Current legal practices about experimental animal care were considered before, during and after the study. Rats were randomly divided into 8 groups (n=6). Experimental groups were named as; Group 1-negative control (completely healthy), group 2-positive control (burnt rats, no treatment), group 3-Silverdin®, group 4-Bepanthol®, group 5-Sudocrem®, group 6-*Aloe vera* 30 mg, group 7-*Aloe vera* 60 mg, group 8-*Aloe vera* 90 mg (Table 1).

Table 1. Experimental groups and applied drugs

Group Name	Applied Drugs
Group 1	None
Group 2	None
Group 3	Silverdin Cream
Group 4	Bepanthol Cream
Group 5	Sudocrem
Group 6	<i>Aloe vera</i> 30 mg gel
Group 7	<i>Aloe vera</i> 60 mg gel
Group 8	<i>Aloe vera</i> 90 mg gel

Rats' backs were shaved under anesthesia. Their backs were sterilized with alcohol cotton. Falcon tubes that has 3 cm diameter were filled with 90°C hot water. Rats were exposed to these water in falcon tubes for 10 seconds. After the exposure, second degree burns were occurred. After this process, rats were injected 5 ml saline to their napes subcutaneously and 1 drop of saline was given to each rats' eyes. Positive and negative control groups were not treated. Other groups of rats were treated with their selected drugs.

Treatment was continued with selected drugs once a day for 15 days. Positive and negative control groups were sacrificed after 2 days from forming burn model. After 15 days, the other groups were sacrificed.

Table 2. Working fiction

Groups							
Group 1	Group 2	Group 3	Group 4	Group 5	Group 6	Group 7	Group 8
After exposing rats to 90°C hot water for 10 seconds							
Sham group (only shaving)	Untreated control group that were formed burnt rat model	Silverdin® cream was applied to burnt area	Bepanthol® cream was applied to burnt area	Sudocrem® was applied to burnt area	<i>Aloe vera</i> 30 mg was applied to burnt area	<i>Aloe vera</i> 60 mg was applied to burnt area	<i>Aloe vera</i> 90 mg was applied to burnt area
Sacrificed after 2 days		Sacrificed after 15 days					

Statistical analysis

Obtained data were analyzed with the use of SPSS v.21 statistic program. The data were analyzed with 1-way ANOVA followed by the Duncan test. Data were shown as mean±SD. Comparison of two data was done by the t test and if $p < 0,05$, it was considered as statistically significant.

RESULTS

Table 3. Burn areas of experimental groups on stated days.

	Silverdin®	Bepanthol®	Sudocrem®	<i>Aloe vera</i> 30 mg	<i>Aloe vera</i> 60 mg	<i>Aloe vera</i> 90 mg	SD (±)
Day 1	7,07	7,07	7,07	7,06	7,07	7,07	0
Day 7	5,30	5,72	5,48	5,24	5,83	5,76	0,24
Day 10	4,75	4,90	3,89	4,39	4,91	4,55	0,38
Day 15	3,73	3,72	2,30	3,06	3,52	3,43	0,54

*The data were analyzed with 1-way ANOVA followed by the Duncan test ($p < 0,05$).

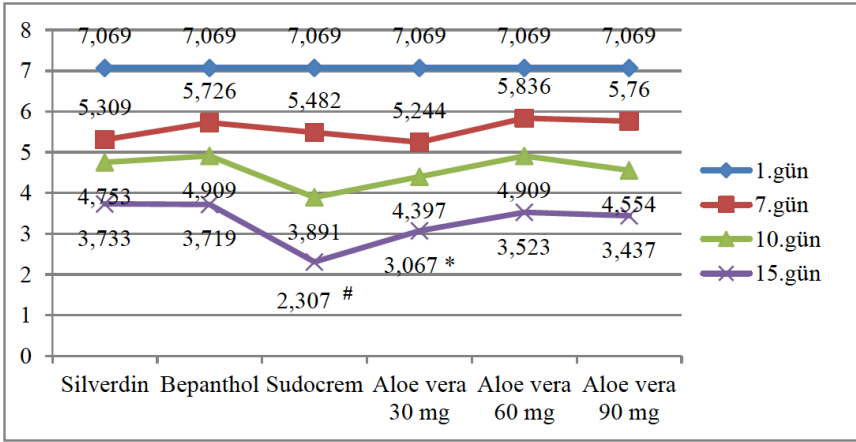


Figure 2. Graphical display of burn areas of experimental groups on stated days.

*: compared with other groups except Sudocream when 15th days of treatment; #: compared with all groups when 15th days of treatment.

At the end of the study, our results showed that area of burn was smaller in Sudocream group compared with those of other groups ($p < 0,05$). It can be shown in Table 3 and Figure 2.




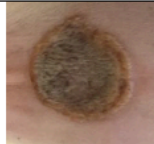









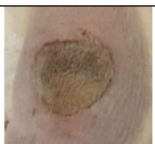
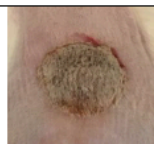

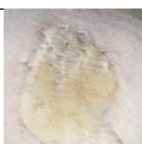
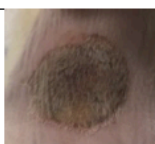






Day Medicine	Day			
	Day 1	Day 7	Day 10	Day 15
Silverdin®				
Bepantol®				
Sudocrem®				
<i>Aloe vera</i> 30 mg				
<i>Aloe vera</i> 60 mg				
<i>Aloe vera</i> 90 mg				

Figure 3. Burnt skin photos of experimental groups of that were taken on different days.

*: compared with other groups except Sudocream when 15th days of treatment; #: compared with all groups when 15th days of treatment.

The result showed that the scar tissue was softer (not stiff or coarse) in the Sudocream and *Aloe vera* 30 mg treated groups when compared with the others (Figure 3). Also, colour of wound secretion is more reddish in *Aloe vera* 30 mg and Sudocream groups compared with other groups on the 15th day of the study (Figure 3).

DISCUSSION AND CONCLUSION

Epidemiological studies around the world have shown that burns are one of the important reasons of death in community.⁹⁻¹¹ The most observed type of burn is second-degree burn and in order to treat, various types of medicines are available. Aloe vera can also be used for healing burns. It has been reported to contain amino acids, tannins, lipids, steroids, enzymes, flavonoids, anthraquinones, phlorotannins, carbohydrates, alkaloids, terpenes, and saponins.¹² These compounds in Aloe vera make it important in traditional and alternative medicine. The enhancing effect of Aloe vera to collagen levels providing strength and integrity to the tissue matrix and playing an important role in homeostasis along with epithelialization were also previously reported.¹³ Our findings showed that *Aloe vera* gel has a potential of healing the burn wounds on rats in line with the study by Farzadinia.¹⁴ On the other hand, contrary to expectations, not all doses of Aloe vera were found as the best drug. Among the *Aloe vera* gel drugs, the most effective dose was 30 mg, only. Aloe vera was better than silver sulfadiazine¹⁵(Silverdin® cream) but not than Sudocrem ® which contains zinc oxide. The other important parameter that shows wound healing is redness and thickness of periphery of burnt area. In accordance with the prior study performed by Emsen, our findings showed that wound periphery was more reddened and softer in groups which were treated with *Aloe vera* 30 mg and Sudocrem®.¹⁶ When comparing with other groups, *Aloe vera* wasn't the most effective drug among them but it was better than silver sulfadiazine which is the most used medicine in market. As a result of comparison, the most effective drug was Sudocrem and used for rashes in babies (burn area decreased to 2,307 cm² from 7,069 cm²). According to our data, the biggest wound area was in the Silverdin® group. Consequently, it can be said Aloe vera can be used in the treatment of second degree burns as an alternative medicine, instead of silver sulfadiazine.

REFERENCES

1. American Burn Association/American College of Surgeons. Guidelines for the operation of burn centers. *J. Burn Care Res.* **2007**, 28(1), 134-141.
2. Jeschke MG, Kamolz LP, Shahrokhi S. Burn Care and Treatment A Practical Guide. Yanık Bakımı ve Tedavisi, Translation into Turkish by: Erkülç A, Yıldırım MS, Anay H. Nobel Tıp Kitabevleri Tic. Ltd. Şti. İstanbul, **2015**.
3. Akyolcu N, Kanan N. Wound and Stoma Care, İstanbul Üniversitesi Florence Nightingale Hemşirelik Fakültesi 50. Yıl Yayınları, Nobel Tıp Kitabevleri Tic. Ltd. Şti. İstanbul, **2015** (in Turkish).
4. Kocattürk BK, Teyin M, Balcı Y, Eşiyok B. Evaluation of burn cases presenting in the Osmangazi University Hospital emergency room. *Türkiye Klinikleri J. Med. Sci.* **2005**, 25(3), 400-406.
5. Treatment Algorithm of Burn Injuries, Turkey Ministry of Health, **2012** (in Turkish).
6. Khorasani G, Hosseinimehr SJ, Azadbakht M, Zamani A, Mahdavi MR. Aloe Versus Silver Sulfadiazine Cream for Second-Degree Burns: A Randomized Controlled Study. *Surg. Today* **2009**, 39(7), 587-591.
7. Rosca-Casian O, Parvu M, Vlase L, Tamas M. Antifungal Activity of Aloe Vera Leaves. *Fitoterapia.* **2007**, 78(3), 219-222.
8. Lee D, Kim HS, Shin E, Do SG, Lee CK, Kim YM, Lee MB, Min KY, Koo J, Kim SJ, Nam ST, Kim HW, Park YH, Choi WS. Polysaccharide isolated from Aloe vera gel suppresses ovalbumin-induced food allergy through inhibition of Th2 immunity in mice. *Biomed. Pharmacother.* **2018**, 101, 201-210.
9. Chalise PR, Shrestha S, Sherpa K, Nepal U, Bhattachan CL, Bhattacharya K. Epidemiological and bacteriological profile of burn patients at Nepal Medical College Teaching Hospital. *Nepal Med. Coll. J.* **2008**, 10, 233-237.
10. Chen Y, Mo F, Yi QL, Jiang Y, Mao Y. Unintentional injury mortality and external causes in Canada from 2001 to 2007. *Chronic Dis. Inj. Can.* **2013**, 33, 95-102.
11. Dale EL, Mueller MA, Wang L, Fogerty MD, Guy JS, Nthumba PM. Epidemiology of operative burns at Kijabe Hospital from 2006 to 2010: pilot study of a web-based tool for creation of the Kenya Burn Repository. *Burns.* **2013**, 39, 788-795.
12. Ejoba R. Phytochemical constituents of some leaves extract of Aloe vera and Azadirachta indica plant species. *Global Adv. Res. J. Environ. Sci. Toxicol.* **2012**, 1, 14-17.
13. Chithra P, Sajithlal GB, Chandrakasan G. Influence of aloe vera on the healing of dermal wounds in diabetic rats. *J. Ethnopharmacol.* **1998**, 59, 195-201.
14. Farzadinia P, Jofreh N, Khatamsaz S, Movahed A, Akbarzadeh S, Mohammadi M, et al. Anti-inflammatory and wound healing activities of Aloe vera, honey and milk ointment on second degree burns in rats. *Int. J. Low Extrem. Wounds.* **2016**, 15, 241-247.
15. Akhoondinasab MR, Akhoondinasab M, Saberi M. Comparison of healing effect of aloe vera extract and silver sulfadiazine in burn injuries in experimental rat model. *World J. Plast. Surg.* **2014**, 3(1), 29-34.
16. Emsen IM. A different and safe method of split thickness skin graft fixation: medical honey application. *Burns.* **2007**, 33, 782-787.

